# LM25148 42-V Synchronous Buck DC/DC Controller with Ultra-Low $I_Q$ and Dual Random Spread Spectrum

## 1 Features

- Functional Safety-Capable
  - Documentation available to aid functional safety system design
- Integrated EMI mitigation
  - Selectable dual random spread spectrum (DRSS) feature for enhanced EMI performance across low and high-frequency bands
  - Optimized for CISPR 32 Class B requirements
- Versatile synchronous buck DC/DC controller
  - Wide input voltage range of 3.5 V to 42 V
  - 1% accurate, fixed 3.3-V, 5-V, 12-V, or adjustable output from 0.8 V to 36 V
  - 150°C maximum junction temperature
  - Lossless DCR or shunt current sensing
  - Shutdown mode current: 2.3 µA
  - No-load sleep current: 9.5 µA
  - Internal 3-ms soft-start ramp
  - Stackable up to two phases
  - Advanced dropout with frequency foldback
  - Internal bootstrap diode
- Switching frequency from 100 kHz to 2.2 MHz
  - SYNC in and SYNC out capability
  - Selectable PFM or FPWM modes
- Inherent protection features for robust design
  - Internal hiccup mode overcurrent protection
  - ENABLE and PGOOD functions
  - VCC, VDDA, and gate-drive UVLO protection
  - Internal or external loop compensation
  - Thermal shutdown protection with hysteresis
- Create a custom design using the LM25148 with WEBENCH® Power Designer

## 2 Applications

- Building automation
- Industrial transport
- Power delivery
- Test and measurement
- Aerospace and defense

## 3 Description

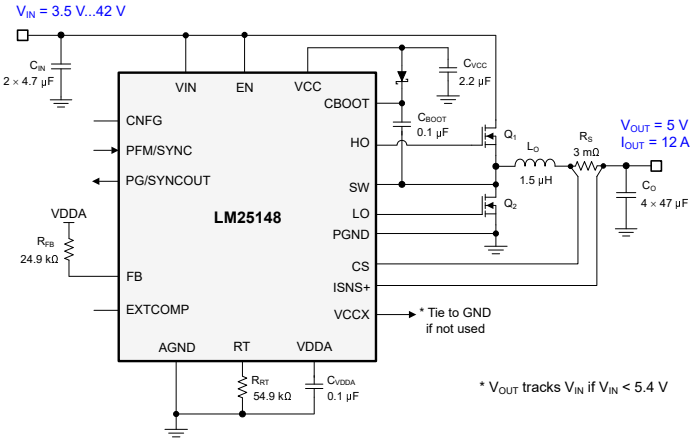
The LM25148 is a 42-V, ultra-low $I_Q$ synchronous buck DC/DC controller for high-current, single-output applications. The controller uses a peak current-mode control architecture for easy loop compensation, fast transient response, and excellent load and line regulation. The LM25148 can be set up in interleaved mode (paralleled output) with accurate current sharing for high-current applications. It can operate at input voltages as low as 3.5 V, at nearly 100% duty cycle if needed.

The LM25148 has a unique EMI reduction feature known as dual random spread spectrum (DRSS). Combining low-frequency triangular and high-frequency random modulations mitigates EMI disturbances across lower and higher frequency bands, respectively. This hybrid technique aligns with the multiple resolution bandwidth (RBW) settings specified in industry-standard EMC tests.

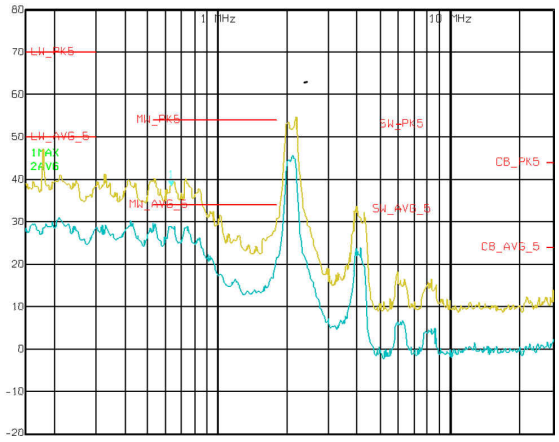
**Device Information**

| PART NUMBER | PACKAGE(1) | BODY SIZE (NOM) |
|---|---|---|
| LM25148 | VQFN (24) | 3.5 mm × 5.5 mm |

(1) For all available packages, see the orderable addendum at the end of the data sheet




**Typical Application Schematic**




**CISPR 25 EMI Performance, 150 kHz to 30 MHz**

An IMPORTANT NOTICE at the end of this data sheet addresses availability, warranty, changes, use in safety-critical applications, intellectual property matters and other important disclaimers. PRODUCTION DATA.

# Table of Contents

**1 Features**....1
**2 Applications**....1
**3 Description**....1
**4 Revision History**....2
**5 Description (continued)**....3
**6 Pin Configuration and Functions**....3
**7 Specifications**....5
7.1 Absolute Maximum Ratings....5
7.2 ESD Ratings....5
7.3 Recommended Operating Conditions....5
7.4 Thermal Information....6
7.5 Electrical Characteristics....6
7.6 Typical Characteristics....9
**8 Detailed Description**....13
8.1 Overview....13
8.2 Functional Block Diagram....14
8.3 Feature Description....15
8.4 Device Functional Modes....24
**9 Application and Implementation**....25
9.1 Application Information....25
9.2 Typical Applications....32
**10 Power Supply Recommendations**....47
**11 Layout**....48
11.1 Layout Guidelines....48
11.2 Layout Example....51
**12 Device and Documentation Support**....53
12.1 Device Support....53
12.2 Documentation Support....54
12.3 Receiving Notification of Documentation Updates....55
12.4 Support Resources....55
12.5 Trademarks....55
12.6 Electrostatic Discharge Caution....55
12.7 Glossary....55
**13 Mechanical, Packaging, and Orderable Information**....55

## 4 Revision History

NOTE: Page numbers for previous revisions may differ from page numbers in the current version.

| DATE | REVISION | NOTES |
|---|---|---|
| December 2021 | * | Initial release |

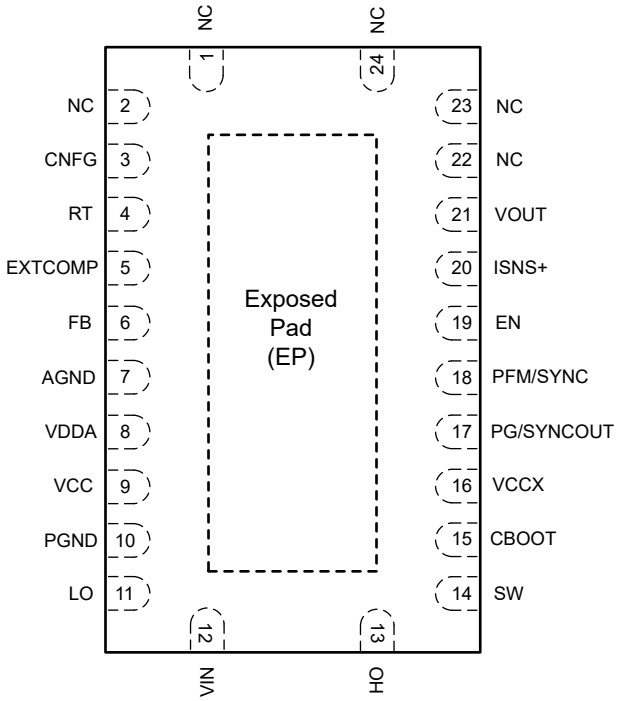

Copyright © 2021 Texas Instruments Incorporated

## 5 Description (continued)

Additional features of the LM25148 include 150°C maximum junction temperature operation, user-selectable diode emulation for lower current consumption at light-load conditions, open-drain power-good flag for fault reporting and output monitoring, precision enable input, monotonic start-up into prebiased load, integrated VCC bias supply regulator, internal 3-ms soft-start time, and thermal shutdown protection with automatic recovery.

The LM25148 controller comes in a 3.5-mm × 5.5-mm thermally enhanced, 24-pin VQFN package.

## 6 Pin Configuration and Functions




Connect the exposed pad to AGND and PGND on the PCB.

**Figure 6-1. (Top View)**

**Table 6-1. Pin Functions**

| PIN | | I/O[1] | DESCRIPTION |
|---|---|---|---|
| NO. | NAME | | |
| 1 | NC | – | Connect to GND at the exposed pad to improve heat spreading. |
| 2 | NC | – | Connect to GND at the exposed pad to improve heat spreading. |
| 3 | CNFG | I | Connect a resistor to ground to set primary/secondary, spread spectrum enable/disable, or interleaved operation. |
| 4 | RT | I | Frequency programming pin. A resistor from RT to AGND sets the oscillator frequency between 100 kHz and 2.2 MHz. |
| 5 | EXTCOMP | O | Transconductance error amplifier output. If used, connect the compensation network from EXTCOMP to AGND. |
| 6 | FB | I | Connect FB to VDDA to set the output voltage to 3.3 V. Connect FB using a 24.9 kΩ or 49.9 kΩ to VDDA to set the output voltage to 5 V or 12 V, respectively. Install a resistor divider from VOUT to AGND to set the output voltage setpoint between 0.8 V and 36 V. The FB regulation voltage is 0.8 V. |
| 7 | AGND | G | Analog ground connection. Ground return for the internal voltage reference and analog circuits |
| 8 | VDDA | O | Internal analog bias regulator. Connect a ceramic decoupling capacitor from VDDA to AGND. |
| 9 | VCC | P | VCC bias supply pin. Connect a ceramic capacitor between VCC and PGND. |
| 10 | PGND | G | Power ground connection pin for low-side MOSFET gate driver |
| 11 | LO | O | Low-side power MOSFET gate driver output |

Copyright © 2021 Texas Instruments Incorporated

**Table 6-1. Pin Functions (continued)**

| PIN | | I/O[1] | DESCRIPTION |
|---|---|---|---|
| NO. | NAME | | |
| 12 | VIN | P | Supply voltage input source for the VCC regulator |
| 13 | HO | O | High-side power MOSFET gate driver output |
| 14 | SW | P | Switching node of the buck regulator and high-side gate driver return. Connect to the bootstrap capacitor, the source terminal of the high-side MOSFET, and the drain terminal of the low-side MOSFET. |
| 15 | CBOOT | P | High-side driver supply for bootstrap gate drive |
| 16 | VCCX | P | Optional input for an external bias supply. If $V_{VCCX}$ > 4.3 V, VCCX is internally connected to VCC and the internal VCC regulator is disabled. |
| 17 | PG/SYNCOUT | O | An open-collector output that goes low if VOUT is outside the specified regulation window. The PG/SYNCOUT pin of the primary controller in dual-phase mode provides a 180° phase-shifted SYNCOUT signal. |
| 18 | PFM/SYNC | I | Connect PFM/SYNC to VDDA to enable diode emulation mode. Connect PFM to AGND to operate the LM25148 in forced PWM (FPWM) mode with continuous conduction at light loads. PFM can also be used as a synchronization input to synchronize the internal oscillator to an external clock signal. |
| 19 | EN | I | An active-high precision input with rising threshold of 1 V and hysteresis current of 10 µA. If the EN voltage is less than 0.5 V, the LM25148 is in shutdown mode, unless a SYNC signal is present on PFM/SYNC. |
| 20 | ISNS+ | I | Current sense amplifier input. Connect this pin to the inductor side of the external current sense resistor (or to the relevant sense capacitor terminal if inductor DCR current sensing is used) using a low-current Kelvin connection. |
| 21 | VOUT | I | Output voltage sense and the current sense amplifier input. Connect VOUT to the output side of the current sense resistor (or to the relevant sense capacitor terminal if inductor DCR current sensing is used). |
| 22 | NC | — | Connect to GND at the exposed pad to improve heat spreading. |
| 23 | NC | — | Connect to GND at the exposed pad to improve heat spreading. |
| 24 | NC | — | Connect to GND at the exposed pad to improve heat spreading. |

(1) P = Power, G = Ground, I = Input, O = Output


Copyright © 2021 Texas Instruments Incorporated

# 7 Specifications

## 7.1 Absolute Maximum Ratings

Over the recommended operating junction temperature range of –40°C to 150°C (unless otherwise noted) (1)

| | | MIN | MAX | UNIT |
|---|---|---|---|---|
| Output voltage | VOUT, ISNS+ to AGND | –0.3 | 36 | V |
| | VOUT to ISNS+ | –0.3 | 0.3 | V |
| Input voltage | VIN to PGND | –0.3 | 47 | V |
| | SW to PGND | –0.3 | 47 | V |
| | SW to PGND, transient < 20 ns | –5 | | V |
| | CBOOT to SW | –0.3 | 6.5 | V |
| | CBOOT to SW, transient < 20 ns | –2 | | V |
| | HO to SW | –0.3 | $V_{HB}$ + 0.3 | V |
| | HO to SW, transient < 20 ns | –5 | | V |
| | LO to PGND | –0.3 | $V_{VCC}$ + 0.3 | V |
| | LO to PGND, transient < 20 ns | –1.5 | | V |
| | EN to PGND | –0.3 | 47 | V |
| | VCC, VCCX, VDDA, PG, FB, PFM/SYNC, RT, EXTCOMP to AGND | –0.3 | 6.5 | V |
| | CNFG to AGND | –0.3 | 5.5 | V |
| Operating junction temperature, $T_J$ | | –40 | 150 | °C |
| Storage temperature, $T_{stg}$ | | –55 | 150 | °C |

(1) Operation outside the *Absolute Maximum Ratings* may cause permanent device damage. *Absolute Maximum Ratings* do not imply functional operation of the device at these or any other conditions beyond those listed under *Recommended Operating Conditions*. If used outside the *Recommended Operating Conditions* but within the *Absolute Maximum Ratings*, the device may not be fully functional, and this may affect device reliability, functionality, performance, and shorten the device lifetime.

## 7.2 ESD Ratings

| | | | VALUE | UNIT |
|---|---|---|---|---|
| $V_{(ESD)}$ | Electrostatic discharge | Human-body model (HBM), per ANSI/ESDA/JEDEC JS-001 (1) | ±2000 | V |
| | | Charged device model (CDM), per ANSI/ESDA/JEDEC JS-002 (2) | ±750 | |

(1) JEDEC document JEP155 states that 500-V HBM allows safe manufacturing with a standard ESD control process.
(2) JEDEC document JEP157 states that 250-V CDM allows safe manufacturing with a standard ESD control process.

## 7.3 Recommended Operating Conditions

Over the operating junction temperature range of –40°C to 150°C (unless otherwise noted). (1)

| | | MIN | NOM | MAX | UNIT |
|---|---|---|---|---|---|
| $V_{IN}$ | Input supply voltage range | 3.5 | | 42 | V |
| $V_{OUT}$ | Output voltage range | 0.8 | | 36 | V |
| | SW to PGND | –0.3 | | 42 | V |
| | CBOOT to SW | –0.3 | 5 | 5.25 | V |
| | FB, EXTCOMP, RT, CNFG to AGND | –0.3 | | 5.25 | V |
| | EN to PGND | –0.3 | | 42 | V |
| | VCC, VCCX, VDDA, to PGND | –0.3 | 5 | 5.25 | V |
| | VOUT, ISNS+ to PGND | –0.3 | | 36 | V |
| | PGND to AGND | –0.3 | | 0.3 | V |
| | CNFG to AGND | –0.3 | | 5.5 | V |
| $T_J$ | Operating junction temperature | –40 | | 150 | °C |

(1) Recommended operating conditions are conditions under which the device is intended to be functional. For specifications and test conditions, see the *Electrical Characteristics*.

Copyright © 2021 Texas Instruments Incorporated

## 7.4 Thermal Information

| THERMAL METRIC(1) | | LM25148 RGY (VQFN) 24 PINS | UNIT |
|---|---|---|---|
| $R_{\theta JA}$ | Junction-to-ambient thermal resistance | 37.3 | °C/W |
| $R_{\theta JC(top)}$ | Junction-to-case (top) thermal resistance | 32 | °C/W |
| $R_{\theta JB}$ | Junction-to-board thermal resistance | 15.5 | °C/W |
| $\psi_{JT}$ | Junction-to-top characterization parameter | 1.2 | °C/W |
| $\psi_{JB}$ | Junction-to-board characterization parameter | 15.5 | °C/W |
| $R_{\theta JC(bot)}$ | Junction-to-case (bottom) thermal resistance | 5.6 | °C/W |

(1) For more information about traditional and new thermal metrics, see the *Semiconductor and IC Package Thermal Metrics* application note

## 7.5 Electrical Characteristics

$T_J$ = –40°C to 150°C. Typical values are at $T_J$ = 25°C and $V_{IN}$ = 12 V (unless otherwise noted).

| PARAMETER | | TEST CONDITIONS | MIN | TYP | MAX | UNIT |
|---|---|---|---|---|---|---|
| **SUPPLY (VIN)** | | | | | | |
| $I_{Q-VIN1}$ | VIN shutdown current | $V_{EN}$ = 0 V | | 2.3 | 3.8 | µA |
| $I_{Q-VIN2}$ | VIN standby current | Non-switching, 0.5 V ≥ $V_{EN}$ ≤ 1 V | | 124 | | µA |
| $I_{SLEEP1}$ | Sleep current, 3.3 V | 1.03 V ≤ $V_{EN}$ ≤ 42 V, $V_{VOUT}$ = 3.3 V, in regulation, no-load, not switching, $V_{PFM/SYNC}$ = 0 V | | 9.5 | 19.7 | µA |
| $I_{SLEEP2}$ | Sleep current, 5 V | $V_{EN}$ = 5 V, $V_{VOUT}$ = 5 V, in regulation, no-load, not switching, $V_{PFM/SYNC}$ = 0 V | | 9.9 | 19.9 | µA |
| **ENABLE (EN)** | | | | | | |
| $V_{SDN}$ | Shutdown to standby threshold | $V_{EN}$ rising | | 0.5 | | V |
| $V_{EN-HIGH}$ | Enable voltage rising threshold | $V_{EN}$ rising, enable switching | 0.95 | 1.0 | 1.05 | V |
| $I_{EN-HYS}$ | Enable hysteresis | $V_{EN}$ = 1.1 V | –12 | –10 | –8 | µA |
| **INTERNAL LDO (VCC)** | | | | | | |
| $V_{VCC-REG}$ | VCC regulation voltage | $I_{VCC}$ = 0 mA to 100 mA | 4.7 | 5 | 5.3 | V |
| $V_{VCC-UVLO}$ | VCC UVLO rising threshold | | 3.3 | 3.4 | 3.5 | V |
| $V_{VCC-HYST}$ | VCC UVLO hysteresis | | | 148 | | mV |
| $I_{VCC-REG}$ | Internal LDO short-circuit current limit | | 115 | 170 | | mA |
| **INTERNAL LDO (VDDA)** | | | | | | |
| $V_{VDDA-REG}$ | VDDA regulation voltage | | 4.75 | 5 | 5.25 | V |
| $V_{VDDA-UVLO}$ | VDDA UVLO rising | $V_{VCC}$ rising, $V_{VCCX}$ = 0 V | 3 | 3.2 | 3.3 | V |
| $V_{VDDA-HYST}$ | VDDA UVLO hysteresis | $V_{VCCX}$ = 0 V | | 120 | | mV |
| $R_{VDDA}$ | VDDA resistance | $V_{VCCX}$ = 0 V | | 5.5 | | Ω |
| **EXTERNAL BIAS (VCCX)** | | | | | | |
| $V_{VCCX-ON}$ | VCCX rising threshold | | 4.1 | 4.3 | 4.4 | V |
| $V_{VCCX-HYST}$ | VCCX hysteresis voltage | $V_{VCCX}$ = 5 V | | 130 | | mV |
| $R_{VCCX}$ | VCCX resistance | $V_{VCCX}$ = 5 V | | 2 | | Ω |
| **REFERENCE VOLTAGE** | | | | | | |
| $V_{REF}$ | Regulated FB voltage | | 795 | 800 | 808 | mV |
| **OUTPUT VOLTAGE (VOUT)** | | | | | | |
| $V_{OUT-3.3V-INT}$ | 3.3-V output voltage setpoint | $R_{FB}$ = 0 Ω, $V_{IN}$ = 3.8 V to 42 V, internal COMP | 3.267 | 3.3 | 3.333 | V |
| $V_{OUT-3.3V-EXT}$ | 3.3-V output voltage setpoint | $R_{FB}$ = 0 Ω, $V_{IN}$ = 3.8 V to 42 V, external COMP | 3.267 | 3.3 | 3.333 | V |
| $V_{OUT-5V-INT}$ | 5-V output voltage setpoint | $R_{FB}$ = 24.9 kΩ, $V_{IN}$ = 5.5 V to 42 V, internal COMP | 4.95 | 5.0 | 5.05 | V |
| $V_{OUT-5V-EXT}$ | 5-V output voltage setpoint | $R_{FB}$ = 24.9 kΩ, $V_{IN}$ = 5.5 V to 42 V, external COMP | 4.95 | 5.0 | 5.05 | V |


Copyright © 2021 Texas Instruments Incorporated

$T_J$ = –40°C to 150°C. Typical values are at $T_J$ = 25°C and $V_{IN}$ = 12 V (unless otherwise noted).

| PARAMETER | | TEST CONDITIONS | MIN | TYP | MAX | UNIT |
|---|---|---|---|---|---|---|
| $V_{OUT-12V-INT}$ | 12-V output setpoint | $R_{FB}$ = 48.7 kΩ, $V_{IN}$ = 24 V to 42 V, internal COMP COMP | 11.88 | 12 | 12.12 | V |
| $V_{OUT-12V-EXT}$ | 12-V output setpoint | $R_{FB}$ = 48.7 kΩ, $V_{IN}$ = 24 V to 42 V, external COMP | 11.88 | 12 | 12.12 | V |
| $R_{FB-OPT1}$ | 5-V output select | | 23 | 25 | 27 | kΩ |
| $R_{FB-OPT2}$ | 12-V output select | | 47 | 50 | 53 | kΩ |
| **ERROR AMPLIFIER (COMP)** | | | | | | |
| $g_{m-EXTERNAL}$ | EA transconductance, external compensation | FB to EXTCOMP | 1020 | 1200 | | µS |
| $g_{m-INTERNAL}$ | EA transconductance, internal compensation | FB to EXTCOMP 100 kΩ to VDDA | | 30 | | µS |
| $I_{FB}$ | Error amplifier input bias current | | | | 75 | nA |
| $V_{COMP-CLAMP}$ | COMP clamp voltage | $V_{FB}$ = 0 V | | 2.1 | | V |
| $I_{COMP-SRC}$ | EA source current | $V_{EXTCOMP}$ = 1 V, $V_{FB}$ = 0.6 V | | 180 | | µA |
| $I_{COMP-SINK}$ | EA sink current | $V_{EXTCOMP}$ = 1 V, $V_{FB}$ = 1 V | | 180 | | µA |
| $R_{COMP}$ | Internal compensation | EXTCOMP 100 kΩ to VDDA | | 400 | | kΩ |
| $C_{COMP}$ | Internal compensation | EXTCOMP 100 kΩ to VDDA | | 50 | | pF |
| $C_{COMP-HF}$ | Internal compensation | EXTCOMP 100 kΩ to VDDA | | 1 | | pF |
| **PULSE FREQUENCY MODULATION (PFM/SYNC)** | | | | | | |
| $V_{PFM-LO}$ | PFM detection threshold low | | 0.8 | | | V |
| $V_{PFM-HI}$ | PFM decection threshold high | | | | 2.0 | V |
| $V_{ZC-SW}$ | Zero-cross threshold | | | –5.5 | | mV |
| $V_{ZC-DIS}$ | Zero-cross threshold disable | PFM = VDDA, 1000 SW cycles after first HO pulse | | 100 | | mV |
| $F_{SYNCIN3}$ | Frequency sync range | $R_{RT}$ = 9.53 kΩ, ±20% of the nominal oscillator frequency | 1.74 | | 2.7 | MHz |
| $t_{SYNC-MIN3}$ | Minimum pulse-width of external synchronization signal | | 20 | | 250 | ns |
| $t_{SYNCIN-HO}$ | Delay from PFM faling edge to HO rising edge | | | 45 | | ns |
| $t_{PFM-FILTER}$ | SYNCIN to PFM mode | | 13 | | 45 | µs |
| **DUAL RANDOM SPREAD SPECTRUM (DRSS)** | | | | | | |
| $\Delta f_C$ | Modulation frequency percentage change | | | 7% | | |
| $f_m$ | Modulation frequency | | 8.2 | | 16.2 | kHz |
| **SWITCHING FREQUENCY** | | | | | | |
| $V_{RT}$ | RT pin regulation voltage | 10 kΩ < $R_{RT}$ < 100 kΩ | | 0.5 | | V |
| $F_{SW1}$ | Switching frequency 1 | $R_{RT}$ = 97.6 kΩ to AGND | | 0.22 | | MHz |
| $F_{SW2}$ | Switching frequency 2 | $V_{IN}$ = 12 V, $R_{RT}$ = 9.09 kΩ to AGND | 1.98 | 2.2 | 2.42 | MHz |
| $F_{SW3}$ | Switching frequency 3 | $R_{RT}$ = 220 kΩ to AGND | | 100 | | kHz |
| $SLOPE_1$ | Internal slope compensation 1 | $R_{RT}$ = 9.09 kΩ | | 600 | | mV/µs |
| $SLOPE_2$ | Internal slope compensation 2 | $R_{RT}$ = 97.6 kΩ | | 50 | | mV/µs |
| $t_{ON(min)}$ | Minimum on time | | | 50 | | ns |
| $t_{OFF(min)}$ | Minimum off time | | | 90 | | ns |
| **POWER GOOD (PG)** | | | | | | |
| $V_{PG-UV}$ | Power-good UV trip level | Falling with respect to the regulated voltage | 90% | 92% | 94% | |
| $V_{PG-OV}$ | Power-good OV trip level | Rising with respect to the regulation voltage | 108% | 110% | 112% | |
| $V_{PG-UV-HYST}$ | Power-good UV hysteresis | Falling with respect to the regulated output | | 3.6% | | |
| $V_{PG-OV-HYST}$ | Power-good OV hysteresis | Rising with respect to the regulation voltage | | 3.4% | | |
| $t_{OV-DLY}$ | OV filter time | $V_{OUT}$ rising | | 25 | | µs |
| $t_{UV-DLY}$ | UV filter time | $V_{OUT}$ falling | | 25 | | µs |
| $V_{PG-OL}$ | PG voltage | Open collector, PG/SYNC = 4 mA | | | 0.8 | V |
| **SYNCHRONIZATION OUTPUT (PG/SYNCOUT)** | | | | | | |

Copyright © 2021 Texas Instruments Incorporated

$T_J$ = –40°C to 150°C. Typical values are at $T_J$ = 25°C and $V_{IN}$ = 12 V (unless otherwise noted).

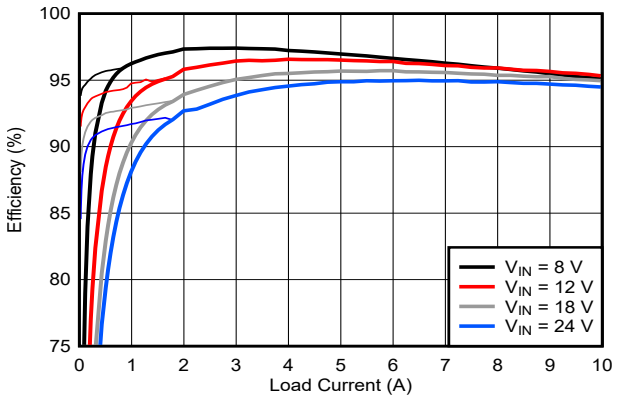
| PARAMETER | | TEST CONDITIONS | MIN | TYP | MAX | UNIT |
|---|---|---|---|---|---|---|
| $V_{SYNCOUT-LO}$ | SYNCOUT-LO low-state voltage | $R_{CNFG}$ = 54.9 kΩ or 71.5 kΩ to VDDA (primary), PFM/SYNC = 2 mA | | | 0.8 | V |
| $V_{SYNCOUT-HO}$ | SYNCO-HO high-state voltage | $R_{CNFG}$ = 54.9 kΩ, or 71.5 kΩ to VDDA (primary) PFM/SYNC = 2 mA | 2.0 | | | V |
| $t_{SYNCOUT}$ | Delay from HO rising edge to SYNCOUT (PG pin in primary mode) | $V_{PFM}$ = 0 V, $F_{SW}$ set by $R_{RT}$ = 100 kΩ | | 2.1 | | µs |
| **STARTUP (Soft Start)** | | | | | | |
| $t_{SS-INT}$ | Internal fixed soft-start time | | 1.9 | 3 | 4.6 | ms |
| **BOOT CIRCUIT** | | | | | | |
| $V_{BOOT-DROP}$ | Internal diode forward drop | $I_{CBOOT}$ = 20 mA, VCC to CBOOT | 0.63 | 0.8 | | V |
| $I_{BOOT}$ | CBOOT to SW quiescent current, not switching | $V_{EN}$ = 5 V, $V_{CBOOT-SW}$ = 5 V | 3.0 | | 4.2 | µA |
| $V_{BOOT-SW-UV-R}$ | CBOOT to SW UVLO rising threshold | $V_{CBOOT-SW}$ rising | | 2.83 | | V |
| $V_{BOOT-SW-UV-F}$ | CBOOT to SW UVLO falling threshold | $V_{CBOOT-SW}$ falling | | 2.5 | | V |
| $V_{BOOT-SW-UV-HYS}$ | CBOOT to SW UVLO hysteresis | | | 0.05 | | V |
| **HIGH-SIDE GATE DRIVER (HO)** | | | | | | |
| $V_{HO-HIGH}$ | HO high-state output voltage | $I_{HO}$ = –100 mA, $V_{HO-HIGH}$ = $V_{CBOOT}$ – $V_{HO}$ | | 106 | | mV |
| $V_{HO-LOW}$ | HO low-state output voltage | $I_{HO}$ = 100 mA | | 50 | | mV |
| $t_{HO-RISE}$ | HO rise time (10% to 90%) | $C_{LOAD}$ = 2.7 nF | | 7 | | ns |
| $t_{HO-FALL}$ | HO fall time (90% to 10%) | $C_{LOAD}$ = 2.7 nF | | 7 | | ns |
| $I_{HO-SRC}$ | HO peak source current | $V_{HO}$ = $V_{SW}$ = 0 V, $V_{CBOOT}$ = $V_{VCCX}$ = 5 V | | 2.2 | | A |
| $I_{HO-SINK}$ | HO peak sink current | $V_{VCCX}$ = 5 V | | 3.2 | | A |
| **LOW-SIDE GATE DRIVER (LO)** | | | | | | |
| $V_{LO-LOW}$ | LO low-state output voltage | $I_{LO}$ = 100 mA | | 50 | | mV |
| $V_{LO-HIGH}$ | LO high-state output voltage | $I_{LO}$ = –100 mA | | 130 | | mV |
| $t_{LO-RISE}$ | LO rise time (10% to 90%) | $C_{LOAD}$ = 2.7 nF | | 7 | | ns |
| $t_{LO-FALL}$ | LO fall time (90% to 10%) | $C_{LOAD}$ = 2.7 nF | | 7 | | ns |
| $I_{LO-SRC}$ | LO peak source current | $V_{HO}$ = $V_{SW}$ = 0 V, $V_{CBOOT}$ = $V_{VCCX}$ = 5 V | | 2.2 | | A |
| $I_{LO-SINK}$ | LO peak sink current | $V_{VCCX}$ = 5 V | | 3.2 | | A |
| **ADAPTIVE DEADTIME CONTROL** | | | | | | |
| $t_{DEAD1}$ | HO off to LO on deadtime | | | 20 | | ns |
| $t_{DEAD2}$ | LO off to HO on deadtime | | | 20 | | ns |
| **INTERNAL HICCUP MODE** | | | | | | |
| $HIC_{DLY}$ | Hiccup mode activation delay | $V_{ISNS+}$ –$V_{VOUT}$ > 60 mV | | 512 | | cycles |
| $HIC_{CYCLES}$ | HICCUP mode fault | $V_{ISNS+}$ –$V_{VOUT}$ > 60 mV | | 16384 | | cycles |
| **OVERCURRENT PROTECTION** | | | | | | |
| $V_{CS-TH}$ | Current limit threshold | Measured from ISNS+ to VOUT | 49 | 60 | 73 | mV |
| $t_{DELAY-ISNS+}$ | ISNS+ delay to output | | | 65 | | ns |
| $G_{CS}$ | CS amplifier gain | | 9 | 10 | 10.8 | V/V |
| $I_{BIAS-ISNS+}$ | CS amplifier input bias current | | | 15 | | nA |
| **CONFIGURATION** | | | | | | |
| $R_{CONF-OPT1}$ | Primary, no spread spectrum | | 28.7 | 29.4 | 31 | kΩ |
| $R_{CONF-OPT2}$ | Primary, with spread spectrum | | 40.2 | 41.2 | 43.2 | kΩ |
| $R_{CONF-OPT3}$ | Primary, interleaved, no spread spectrum | | 53.6 | 54.9 | 57.6 | kΩ |
| $R_{CONF-OPT4}$ | Primary, interleaved, with spread spectrum | | 69.8 | 71.5 | 73.2 | kΩ |
| $R_{CONF-OPT5}$ | Secondary | | 87 | 90.9 | 93.1 | kΩ |
| **THERMAL SHUTDOWN** | | | | | | |
| $T_{J-SD}$ | Thermal shutdown threshold (1) | Temperature rising | | 175 | | °C |
| $T_{J-HYS}$ | Thermal shutdown hysteresis (1) | | | 15 | | °C |

(1) Specified by design. Not production tested.


Copyright © 2021 Texas Instruments Incorporated

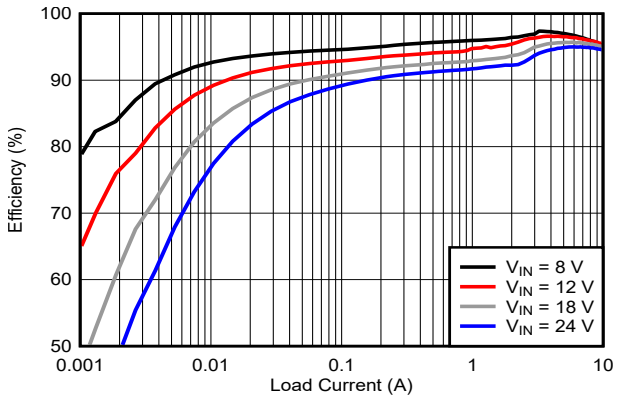
## 7.6 Typical Characteristics

$V_{IN}$ = 12 V, unless otherwise specified



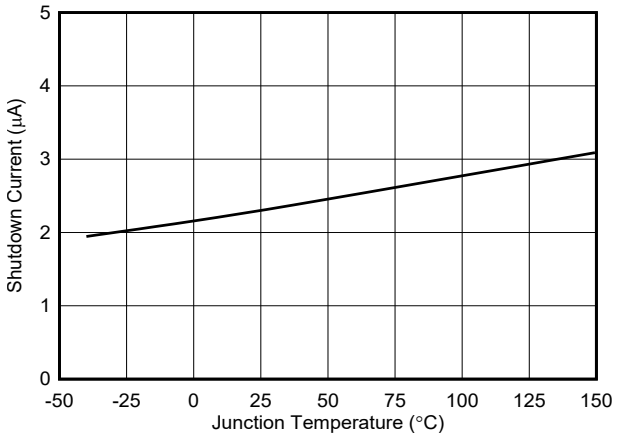

$V_{OUT}$ = 5 V $F_{SW}$ = 440 kHz

**Figure 7-1. Efficiency vs. Load**



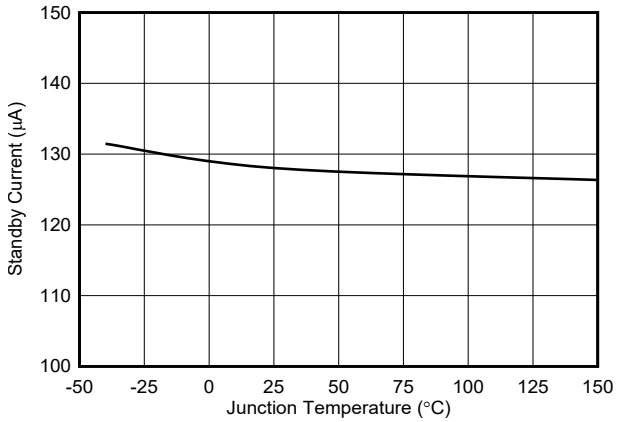

$V_{OUT}$ = 5 V $F_{SW}$ = 440 kHz

**Figure 7-2. Efficiency vs. Load, Log Scale**



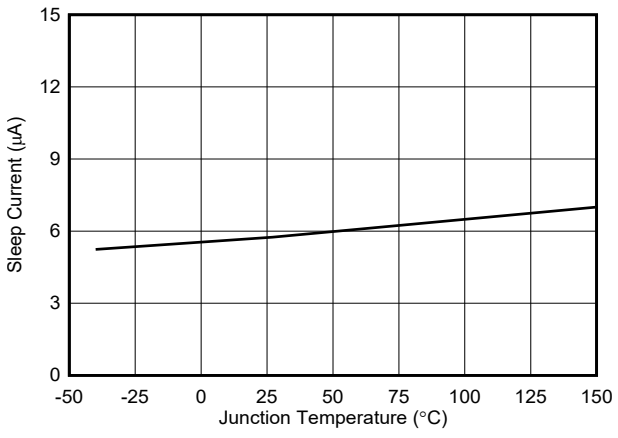

$V_{EN}$ = 0 V

**Figure 7-3. Shutdown Current vs. Temperature**



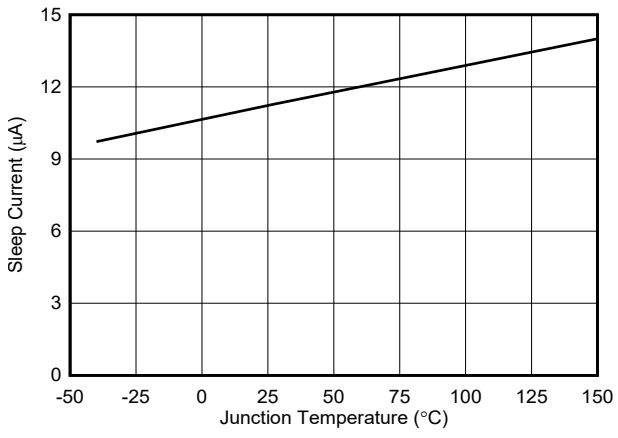

0.5 V ≤ $V_{EN}$ ≤ 1 V

**Figure 7-4. Standby Current vs. Temperature**




$V_{VOUT}$ = 3.3 V 1.03 V ≤ $V_{EN}$ ≤ 42 V

**Figure 7-5. Sleep Current vs. Temperature**




$V_{VOUT}$ = 5 V 1.03 V ≤ $V_{EN}$ ≤ 42 V

**Figure 7-6. Sleep Current vs. Temperature**

Copyright © 2021 Texas Instruments Incorporated

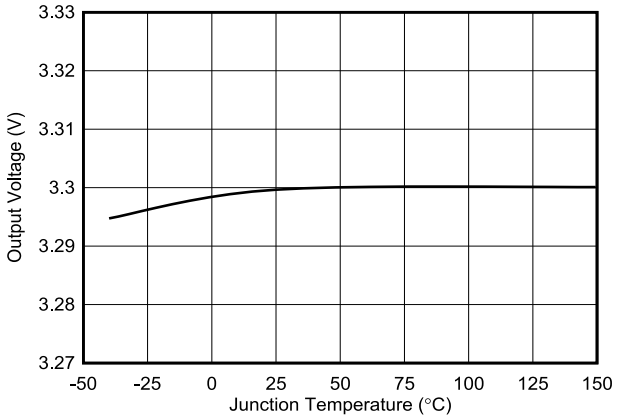



**Figure 7-7. Fixed 3.3-V Output Voltage vs. Temperature**

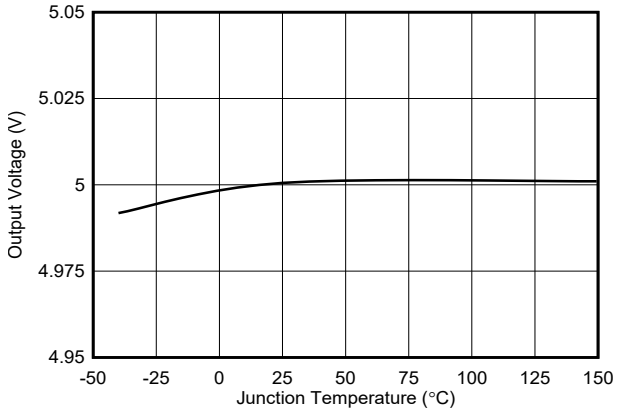



**Figure 7-8. Fixed 5-V Output Voltage vs. Temperature**

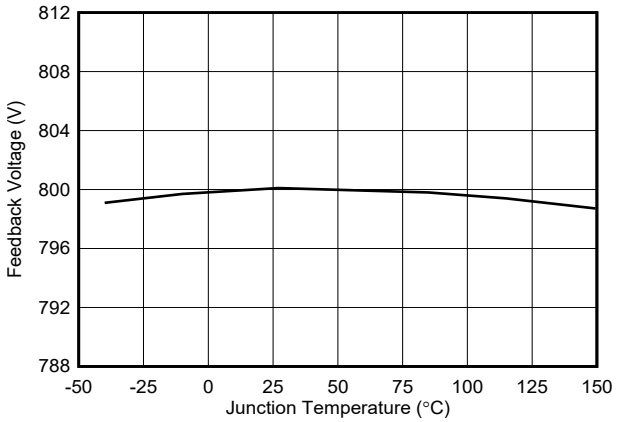



**Figure 7-9. Feedback Voltage vs. Temperature**

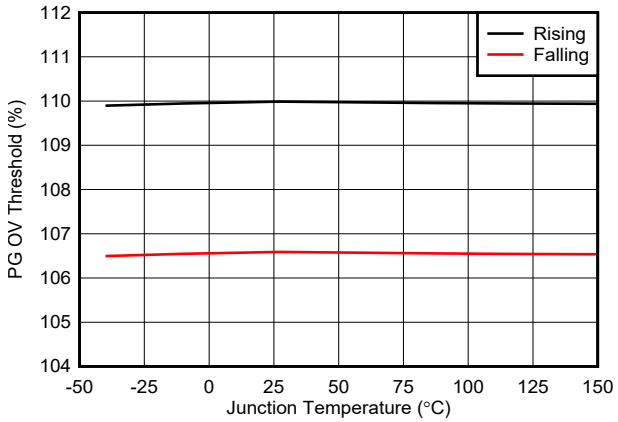



**Figure 7-10. PG OV Thresholds vs. Temperature**

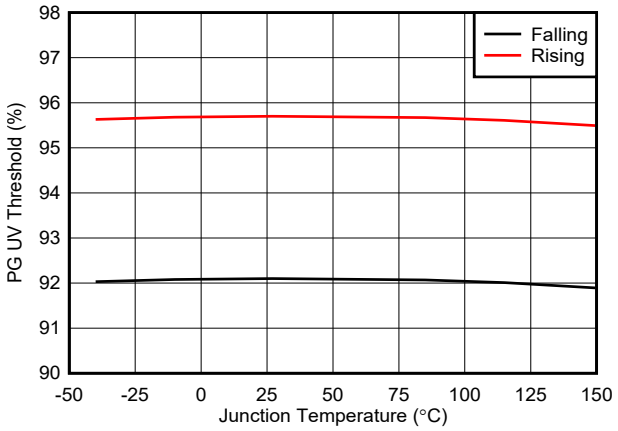



**Figure 7-11. PG UV Thresholds vs. Temperature**

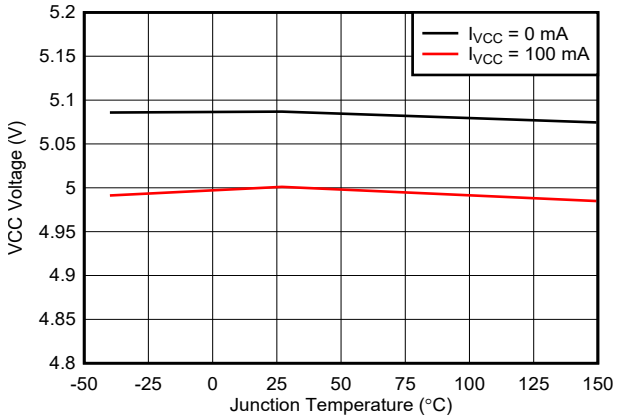



**Figure 7-12. VCC Regulation Voltage vs. Temperature**


Copyright © 2021 Texas Instruments Incorporated

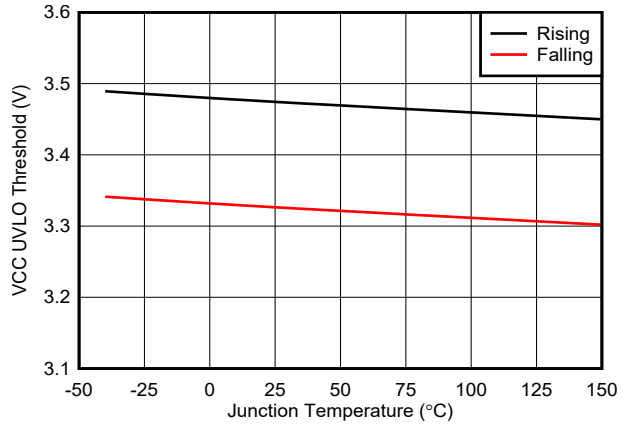



**Figure 7-13. VCC UVLO Thresholds vs. Temperature**

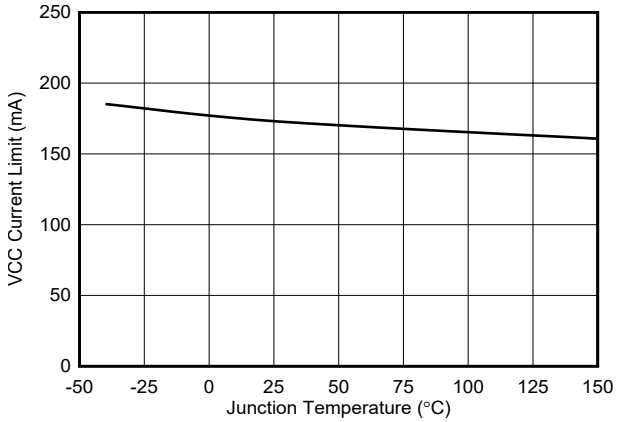



**Figure 7-14. VCC Current Limit vs. Temperature**

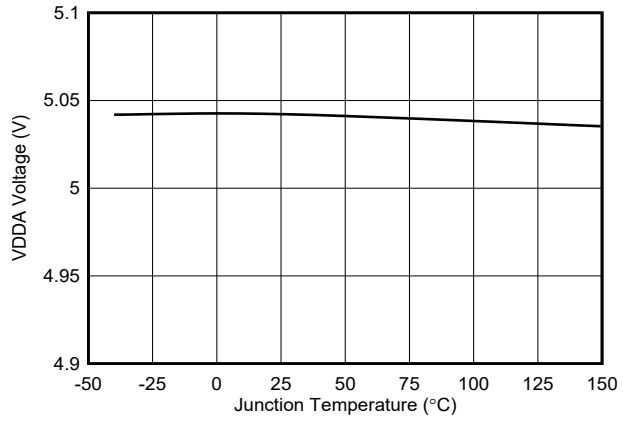



**Figure 7-15. VDDA Regulation Voltage vs. Temperature**

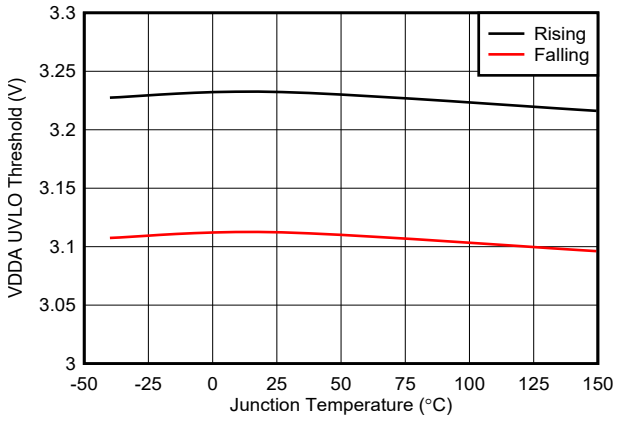



**Figure 7-16. VDDA UVLO Thresholds vs. Temperature**

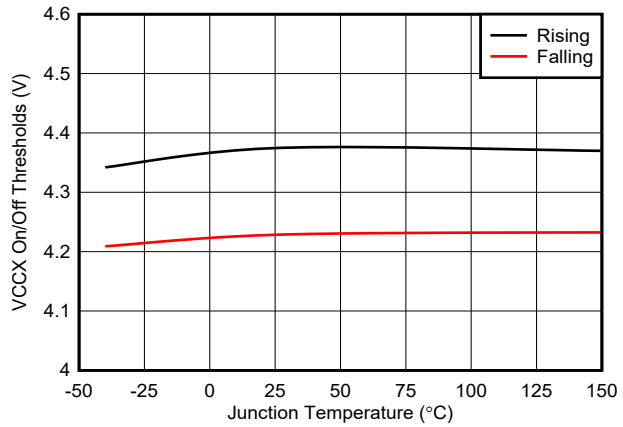



**Figure 7-17. VCCX On/Off Thresholds vs. Temperature**

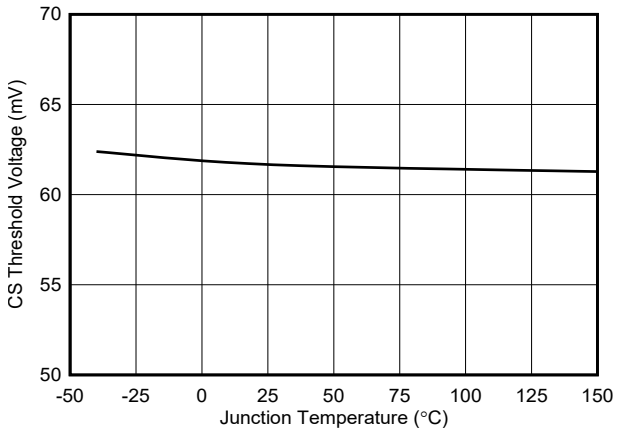



**Figure 7-18. Current Sense (CS) Threshold vs. Temperature**

Copyright © 2021 Texas Instruments Incorporated

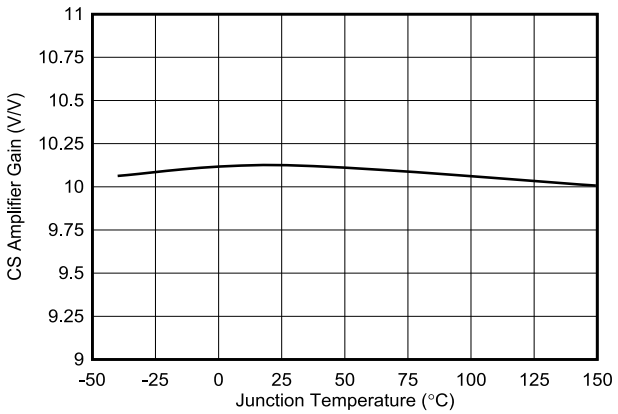



**Figure 7-19. Current Sense (CS) Amplifier Gain vs. Temperature**

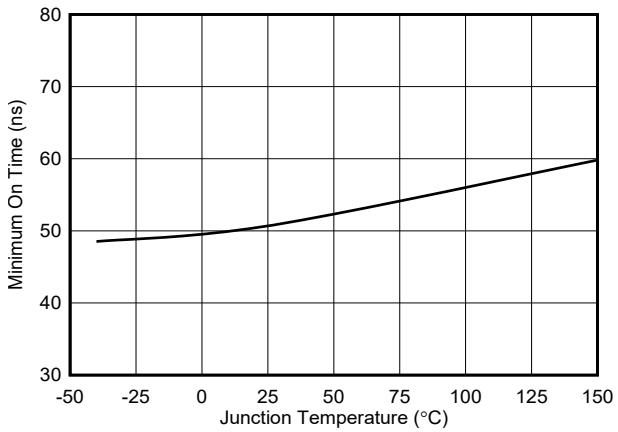



**Figure 7-20. Minimum On Time (HO) vs. Temperature**

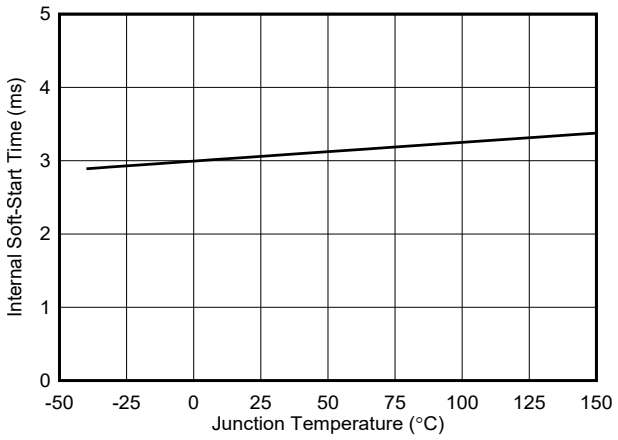
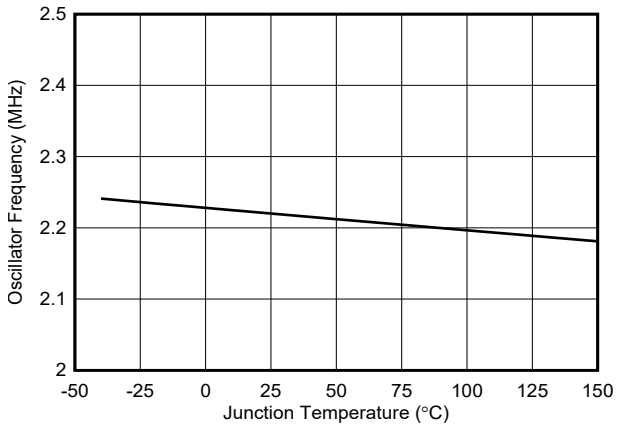



**Figure 7-21. Soft-Start Time vs. Temperature**




$R_{RT}$ = 9.09 kΩ

**Figure 7-22. Switching Frequency vs. Temperature**


Copyright © 2021 Texas Instruments Incorporated

# 8 Detailed Description

## 8.1 Overview

The LM25148 is a switching DC/DC controller that features all of the functions necessary to implement a high-efficiency synchronous buck power supply operating over a wide input voltage range from 3.5 V to 42 V. The LM25148 is configured to provide a fixed 3.3-V, 5-V, or 12-V output, or an adjustable output from 0.8 V to 36 V. This easy-to-use controller integrates high-side and low-side MOSFET gate drivers capable of sourcing and sinking peak currents of 2.2 A and 3.2 A, respectively. Adaptive dead-time control is designed to minimize body diode conduction during switching transitions.

Current-mode control using a shunt resistor or inductor DCR current sensing provides inherent line feedforward, cycle-by-cycle peak current limiting, and easy loop compensation. It also supports a wide duty cycle range for high input voltage and low-dropout applications as well as when application require a high step-down conversion ratio (for example, 10-to-1). The oscillator frequency is user-programmable between 100 kHz to 2.2 MHz, and the frequency can be synchronized as high as 2.5 MHz by applying an external clock to the PFM/SYNC pin.

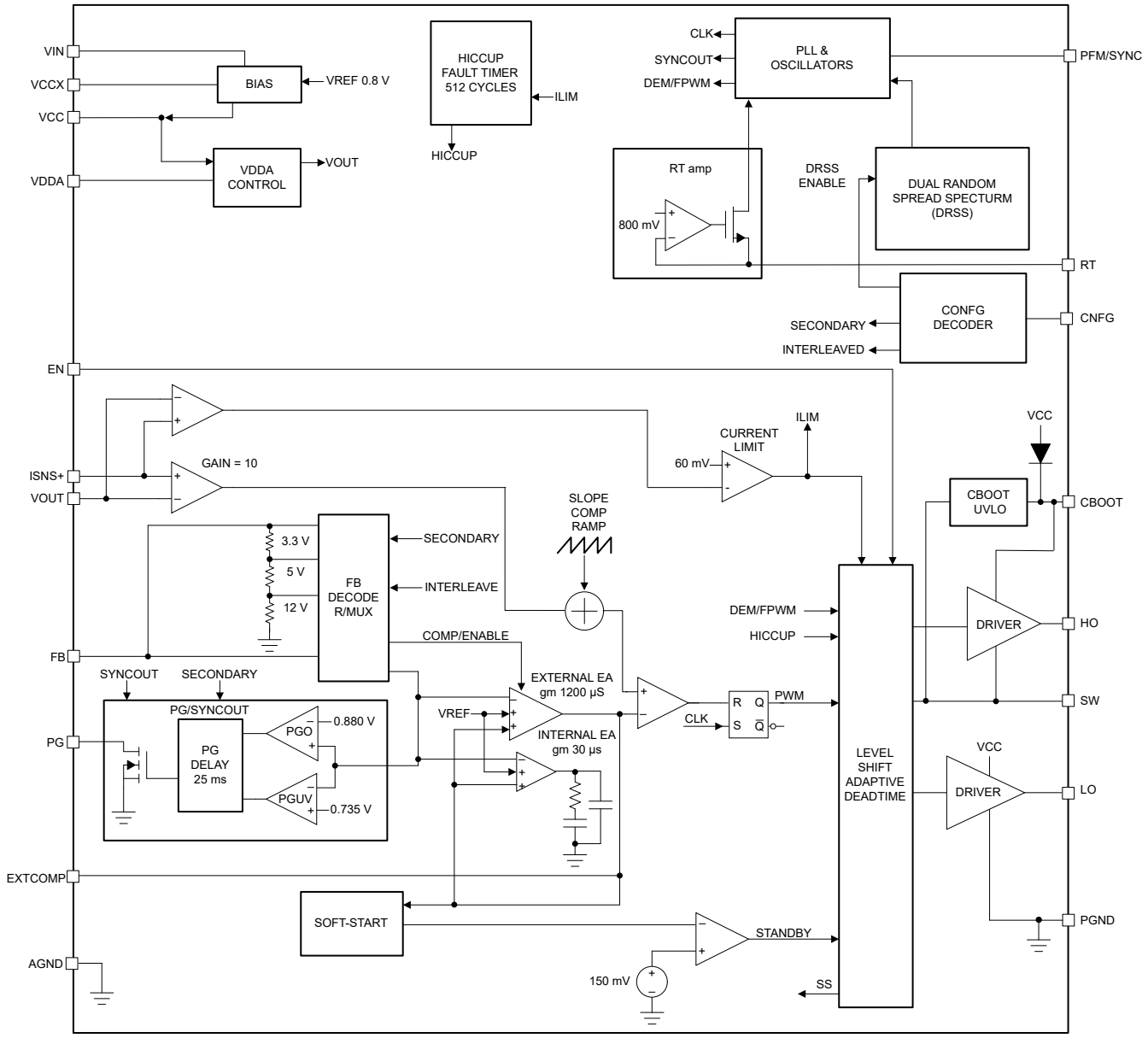
An external bias supply can be connected to VCCX to maximize efficiency in high input voltage applications. A user-selectable diode emulation feature enables discontinuous conduction mode (DCM) operation to further improve efficiency and reduce power dissipation during light-load conditions. Fault protection features include current limiting, thermal shutdown, UVLO, and remote shutdown capability.

The LM25148 incorporates features to simplify the compliance with various EMI standards, for example CISPR 11 and CISPR 32 Class B requirements. DRSS techniques reduce the peak harmonic EMI signature.

The LM25148 is provided in a 24-pin VQFN package with an exposed pad to aid in thermal dissipation.

Copyright © 2021 Texas Instruments Incorporated

## 8.2 Functional Block Diagram





Copyright © 2021 Texas Instruments Incorporated

## 8.3 Feature Description

### 8.3.1 Input Voltage Range ($V_{IN}$)

The LM25148 operational input voltage range is from 3.5 V to 42 V. The device is intended for step-down conversions from 12-V, 24-V, and 48-V supply rails. The application circuit in Figure 9-4 shows all the necessary components to implement an LM25148 based wide-$V_{IN}$ single-output step-down regulator using a single supply. The LM25148 uses an internal LDO to provide a 5-V VCC bias rail for the gate drive and control circuits (assuming the input voltage is higher than 5 V with additional voltage margin necessary for the subregulator dropout specification).

In high input voltage applications, take extra care to ensure that the VIN and SW pins do not exceed their absolute maximum voltage rating of 47 V during line or load transient events. Voltage excursions that exceed the applicable voltage specifications can damage the device.

Care should be taken in applications where there are fast input transients that cause the voltage at VIN to suddenly drop more than 2 V below the VOUT setpoint. The LM25148 has an internal ESD diode from the VOUT to the VIN pins that can conduct under such conditions causing the output to discharge. To prevent damage to the internal ESD diode under the said conditions, TI recommends adding a Schottky diode in series with the VIN pin of the LM25148 to prevent reverse current flow from VOUT to VIN.

### 8.3.2 High-Voltage Bias Supply Regulator (VCC, VCCX, VDDA)

The LM25148 contains an internal high-voltage VCC bias regulator that provides the bias supply for the PWM controller and the gate drivers for the external MOSFETs. The input voltage pin (VIN) can be connected directly to an input voltage source up to 42 V. However, when the input voltage is below the VCC setpoint level, the VCC voltage tracks $V_{IN}$ minus a small voltage drop.

The VCC regulator output current limit is 115 mA (minimum). At power up, the controller sources current into the capacitor connected at the VCC pin. When the VCC voltage exceeds 3.3 V and the EN pin is connected to a voltage greater than 1 V, the soft-start sequence begins. The output remains active unless the VCC voltage falls below the VCC UVLO falling threshold of 3.1 V (typical) or EN is switched to a low state. Connect a ceramic capacitor from VCC to PGND. The recommended range of the VCC capacitor is from 2.2 µF to 10 µF.

An internal 5-V linear regulator generates the VDDA bias supply. Bypass VDDA with a 100-nF or higher ceramic capacitor to achieve a low-noise internal bias rail. Normally, VDDA is 5 V. However, there is one condition where VDDA regulates at 3.3 V. This is in PFM mode with a light or no-load on the output.

Minimize the internal power dissipation of the VCC regulator by connecting VCCX to a 5-V output or to an external 5-V supply. If the VCCX voltage is above 4.3 V, VCCX is internally connected to VCC and the internal VCC regulator is disabled. Tie VCCX to PGND if it is unused. Never connect VCCX to a voltage greater than 6.5 V. If an external supply is connected to VCCX to power the LM25148, $V_{IN}$ must be greater than the external bias voltage during all conditions to avoid damage to the controller.

### 8.3.3 Precision Enable (EN)

The EN pin can be connected to a voltage as high as 42 V. The LM25148 has a precision enable. When the EN voltage is greater than 1 V, controller switching is enabled. If the EN pin is pulled below 0.5 V, the LM25148 is in shutdown with an $I_Q$ of 2.3 µA (typical) current consumption from $V_{IN}$. When the enable voltage is between 0.5 V and 1 V, the LM25148 is in standby mode with the VCC regulator active but the controller is not switching. In standby mode, the non-switching input quiescent current is 124-µA typical. The LM25148 is enabled with a voltage greater than 1.0 V. However, many applications benefit from using a resistor divider $R_{UV1}$ and $R_{UV2}$, as shown in Figure 8-1, to establish a precision UVLO level. TI does not recommend leaving the EN pin floating.

When using precision enable and a VCCX supply, place a series diode with the cathode connected to the LM25148 VCCX pin.

Use Equation 1 and Equation 2 to calculate the UVLO resistors given the required input turn-on and turn-off voltages.

Copyright © 2021 Texas Instruments Incorporated

$$R_{UV1} = \frac{V_{IN(on)} - V_{IN(off)}}{I_{HYS}} \quad (1)$$

$$R_{UV2} = R_{UV1} \cdot \frac{V_{EN}}{V_{IN(on)} - V_{EN}} \quad (2)$$

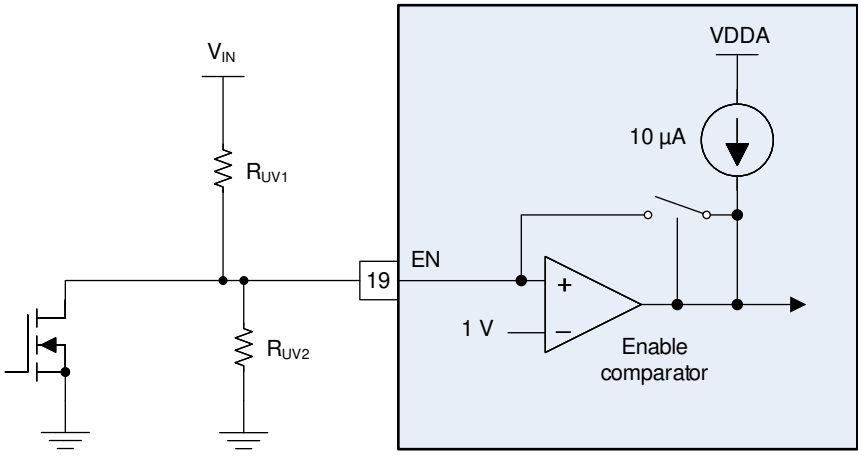



**Figure 8-1. Programmable Input Voltage UVLO Turn-On**

### 8.3.4 Power-Good Monitor (PG)

The LM25148 includes an output voltage monitoring signal for $V_{OUT}$ to simplify sequencing and supervision. The power-good signal is used for start-up sequencing of downstream converters, fault protection, and output monitoring. The power-good output (PG) switches to a high impedance open-drain state when the output voltage is in regulation. The PG switches low when the output voltage drops below the lower power-good threshold (92% typical) or rises above the upper power-good threshold (110% typical). A 25-µs deglitch filter prevents false tripping of the power-good signal during transients. TI recommends a pullup resistor of 100 kΩ (typical) from PG to the relevant logic rail. PG is asserted low during soft start and when the buck regulator is disabled.

When the LM25148 is configured as a primary controller, the PG/SYNC pin becomes a synchronization clock output for the secondary controller. The synchronization signal is 180° out-of-phase with the primary HO driver output.

### 8.3.5 Switching Frequency (RT)

Program the LM25148 oscillator with a resistor from RT to AGND to set an oscillator frequency from 100 kHz and 2.2 MHz. Calculate the RT resistance for a given switching frequency using Equation 3.

$$R_T(k\Omega) = \frac{\frac{10^6}{F_{SW}(kHz)} - 53}{45} \quad (3)$$

Under low $V_{IN}$ conditions when the on time of the high-side MOSFET exceeds the programmed oscillator period, the LM25148 extends the switching period until the PWM latch is reset by the current sense ramp exceeding the controller compensation voltage.

The approximate input voltage level at which this occurs is given by Equation 4.

$$V_{IN(min)} = V_{OUT} \cdot \frac{t_{SW}}{t_{SW} - t_{OFF(min)}} \quad (4)$$


Copyright © 2021 Texas Instruments Incorporated

where

- $t_{SW}$ is the switching period.
- $t_{OFF(min)}$ is the minimum off time of 90 ns.

### 8.3.6 Dual Random Spread Spectrum (DRSS)

The LM25148 provides a digital spread spectrum, which reduces the EMI of the power supply over a wide frequency range. DRSS combines a low-frequency triangular modulation profile with a high frequency cycle-by-cycle random modulation profile. The low-frequency triangular modulation improves performance in lower radio-frequency bands, while the high-frequency random modulation improves performance in higher radio frequency bands.

Spread spectrum works by converting a narrowband signal into a wideband signal that spreads the energy over multiple frequencies. Since industry standards require different EMI receiver resolution bandwidth (RBW) settings for different frequency bands, the RBW has an impact on the spread spectrum performance. For example, the CISPR 25 spectrum analyzer RBW in the frequency band from 150 kHz to 30 MHz is 9 kHz. For frequencies greater than 30 MHz, the RBW is 120 kHz. DRSS is able to simultaneously improve the EMI performance in the low and high RBWs using its low-frequency triangular modulation profile and at high frequency cycle-by-cycle random modulation, respectively. DRSS can reduce conducted emissions up to 15 dBµV in the low-frequency band (150 kHz to 30 MHz) and 5 dBµV in the high-frequency band (30 MHz to 108 MHz).

To enable DRSS, connect either a 41.2-kΩ or 71.5-kΩ resistor from CNFG to AGND. DRSS is disabled when an external clock is applied to the PFM/SYNC pin.

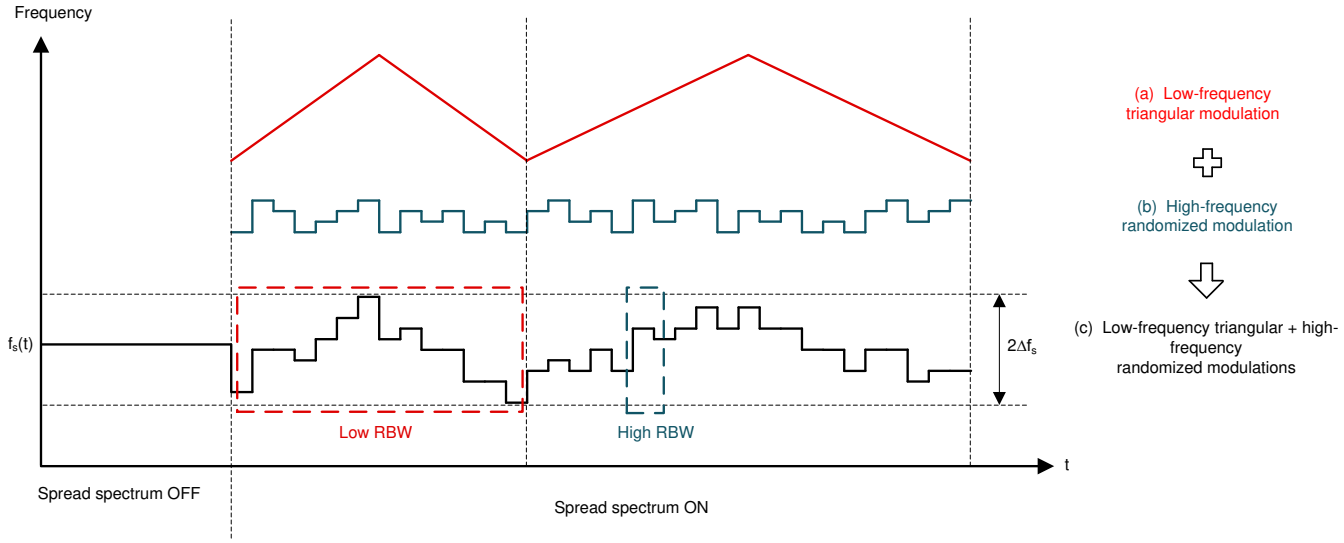



**Figure 8-2. Dual Random Spread Spectrum Implementation**

### 8.3.7 Soft Start

The LM25148 has an internal 3-ms soft-start timer (typical). The soft-start feature allows the regulator to gradually reach the steady-state operating point, thus reducing start-up stresses and surges.

### 8.3.8 Output Voltage Setpoint (FB)

The LM25148 output can be independently configured for one of three fixed output voltages without external feedback resistors, or adjusted to a desired voltage using an external resistor divider. Set the output to 3.3 V by connecting FB directly to VDDA. Alternatively, set the output to either 5 V or 12 V by installing a 24.9-kΩ or 49.9-kΩ resistor between FB and VDDA, respectively. See Table 8-1.

Copyright © 2021 Texas Instruments Incorporated

**Table 8-1. Feedback Configuration Resistors**

| PULLUP RESISTOR TO VDDA | $V_{OUT}$ SETPOINT |
|---|---|
| 0 Ω | 3.3 V |
| 24.9 kΩ | 5 V |
| 49.9 kΩ | 12 V |
| Not installed | External FB divider setting |

The configuration settings are latched and cannot be changed until the LM25148 is powered down (with the VCC voltage decreasing below its falling UVLO threshold) and then powered up again (VCC rises above 3.4-V typical). Alternatively, set the output voltage with an external resistor divider from the output to AGND. The output voltage adjustment range is between 0.8 V and 36 V. The regulation voltage at FB is 0.8 V ($V_{REF}$). Use Equation 5 to calculate the upper and lower feedback resistors, designated as $R_{FB1}$ and $R_{FB2}$, respectively.

$$R_{FB1} = \left( \frac{V_{OUT}}{V_{REF}} - 1 \right) \cdot R_{FB2} \tag{5}$$

The recommended starting value for $R_{FB2}$ is between 10 kΩ and 20 kΩ.

If low-$I_Q$ operation is required, take care when selecting the external feedback resistors. The current consumption of the external divider adds to the LM25148 sleep current (9.5 µA typical). The divider current reflected to $V_{IN}$ is scaled by the ratio of $V_{OUT}$ / $V_{IN}$.

### 8.3.9 Minimum Controllable On Time

There are two limitations to the minimum output voltage adjustment range: the LM25148 voltage reference of 0.8 V and the minimum controllable switch-node pulse width, $t_{ON(min)}$.

$t_{ON(min)}$ effectively limits the voltage step-down conversion ratio $V_{OUT}$ / $V_{IN}$ at a given switching frequency. For fixed-frequency PWM operation, the voltage conversion ratio must satisfy Equation 6.

$$\frac{V_{OUT}}{V_{IN}} > t_{ON(min)} \cdot F_{SW} \tag{6}$$

where

- $t_{ON(min)}$ is 50 ns (typical).
- $F_{SW}$ is the switching frequency.

If the desired voltage conversion ratio does not meet the above condition, the LM25148 transitions from fixed switching frequency operation to a pulse-skipping mode to maintain output voltage regulation. For example, if the desired output voltage is 5 V with an input voltage of 24 V and switching frequency of 2.1 MHz, use Equation 7 to check the conversion ratio.

$$\frac{5\,V}{24\,V} > 50\,ns \cdot 2.1\,MHz$$

$$0.208 > 0.105 \tag{7}$$

For wide $V_{IN}$ applications and low output voltages, an alternative is to reduce the LM25148 switching frequency to meet the requirement of Equation 6.

### 8.3.10 Error Amplifier and PWM Comparator (FB, EXTCOMP)

The LM25148 has a high-gain transconductance amplifier that generates an error current proportional to the difference between the feedback voltage and an internal precision reference (0.8 V). The control loop compensation is configured two ways. The first is using the internal compensation amplifier, which has a


Copyright © 2021 Texas Instruments Incorporated

transconductance of 30 µS. Internal compensation is configured by connecting the EXTCOMP pin through a 100-kΩ resistance to VDDA. If a 100-kΩ resistor is not detected, the LM25148 defaults to the external loop compensation network. The transconductance of the amplifier for external compensation is 1200 µS. This is latched and cannot be reconfigured once programmed unless power to the device is recycled. Use an external compensation network if higher performance is required to meet a stringent transient response specification. To reconfigure the compensation (internal or external), remove power and allow VCC to drop below its $VCC_{UVLO}$ threshold, which is 3.3 V (typical).

A type-II compensation network is generally recommended for peak current-mode control.

### 8.3.11 Slope Compensation

The LM25148 provides internal slope compensation for stable operation with peak current-mode control and a duty cycle greater than 50%. Calculate the buck inductance to provide a slope compensation contribution equal to one times the inductor downslope using Equation 8.

$$L_{O\text{-}IDEAL}(\mu H) = \frac{V_{OUT}(V) \cdot R_S(m\Omega)}{24 \cdot F_{SW}(MHz)} \quad (8)$$

- A lower inductance value generally increases the peak-to-peak inductor current, which minimizes size and cost, and improves transient response at the cost of reduced light-load efficiency due to higher cores losses and peak currents.
- A higher inductance value generally decreases the peak-to-peak inductor current, reducing switch peak and RMS currents at the cost of requiring larger output capacitors to meet load-transient specifications.

### 8.3.12 Inductor Current Sense (ISNS+, VOUT)

There are two methods to sense the inductor current of the buck power stage. The first uses a current sense resistor (also known as a shunt) in series with the inductor, and the second avails of the DC resistance of the inductor (DCR current sensing).

#### *8.3.12.1 Shunt Current Sensing*

Figure 8-3 illustrates inductor current sensing using a shunt resistor. This configuration continuously monitors the inductor current to provide accurate overcurrent protection across the operating temperature range. For optimal current sense accuracy and overcurrent protection, use a *low inductance* ±1% tolerance shunt resistor between the inductor and the output, with a Kelvin connection to the LM25148 current sense amplifier.

If the peak voltage signal sensed from ISNS+ to VOUT exceeds the current limit threshold of 60 mV, the current limit comparator immediately terminates the HO output for cycle-by-cycle current limiting. Calculate the shunt resistance using Equation 9.

$$R_S = \frac{V_{CS\text{-}TH}}{I_{OUT(CL)} + \frac{\Delta I_L}{2}} \quad (9)$$

where

- $V_{CS\text{-}TH}$ is current sense threshold of 60 mV.
- $I_{OUT(CL)}$ is the overcurrent setpoint that is set higher than the maximum load current to avoid tripping the overcurrent comparator during load transients.
- $\Delta I_L$ is the peak-to-peak inductor ripple current.

Copyright © 2021 Texas Instruments Incorporated

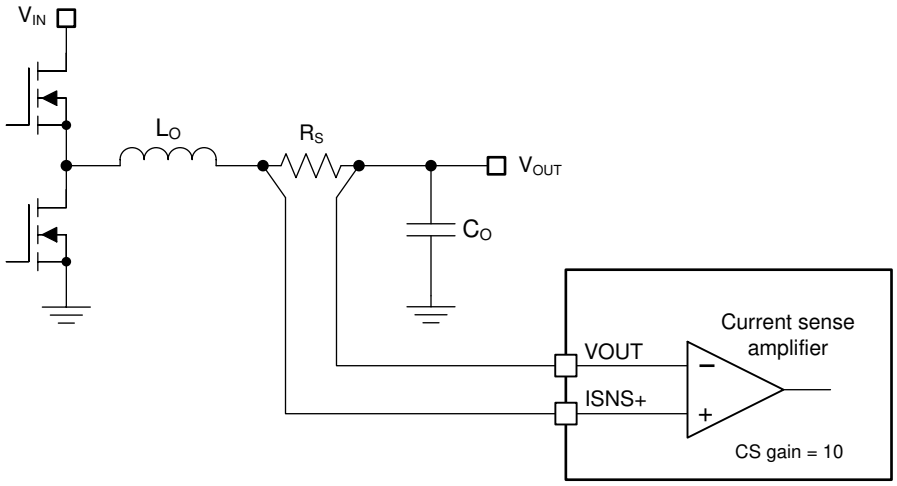



**Figure 8-3. Shunt Current Sensing Implementation**

The soft-start voltage is clamped 150 mV above FB during an overcurrent condition. Sixteen overcurrent events must occur before the SS clamp is enabled. This ensures that SS can be pulled low during brief overcurrent events, preventing output voltage overshoot during recovery.

### *8.3.12.2 Inductor DCR Current Sensing*

For high-power applications that do not require accurate current-limit protection, inductor DCR current sensing is preferable. This technique provides lossless and continuous monitoring of the inductor current using an RC sense network in parallel with the inductor. Select an inductor with a low DCR tolerance to achieve a typical current limit accuracy within the range of 10% to 15% at room temperature. Components $R_{CS}$ and $C_{CS}$ in Figure 8-4 create a low-pass filter across the inductor DCR.

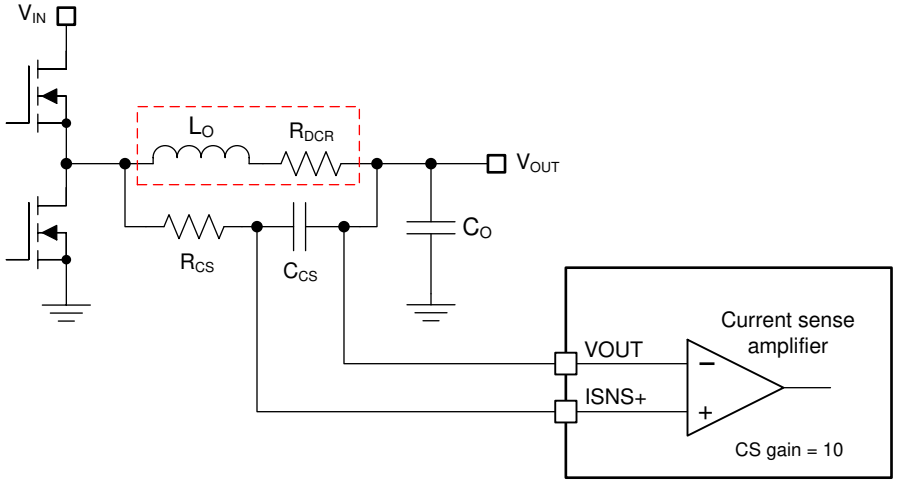



**Figure 8-4. Inductor DCR Current Sensing Implementation**

The voltage drop across the sense capacitor in the s-domain is given by Equation 10. When the $R_{CS}C_{CS}$ time constant is equal to $L_O/R_{DCR}$, the voltage developed across the sense capacitor, $C_{CS}$, is a replica of the inductor DCR voltage and accurate current sensing is achieved. If the $R_{CS}C_{CS}$ time constant is not equal to the $L_O/R_{DCR}$ time constant, there is a sensing error as follows:

- $R_{CS}C_{CS} > L_O/R_{DCR}$ → the DC level is correct, but the AC amplitude is attenuated.
- $R_{CS}C_{CS} < L_O/R_{DCR}$ → the DC level is correct, but the AC amplitude is amplified.


Copyright © 2021 Texas Instruments Incorporated

$$V_{CS}(s) = \frac{1 + s \cdot \frac{L_O}{R_{DCR}}}{1 + s \cdot R_{CS} \cdot C_{CS}} \cdot R_{DCR} \cdot \left( I_{OUT(CL)} + \frac{\Delta I_L}{2} \right) \quad (10)$$

Choose the $C_{CS}$ capacitance greater than or equal to 0.1 µF to maintain a low-impedance sensing network, thus reducing the susceptibility of noise pickup from the switch node. Carefully observe Section 11.1 to make sure that noise and DC errors do not corrupt the current sense signals applied between the ISNS+ and VOUT pins.

### 8.3.13 Hiccup Mode Current Limiting

The LM25148 includes an internal hiccup-mode protection function. After an overload is detected, 512 cycles of cycle-by-cycle current limiting occurs. The 512-cycle counter is reset if four consecutive switching cycles occur without exceeding the current limit threshold. Once the 512-cycle counter has expired, the internal soft start is pulled low, the HO and LO driver outputs are disabled, and the 16384 counter is enabled. After the counter reaches 16384, the internal soft start is enabled and the output restarts. The hiccup-mode current limit is disabled during soft start until the FB voltage exceeds 0.4 V.

### 8.3.14 High-Side and Low-Side Gate Drivers (HO, LO)

The LM25148 contains gate drivers and an associated high-side level shifter to drive the external N-channel power MOSFETs. The high-side gate driver works in conjunction with an internal bootstrap diode $D_{BOOT}$ and bootstrap capacitor $C_{BOOT}$. During the conduction interval of the low-side MOSFET, the SW voltage is approximately 0 V and CBOOT charges from VCC through the internal $D_{BOOT}$. TI recommends a 0.1-µF ceramic capacitor connected with short traces between the CBOOT and SW pins.

The HO and LO outputs are controlled with an adaptive dead-time methodology so that both outputs (HO and LO) are never on at the same time, preventing cross conduction. Before the LO driver output is allowed to turn on, the adaptive dead-time logic first disables HO and waits for the HO-SW voltage to drop below 2 V typical. LO is allowed to turn on after a small delay (HO fall to LO rising delay). Similarly, the HO turn-on is delayed until the LO voltage has dropped below 2 V. This technique ensures adequate dead-time for any size N-channel power MOSFET implementations, including parallel MOSFET configurations.

Caution is advised when adding series gate resistors, as this can impact the effective dead-time. The selected high-side MOSFET determines the appropriate bootstrap capacitance value $C_{BOOT}$ in accordance with Equation 11.

$$C_{BOOT} = \frac{Q_G}{\Delta V_{CBOOT}} \quad (11)$$

where

- $Q_G$ is the total gate charge of the high-side MOSFET at the applicable gate drive voltage.
- $\Delta V_{CBOOT}$ is the voltage variation of the high-side MOSFET driver after turn-on.

To determine $C_{BOOT}$, choose $\Delta V_{CBOOT}$ such that the available gate drive voltage is not significantly impacted. An acceptable range of $\Delta V_{CBOOT}$ is 100 mV to 300 mV. The bootstrap capacitor must be a low-ESR ceramic capacitor, typically 0.1 µF. Use high-side and low-side MOSFETs with logic-level gate threshold voltages.

### 8.3.15 Output Configurations (CNFG)

The LM25148 can be configured as a primary controller (interleaved mode) or as a secondary controller for paralleling the outputs for high-current applications with a resistor $R_{CNFG}$. This resistor also configures if spread spectrum is enabled or disabled. See Table 8-2. Once the VCC voltage is above 3.3 V (typical), the CNFG pin voltage is monitored and latched. To change the configuration mode, the LM25148 must be powered down, and VCC must drop below 3.3 V. Figure 8-5 shows the configuration timing diagram.

When the LM25148 is configured as a primary controller with spread spectrum enabled ($R_{CNFG}$ of 41.2 kΩ or 71.5 kΩ), the LM25148 cannot be synchronized to an external clock.

Copyright © 2021 Texas Instruments Incorporated

**Table 8-2. Configuration Modes**

| $R_{CNFG}$ | PRIMARY/ SECONDARY | SPREAD SPECTRUM | DUAL PHASE |
|---|---|---|---|
| 29.9 kΩ | Primary | OFF | Disabled |
| 41.2 kΩ | Primary | ON | Disabled |
| 54.9 kΩ | Primary | OFF | Enabled |
| 71.5 kΩ | Primary | ON | Enabled |
| 90.9 kΩ | Secondary | N/A | Enabled |

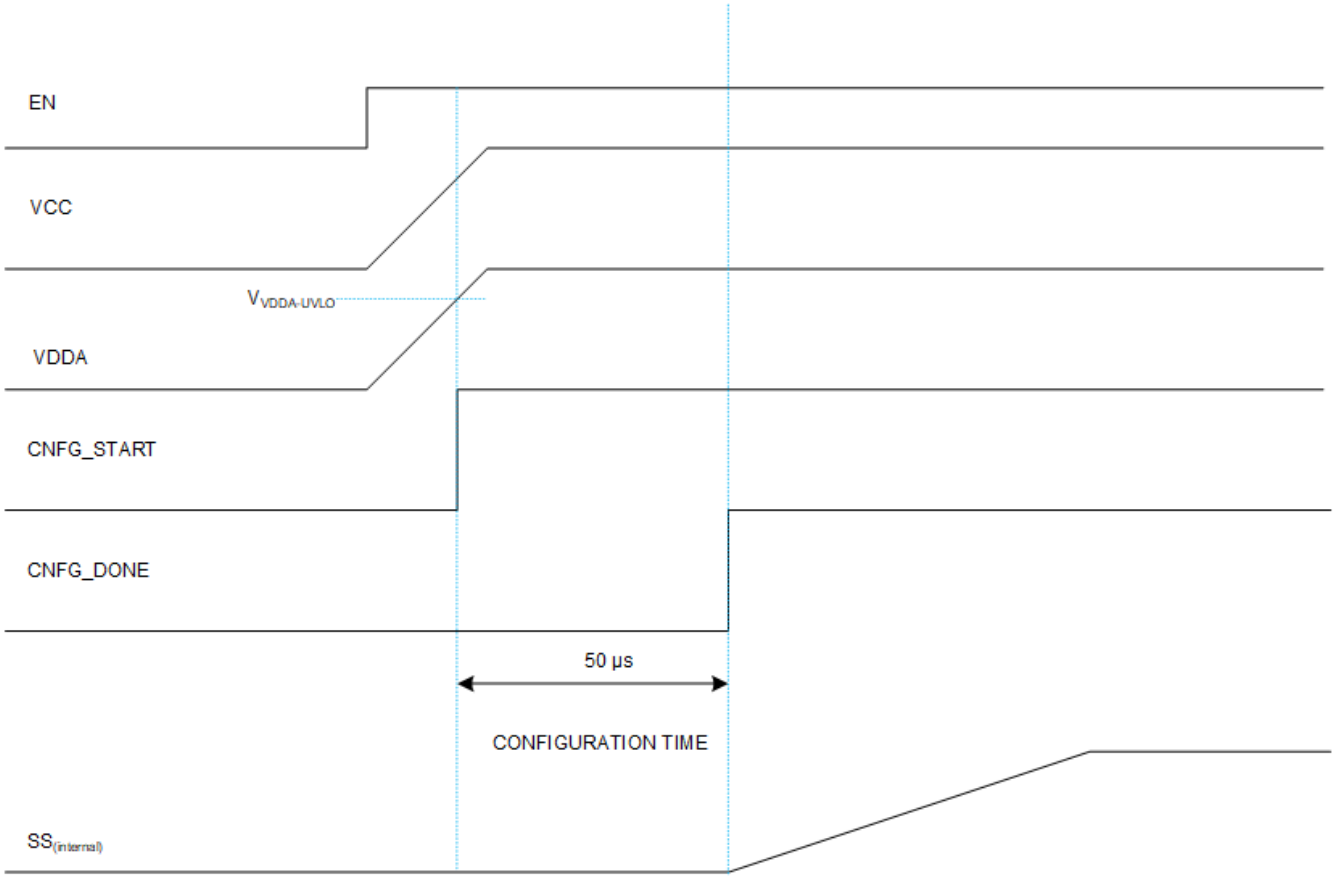



**Figure 8-5. Configuration Timing**

### 8.3.16 Single-Output Dual-Phase Operation

To configure for dual-phase operation, two LM25148 controllers are required. The LM25148 can only be configured in a single or dual-phase configuration where both outputs are tied together. Additional phases cannot be added. Refer to Figure 8-6. Configure the first controller (CNTRL1) as a primary controller and the second controller (CNTRL2) as a secondary. To configure CNTRL1 as a primary controller, install a 54-kΩ or a 71.5-kΩ resistor from CNFG to AGND. To configure the CNTRL2 as a secondary controller, install a 90.9-kΩ resistor from CNFG to AGND. This disables the error amplifier of CNTRL2, placing it into a high-impedance state. Connect the EXTCOMP pins of the primary and secondary controllers together. The internal compensation amplifier feature is not supported when the controller is in dual-phase mode.

In dual-phase mode, the PG pin of the primary controller becomes a SYNCOUT. Refer to *Electrical Characteristics* for voltage levels. Connect PG of the primary to PFM/SYNC (SYNCIN) of the secondary controller. The PG/SYNCOUT signal of the primary controller is 180° out-of-phase and facilitates interleaved operation. RT is not used for the oscillator when the LM25148 is in Secondary Controller mode, but instead is used for slope compensation. Therefore, select the RT resistance to be the same as that of the primary controller. The oscillator is derived from the primary controller. When in primary/secondary mode, enable both


Copyright © 2021 Texas Instruments Incorporated

controllers simultaneously for start-up. After the regulator has started, pull the secondary EN pin low (< 0.8 V) for phase shedding if needed at light load to increase the efficiency.

Configure PFM mode by connecting the PFM/SYNC of the primary to VDDA and the FB of the secondary to VDDA as shown in Figure 8-6. Configure FPWM mode by connecting PFM/SYNC of the primary and FB of the secondary both to AGND. An external synchronization signal can be applied to the primary PFM/SYNC (SYNCIN), and the secondary FB must be configured for FPWM. If an external SYNCIN signal is applied after start-up while in primary/secondary mode, there is a two-clock cycle delay before the LM25148 locks on to the external synchronization signal.

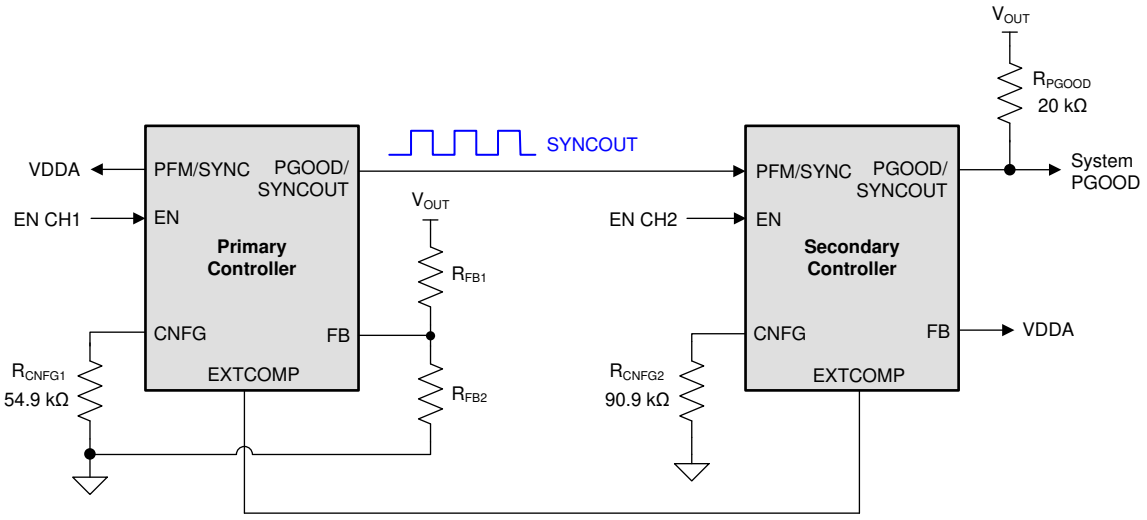



**Figure 8-6. Schematic Configured for Single-Output Dual-Phase Operation**

In PFM mode, the controller enters pulse skipping to reduce the $I_Q$ current and improve the light-load efficiency. When this occurs, the primary controller disables its synchronization clock output, so phase shedding is not supported. In PFM mode connect the two enable pins together. Phase shedding is supported in FPWM only. In FPWM, enable or disable the secondary controller as needed to support higher load current or better light-load efficiency, respectively. When the secondary controller is disabled and then re-enabled, its internal soft start is pulled low and the LM25148 goes through a normal soft-start turn-on.

When the LM25148 is configured for a single-output dual-phase operation using the internal 3.3-V feedback resistor divider, the internal bootstrap UV circuit can source current out of the SW pin, charging up the output capacitors approximately to 3.6 V. If this behavior is undesirable, you can add a 100-kΩ resistor from VOUT to GND to bleed off the charge on the output capacitors.

For more information, see the *Benefits of a Multiphase Buck Converter Technical Brief* and *Multiphase Buck Design From Start to Finish Application Report*.

Copyright © 2021 Texas Instruments Incorporated

## 8.4 Device Functional Modes

### 8.4.1 Sleep Mode

The LM25148 operates with peak current-mode control such that the compensation voltage is proportional to the peak inductor current. During no-load or light-load conditions, the output capacitor discharges very slowly. As a result, the compensation voltage does not demand the driver output pulses on a cycle-by-cycle basis. When the LM25148 controller detects 16 missed switching cycles, it enters sleep mode and switches to a low $I_Q$ state to reduce the current drawn from the input. For the LM25148 to go into sleep mode, the controller must be programmed for diode emulation (tie PFM/SYNC to VDDA).

The typical controller $I_Q$ in sleep mode is 9.5 µA with a 3.3-V output.

### 8.4.2 Pulse Frequency Modulation and Synchronization (PFM/SYNC)

A synchronous buck regulator implemented with a low-side synchronous MOSFET rather than a diode has the capability to sink negative current from the output during conditions of, light-load, output overvoltage, and pre-bias start-up conditions. The LM25148 provides a diode emulation feature that can be enabled to prevent reverse (drain-to-source) current flow in the low-side MOSFET. When configured for Diode Emulation mode, the low-side MOSFET is switched off when reverse current flow is detected by sensing the SW voltage using a zero-cross comparator. The benefit of this configuration is lower power loss during light-load conditions. The disadvantage of diode emulation mode is slower light-load transient response.

The PFM/SYNC pin configures diode emulation. To enable diode emulation and thus achieve low-$I_Q$ current at light loads, connect PFM/SYNC to VDDA. If FPWM with continuous conduction mode (CCM) operation is desired, tie PFM/SYNC to AGND. Note that diode emulation is automatically engaged to prevent reverse current flow during a prebias start-up. A gradual change from DCM to CCM operation provides monotonic start-up performance.

To synchronize the LM25148 to an external source, apply a logic-level clock to the PFM/SYNC pin. The LM25148 can be synchronized to ±20% of the programmed frequency up to a maximum of 2.5 MHz. If there is an RT resistor and a synchronization signal, the LM25148 ignores the RT resistor and synchronizes to the external clock. Under low $V_{IN}$ conditions when the minimum off time is reached, the synchronization signal is ignored, allowing the switching frequency to reduce to maintain output voltage regulation.

### 8.4.3 Thermal Shutdown

The LM25148 includes an internal junction temperature monitor. If the temperature exceeds 175°C (typical), thermal shutdown occurs. When entering thermal shutdown, the device:

1. Turns off the high-side and low-side MOSFETs.
2. PG/SYNCOUT switches low.
3. Turns off the VCC regulator.
4. Initiates a soft-start sequence when the die temperature decreases by the thermal shutdown hysteresis of 15°C (typical).

This is a non-latching protection, and, as such, the device cycles into and out of thermal shutdown if the fault persists.


Copyright © 2021 Texas Instruments Incorporated

# 9 Application and Implementation

**Note**

Information in the following applications sections is not part of the TI component specification, and TI does not warrant its accuracy or completeness. TI's customers are responsible for determining suitability of components for their purposes, as well as validating and testing their design implementation to confirm system functionality.

## 9.1 Application Information

### 9.1.1 Power Train Components

A comprehensive understanding of the buck regulator power train components is critical to successfully completing a synchronous buck regulator design. The following sections discuss the output inductor, input and output capacitors, power MOSFETs, and EMI input filter.

#### *9.1.1.1 Buck Inductor*

For most applications, choose a buck inductance such that the inductor ripple current, $\Delta I_L$, is between 30% to 50% of the maximum DC output current at nominal input voltage. Choose the inductance using Equation 12 based on a peak inductor current given by Equation 13.

$$L_O = \frac{V_{OUT}}{\Delta I_L \cdot F_{SW}} \cdot \left(1 - \frac{V_{OUT}}{V_{IN}}\right) \tag{12}$$

$$I_{L(peak)} = I_{OUT} + \frac{\Delta I_L}{2} \tag{13}$$

Check the inductor data sheet to make sure that the saturation current of the inductor is well above the peak inductor current of a particular design. Ferrite designs have very low core loss and are preferred at high switching frequencies, so design goals can then concentrate on copper loss and preventing saturation. Low inductor core loss is evidenced by reduced no-load input current and higher light-load efficiency. However, ferrite core materials exhibit a hard saturation characteristic and the inductance collapses abruptly when the saturation current is exceeded. This results in an abrupt increase in inductor ripple current and higher output voltage ripple, not to mention reduced efficiency and compromised reliability. Note that the saturation current of an inductor generally decreases as its core temperature increases. Of course, accurate overcurrent protection is key to avoiding inductor saturation.

#### *9.1.1.2 Output Capacitors*

Ordinarily, the output capacitor energy storage of the regulator combined with the control loop response are prescribed to maintain the integrity of the output voltage within the dynamic (transient) tolerance specifications. The usual boundaries restricting the output capacitor in power management applications are driven by finite available PCB area, component footprint and profile, and cost. The capacitor parasitics – equivalent series resistance (ESR) and equivalent series inductance (ESL) – take greater precedence in shaping the load transient response of the regulator as the load step amplitude and slew rate increase.

The output capacitor, $C_{OUT}$, filters the inductor ripple current and provides a reservoir of charge for step-load transient events. Typically, ceramic capacitors provide extremely low ESR to reduce the output voltage ripple and noise spikes, while tantalum and electrolytic capacitors provide a large bulk capacitance in a relatively compact footprint for transient loading events.

Based on the static specification of peak-to-peak output voltage ripple denoted by $\Delta V_{OUT}$, choose an output capacitance that is larger than that given by Equation 14.

Copyright © 2021 Texas Instruments Incorporated

$$C_{OUT} \geq \frac{\Delta I_L}{8 \cdot F_{SW} \sqrt{\Delta V_{OUT}^2 - \left(R_{ESR} \cdot \Delta I_L\right)^2}} \quad (14)$$

Figure 9-1 conceptually illustrates the relevant current waveforms during both load step-up and step-down transitions. As shown, the large-signal slew rate of the inductor current is limited as the inductor current ramps to match the new load-current level following a load transient. This slew-rate limiting exacerbates the deficit of charge in the output capacitor, which must be replenished as fast as possible during and after the load step-up transient. Similarly, during and after a load step-down transient, the slew rate limiting of the inductor current adds to the surplus of charge in the output capacitor that must be depleted as quickly as possible.

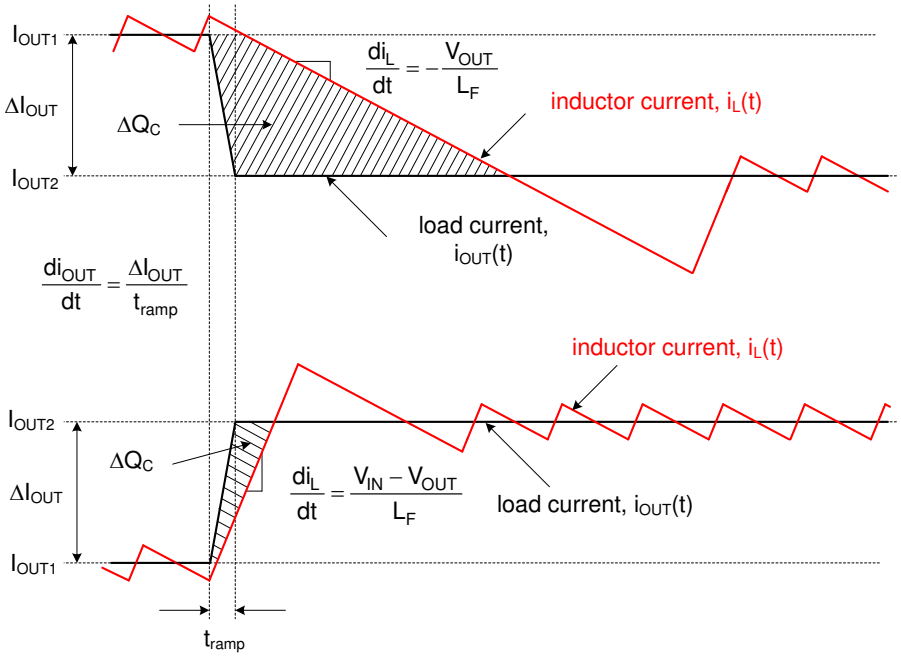



**Figure 9-1. Load Transient Response Representation Showing $C_{OUT}$ Charge Surplus or Deficit**

In a typical regulator application of 12-V input to low output voltage (for example, 3.3 V), the load-off transient represents the worst case in terms of output voltage transient deviation. In that conversion ratio application, the steady-state duty cycle is approximately 28% and the large-signal inductor current slew rate when the duty cycle collapses to zero is approximately $-V_{OUT}$ / L. Compared to a load-on transient, the inductor current takes much longer to transition to the required level. The surplus of charge in the output capacitor causes the output voltage to significantly overshoot. In fact, to deplete this excess charge from the output capacitor as quickly as possible, the inductor current must ramp below its nominal level following the load step. In this scenario, a large output capacitance can be advantageously employed to absorb the excess charge and minimize the voltage overshoot.

To meet the dynamic specification of output voltage overshoot during such a load-off transient (denoted as $\Delta V_{OVERSHOOT}$ with step reduction in output current given by $\Delta I_{OUT}$), the output capacitance should be larger than:

$$C_{OUT} \geq \frac{L_O \cdot \Delta I_{OUT}^2}{\left(V_{OUT} + \Delta V_{OVERSHOOT}\right)^2 - V_{OUT}^2} \quad (15)$$

The ESR of a capacitor is provided in the manufacturer's data sheet either explicitly as a specification or implicitly in the impedance versus frequency curve. Depending on type, size, and construction, electrolytic capacitors have significant ESR, 5 mΩ and above, and relatively large ESL, 5 nH to 20 nH. PCB traces contribute some parasitic resistance and inductance as well. Ceramic output capacitors, on the other hand,


Copyright © 2021 Texas Instruments Incorporated

have low-ESR and ESL contributions at the switching frequency, and the capacitive impedance component dominates. However, depending on package and voltage rating of the ceramic capacitor, the effective capacitance can drop quite significantly with applied DC voltage and operating temperature.

Ignoring the ESR term in Equation 14 gives a quick estimation of the minimum ceramic capacitance necessary to meet the output ripple specification. Two to four 47-µF, 10-V, X7R capacitors in 1206 or 1210 footprint is a common choice for a 5-V output. Use Equation 15 to determine if additional capacitance is necessary to meet the load-off transient overshoot specification.

A composite implementation of ceramic and electrolytic capacitors highlights the rationale for paralleling capacitors of dissimilar chemistries yet complementary performance. The frequency response of each capacitor is accretive in that each capacitor provides desirable performance over a certain portion of the frequency range. While the ceramic provides excellent mid- and high-frequency decoupling characteristics with its low ESR and ESL to minimize the switching frequency output ripple, the electrolytic device with its large bulk capacitance provides low-frequency energy storage to cope with load transient demands.

#### *9.1.1.3 Input Capacitors*

Input capacitors are necessary to limit the input ripple voltage to the buck power stage due to switching-frequency AC currents. TI recommends using X7S or X7R dielectric ceramic capacitors to provide low impedance and high RMS current rating over a wide temperature range. To minimize the parasitic inductance in the switching loop, position the input capacitors as close as possible to the drain of the high-side MOSFET and the source of the low-side MOSFET. The input capacitor RMS current for a single-channel buck regulator is given by Equation 16.

$$I_{CIN,rms} = \sqrt{D \cdot \left( {I_{OUT}}^2 \cdot (1-D) + \frac{\Delta I_L^2}{12} \right)} \tag{16}$$

The highest input capacitor RMS current occurs at D = 0.5, at which point, the RMS current rating of the input capacitors should be greater than half the output current.

Ideally, the DC component of input current is provided by the input voltage source and the AC component by the input filter capacitors. Neglecting inductor ripple current, the input capacitors source current of amplitude ($I_{OUT}$ − $I_{IN}$) during the D interval and sinks $I_{IN}$ during the 1−D interval. Thus, the input capacitors conduct a square-wave current of peak-to-peak amplitude equal to the output current. It follows that the resultant capacitive component of AC ripple voltage is a triangular waveform. Together with the ESR-related ripple component, the peak-to-peak ripple voltage amplitude is given by Equation 17.

$$\Delta V_{IN} = \frac{I_{OUT} \cdot D \cdot (1-D)}{F_{SW} \cdot C_{IN}} + I_{OUT} \cdot R_{ESR} \tag{17}$$

The input capacitance required for a particular load current, based on an input voltage ripple specification of $\Delta V_{IN}$, is given by Equation 18.

$$C_{IN} \geq \frac{D \cdot (1-D) \cdot I_{OUT}}{F_{SW} \cdot (\Delta V_{IN} - R_{ESR} \cdot I_{OUT})} \tag{18}$$

Low-ESR ceramic capacitors can be placed in parallel with higher valued bulk capacitance to provide optimized input filtering for the regulator and damping to mitigate the effects of input parasitic inductance resonating with high-Q ceramics. One bulk capacitor of sufficiently high current rating and four 10-µF 50-V X7R ceramic decoupling capacitors are usually sufficient for 12-V battery automotive applications. Select the input bulk capacitor based on its ripple current rating and operating temperature range.

Of course, a two-channel buck regulator with 180° out-of-phase interleaved switching provides input ripple current cancellation and reduced input capacitor current stress. The above equations represent valid calculations when one output is disabled and the other output is fully loaded.

Copyright © 2021 Texas Instruments Incorporated

#### 9.1.1.4 Power MOSFETs

The choice of power MOSFETs has significant impact on DC/DC regulator performance. A MOSFET with low on-state resistance, $R_{DS(on)}$, reduces conduction loss, whereas low parasitic capacitances enable faster transition times and reduced switching loss. Normally, the lower the $R_{DS(on)}$ of a MOSFET, the higher the gate charge and output charge ($Q_G$ and $Q_{OSS}$, respectively), and vice versa. As a result, the product of $R_{DS(on)}$ and $Q_G$ is commonly specified as a MOSFET figure-of-merit. Low thermal resistance of a given package ensures that the MOSFET power dissipation does not result in excessive MOSFET die temperature.

The main parameters affecting power MOSFET selection in a LM25148 application are as follows:

- $R_{DS(on)}$ at $V_{GS}$ = 5 V
- Drain-source voltage rating, $BV_{DSS}$, typically 40 V or 60 V, depending on the maximum input voltage
- Gate charge parameters at $V_{GS}$ = 5 V
- Output charge, $Q_{OSS}$, at the relevant input voltage
- Body diode reverse recovery charge, $Q_{RR}$
- Gate threshold voltage, $V_{GS(th)}$, derived from the Miller plateau evident in the $Q_G$ versus $V_{GS}$ plot in the MOSFET data sheet. With a Miller plateau voltage typically in the range of 2 V to 3 V, the 5-V gate drive amplitude of the LM25148 provides an adequately enhanced MOSFET when on and a margin against Cdv/dt shoot-through when off.

The MOSFET-related power losses for one channel are summarized by the equations presented in Table 9-1, where suffixes one and two represent high-side and low-side MOSFET parameters, respectively. While the influence of inductor ripple current is considered, second-order loss modes, such as those related to parasitic inductances and SW node ringing, are not included. Consult the LM25148 *Quickstart Calculator* to assist with power loss calculations.

**Table 9-1. MOSFET Power Losses**

| POWER LOSS MODE | HIGH-SIDE MOSFET | LOW-SIDE MOSFET |
|---|---|---|
| MOSFET conduction(2) (3) | $P_{cond1} = D \cdot \left( {I_{OUT}}^2 + \frac{\Delta I_L^2}{12} \right) \cdot R_{DS(on)1}$ | $P_{cond2} = D' \cdot \left( {I_{OUT}}^2 + \frac{\Delta I_L^2}{12} \right) \cdot R_{DS(on)2}$ |
| MOSFET switching | $P_{sw1} = \frac{V_{IN} \cdot F_{SW}}{2} \left[ \left( I_{OUT} - \frac{\Delta I_L}{2} \right) \cdot t_R + \left( I_{OUT} + \frac{\Delta I_L}{2} \right) \cdot t_F \right]$ | Negligible |
| MOSFET gate drive(1) | $P_{Gate1} = V_{CC} \cdot F_{SW} \cdot Q_{G1}$ | $P_{Gate2} = V_{CC} \cdot F_{SW} \cdot Q_{G2}$ |
| MOSFET output charge(4) | $P_{Coss} = F_{SW} \cdot (V_{IN} \cdot Q_{oss2} + E_{oss1} - E_{oss2})$ | |
| Body diode conduction | N/A | $P_{cond_{BD}} = V_F \cdot F_{SW} \left[ \left( I_{OUT} + \frac{\Delta I_L}{2} \right) \cdot t_{dt1} + \left( I_{OUT} - \frac{\Delta I_L}{2} \right) \cdot t_{dt2} \right]$ |
| Body diode reverse recovery(5) | $P_{RR} = V_{IN} \cdot F_{SW} \cdot Q_{RR2}$ | |

(1) Gate drive loss is apportioned based on the internal gate resistance of the MOSFET, externally added series gate resistance and the relevant driver resistance of the LM25148.
(2) MOSFET $R_{DS(on)}$ has a positive temperature coefficient of approximately 4500 ppm/°C. The MOSFET junction temperature, $T_J$, and its rise over ambient temperature is dependent upon the device total power dissipation and its thermal impedance. When operating at or near minimum input voltage, make sure that the MOSFET $R_{DS(on)}$ is rated for the available gate drive voltage.
(3) D' = 1–D is the duty cycle complement.
(4) MOSFET output capacitances, $C_{oss1}$ and $C_{oss2}$, are highly non-linear with voltage. These capacitances are charged losslessly by the inductor current at high-side MOSFET turn-off. During turn-on, however, a current flows from the input to charge the output capacitance of the low-side MOSFET. $E_{oss1}$, the energy of $C_{oss1}$, is dissipated at turn-on, but this is offset by the stored energy $E_{oss2}$ on $C_{oss2}$.
(5) MOSFET body diode reverse recovery charge, $Q_{RR}$, depends on many parameters, particularly forward current, current transition speed, and temperature.

The high-side (control) MOSFET carries the inductor current during the PWM on-time (or D interval) and typically incurs most of the switching losses. It is, therefore, imperative to choose a high-side MOSFET that balances conduction and switching loss contributions. The total power dissipation in the high-side MOSFET is the sum of


Copyright © 2021 Texas Instruments Incorporated

the losses due to conduction, switching (voltage-current overlap), output charge, and typically two-thirds of the net loss attributed to body diode reverse recovery.

The low-side (synchronous) MOSFET carries the inductor current when the high-side MOSFET is off (or 1–D interval). The low-side MOSFET switching loss is negligible as it is switched at zero voltage – current just commutates from the channel to the body diode or vice versa during the transition dead-times. LM25148, with its adaptive gate drive timing, minimizes body diode conduction losses when both MOSFETs are off. Such losses scale directly with switching frequency.

In high step-down ratio applications, the low-side MOSFET carries the current for a large portion of the switching period. Therefore, to attain high efficiency, it is critical to optimize the low-side MOSFET for low $R_{DS(on)}$. In cases where the conduction loss is too high or the target $R_{DS(on)}$ is lower than available in a single MOSFET, connect two low-side MOSFETs in parallel. The total power dissipation of the low-side MOSFET is the sum of the losses due to channel conduction, body diode conduction, and typically one-third of the net loss attributed to body diode reverse recovery. The LM25148 is well suited to drive TI's portfolio of NexFET™ power MOSFETs.

#### *9.1.1.5 EMI Filter*

Switching regulators exhibit negative input impedance, which is lowest at the minimum input voltage. An underdamped LC filter exhibits a high output impedance at the resonant frequency of the filter. For stability, the filter output impedance must be less than the absolute value of the converter input impedance.

$$Z_{IN} = \left| -\frac{V_{IN(min)}^{2}}{P_{IN}} \right| \tag{19}$$

The passive EMI filter design steps are as follows:

- Calculate the required attenuation of the EMI filter at the switching frequency, where $C_{IN}$ represents the existing capacitance at the input of the switching converter.
- Input filter inductor $L_{IN}$ is usually selected between 1 µH and 10 µH, but it can be lower to reduce losses in a high-current design.
- Calculate input filter capacitor $C_F$.

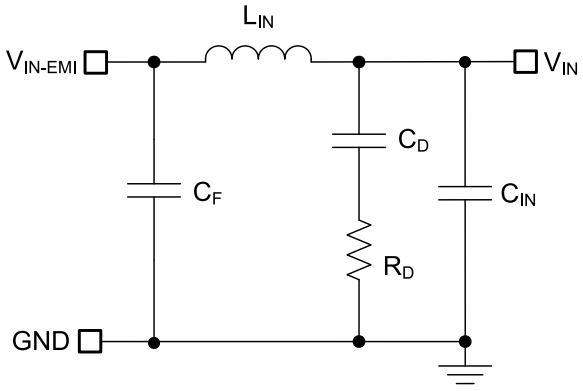



**Figure 9-2. Passive π-Stage EMI Filter for Buck Regulator**

By calculating the first harmonic current from the Fourier series of the input current waveform and multiplying it by the input impedance (the impedance is defined by the existing input capacitor $C_{IN}$), a formula is derived to obtain the required attenuation as shown by Equation 20.

$$Attn = 20\log\left(\frac{I_{L(PEAK)}}{\pi^{2} \cdot F_{SW} \cdot C_{IN}} \cdot \sin\left(\pi \cdot D_{MAX}\right) \cdot \frac{1}{1\,\mu V}\right) - V_{MAX} \tag{20}$$

where

- $V_{MAX}$ is the allowed dBµV noise level for the applicable conducted EMI specification, for example CISPR 32 Class B.
- $C_{IN}$ is the existing input capacitance of the buck regulator.
- $D_{MAX}$ is the maximum duty cycle.
- $I_{PEAK}$ is the peak inductor current.

For filter design purposes, the current at the input can be modeled as a square-wave. Determine the passive EMI filter capacitance $C_F$ from Equation 21.

$$C_F = \frac{1}{L_{IN}} \left( \frac{10^{\frac{|Attn|}{40}}}{2\pi \cdot F_{SW}} \right)^2 \tag{21}$$

Adding an input filter to a switching regulator modifies the control-to-output transfer function. The output impedance of the filter must be sufficiently small so that the input filter does not significantly affect the loop gain of the buck converter. The impedance peaks at the filter resonant frequency. The resonant frequency of the passive filter is given by Equation 22.

$$f_{res} = \frac{1}{2\pi \cdot \sqrt{L_{IN} \cdot C_F}} \tag{22}$$

The purpose of $R_D$ is to reduce the peak output impedance of the filter at the resonant frequency. Capacitor $C_D$ blocks the DC component of the input voltage to avoid excessive power dissipation in $R_D$. Capacitor $C_D$ should have lower impedance than $R_D$ at the resonant frequency with a capacitance value greater than that of the input capacitor $C_{IN}$. This prevents $C_{IN}$ from interfering with the cutoff frequency of the main filter. Added input damping is needed when the output impedance of the filter is high at the resonant frequency (Q of filter formed by $L_{IN}$ and $C_{IN}$ is too high). An electrolytic capacitor $C_D$ can be used for input damping with a value given by Equation 23.

$$C_D \geq 4 \cdot C_{IN} \tag{23}$$

Select the input damping resistor $R_D$ using Equation 24.

$$R_D = \sqrt{\frac{L_{IN}}{C_{IN}}} \tag{24}$$

### 9.1.2 Error Amplifier and Compensation

Figure 9-3 shows a type-II compensator using a transconductance error amplifier (EA). The dominant pole of the EA open-loop gain is set by the EA output resistance, $R_{O\text{-}EA}$, and effective bandwidth-limiting capacitance, $C_{BW}$, as shown by Equation 25.

$$G_{EA(open\,loop)}(s) = -\frac{g_m \cdot R_{O\text{-}EA}}{1 + s \cdot R_{O\text{-}EA} \cdot C_{BW}} \tag{25}$$

The EA high-frequency pole is neglected in the above expression. Equation 26 calculates the compensator transfer function from output voltage to COMP node, including the gain contribution from the (internal or external) feedback resistor network.


Copyright © 2021 Texas Instruments Incorporated

$$G_c(s) = \frac{\hat{v}_c(s)}{\hat{v}_{out}(s)} = -\frac{V_{REF}}{V_{OUT}} \cdot \frac{g_m \cdot R_{O\text{-}EA} \cdot \left(1 + \frac{s}{\omega_{z1}}\right)}{\left(1 + \frac{s}{\omega_{p1}}\right) \cdot \left(1 + \frac{s}{\omega_{p2}}\right)} \quad (26)$$

where

- $V_{REF}$ is the feedback voltage reference of 0.8 V.
- $g_m$ is the EA gain transconductance of 1200 µS.
- $R_{O\text{-}EA}$ is the error amplifier output impedance of 64 MΩ.

$$\omega_{Z1} = \frac{1}{R_{COMP} \cdot C_{COMP}} \quad (27)$$

$$\omega_{p1} = \frac{1}{R_{O\text{-}EA} \cdot (C_{COMP} + C_{HF} + C_{BW})} \cong \frac{1}{R_{O\text{-}EA} \cdot C_{COMP}} \quad (28)$$

$$\omega_{p2} = \frac{1}{R_{COMP} \cdot \left(C_{COMP} \left\| (C_{HF} + C_{BW})\right.\right)} \cong \frac{1}{R_{COMP} \cdot C_{HF}} \quad (29)$$

The EA compensation components create a pole close to the origin, a zero, and a high-frequency pole. Typically, $R_{COMP} << R_{O\text{-}EA}$ and $C_{COMP} >> C_{BW}$ and $C_{HF}$, so the approximations are valid.

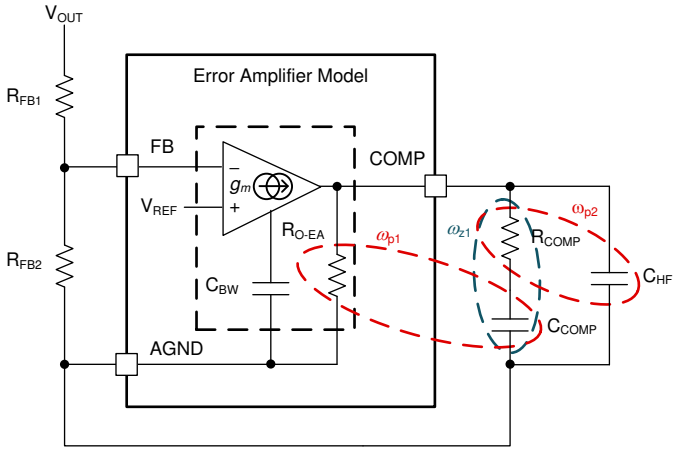



**Figure 9-3. Error Amplifier and Compensation Network**

## 9.2 Typical Applications

### 9.2.1 Design 1 – High Efficiency 2.1-MHz Synchronous Buck Regulator

Figure 9-4 shows the schematic diagram of a single-output synchronous buck regulator with an output voltage of 5 V and a rated load current of 8 A. In this example, the target half-load and full-load efficiencies are 93.5% and 92.5%, respectively, based on a nominal input voltage of 12 V that ranges from 5.5 V to 36 V. The switching frequency is set at 2.1 MHz by resistor $R_{RT}$. The 5-V output is connected to VCCX to reduce IC bias power dissipation and improve efficiency. An output voltage of 3.3 V is also feasible simply by connecting FB to VDDA.

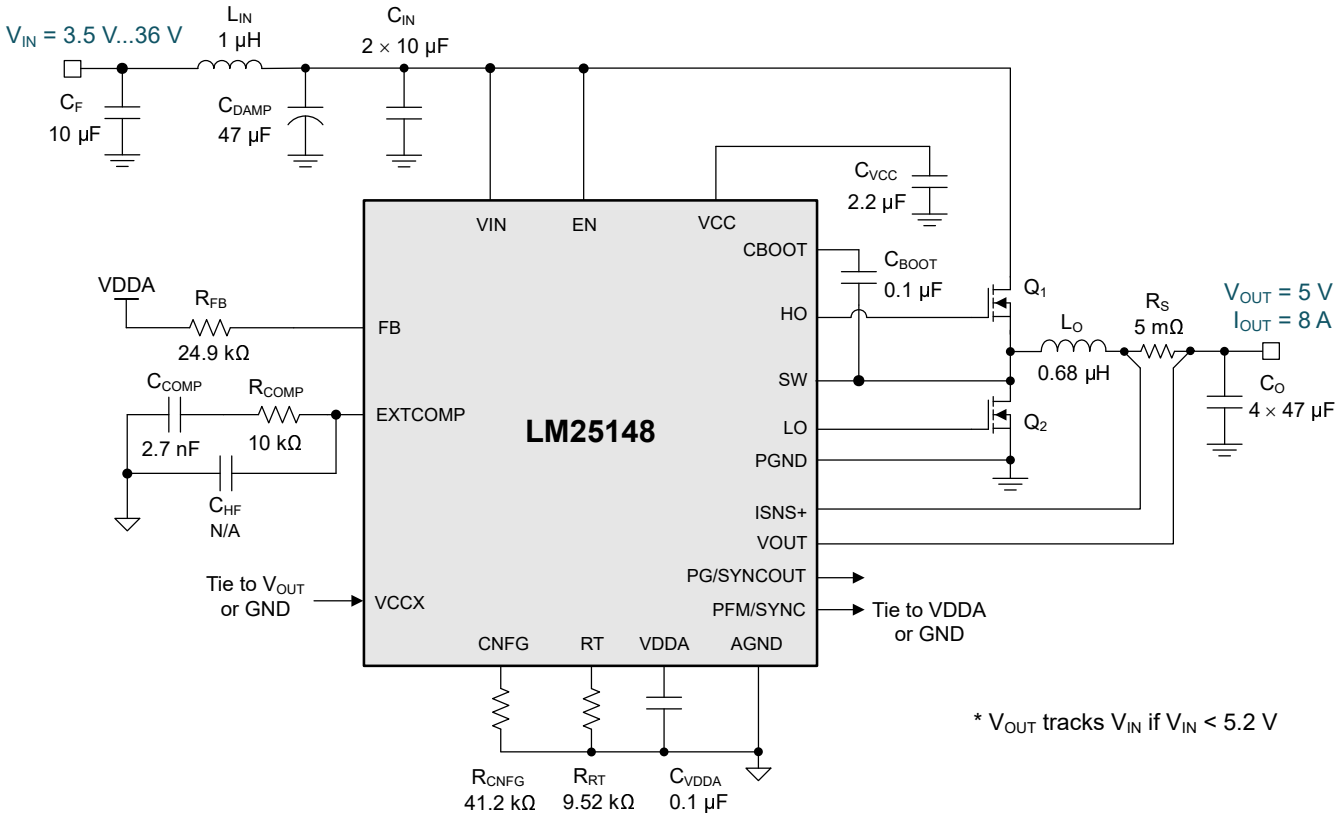



**Figure 9-4. Application Circuit 1 With LM25148 Buck Regulator at 2.1 MHz**

**Note**

This and subsequent design examples are provided herein to showcase the LM25148 controller in several different applications. Depending on the source impedance of the input supply bus, an electrolytic capacitor can be required at the input to ensure stability, particularly at low input voltage and high output current operating conditions. See Section 10 for more details.


Copyright © 2021 Texas Instruments Incorporated

#### 9.2.1.1 Design Requirements

Table 9-2 shows the intended input, output, and performance parameters for this design example.

**Table 9-2. Design Parameters**

| DESIGN PARAMETER | VALUE |
|---|---|
| Input voltage range (steady state) | 8 V to 18 V |
| Min transient input voltage | 5.5 V |
| Max transient input voltage | 36 V |
| Output voltage | 5 V |
| Output current | 8 A |
| Switching frequency | 2.1 MHz |
| Output voltage regulation | ±1% |
| Standby current, no-load | 9.9 µA |
| Shutdown current | 2.3 µA |
| Soft-start time | 3 ms |

The switching frequency is set at 2.1 MHz by resistor $R_{RT}$. In terms of control loop performance, the target loop crossover frequency is 60 kHz with a phase margin greater than 50°.

The selected buck regulator powertrain components are cited in Table 9-3, and many of the components are available from multiple vendors. The MOSFETs in particular are chosen for lowest total conduction and switching power loss, as discussed in detail in Section 9.1.1.4. This design uses a low-DCR composite inductor, and ceramic output capacitor implementation.

**Table 9-3. List of Materials for Application Circuit 1**

| REFERENCE DESIGNATOR | QTY | SPECIFICATION | MANUFACTURER | PART NUMBER |
|---|---|---|---|---|
| $C_{IN}$ | 2 | 10 µF, 50 V, X7S, 1210, ceramic | Taiyo Yuden | UMJ325KB7106KMHT |
| | | | Murata | GCM32EC71H106KA03 |
| | | | TDK | CGA6P3X7S1H106K250AB |
| $C_O$ | 4 | 47 µF, 6.3 V, X7R, 1210, ceramic | Murata | GCM32ER70J476KE19L |
| | | | Taiyo Yuden | JMK325B7476KMHTR |
| | | 47 µF, 10 V, X7S, 1210, ceramic | TDK | CGA6P1X7S1A476M250AC |
| $L_O$ | 1 | 0.56 µH, 3.6 mΩ, 13 A, 6.6 × 6.6 × 4.8 mm | Würth Electronik | 744373490056 |
| | | 0.68 µH, 2.9 mΩ, 22 A, 6.7 × 6.5 × 3.1 mm | Colicraft | XGL6030-681 |
| $Q_1$ | 1 | 40 V, 4.7 mΩ, 12 nC, SON 5 × 6 | Texas Instruments | CSD18503Q5A |
| $Q_2$ | 1 | 40 V, 2.7 mΩ, 35 nC, SON 5 × 6 | Texas Instruments | CSD18511Q5A |
| $R_S$ | 1 | Shunt, 5 mΩ, 0508, 1 W | Susumu | KRL2012E-M-R005-F-T5 |
| $U_1$ | 1 | LM25148 42-V synchronous buck controller | Texas Instruments | LM25148RGYR |

Copyright © 2021 Texas Instruments Incorporated

### 9.2.1.2 Detailed Design Procedure

#### 9.2.1.2.1 Custom Design With WEBENCH® Tools

Click here to create a custom design using the LM25148 device with the WEBENCH® Power Designer.

1. Start by entering the input voltage ($V_{IN}$), output voltage ($V_{OUT}$), and output current ($I_{OUT}$) requirements.
2. Optimize the design for key parameters such as efficiency, footprint, and cost using the optimizer dial.
3. Compare the generated design with other possible solutions from Texas Instruments.

The WEBENCH Power Designer provides a customized schematic along with a list of materials with real-time pricing and component availability.

In most cases, these actions are available:

- Run electrical simulations to see important waveforms and circuit performance
- Run thermal simulations to understand board thermal performance
- Export customized schematic and layout into popular CAD formats
- Print PDF reports for the design, and share the design with colleagues

Get more information about WEBENCH tools at www.ti.com/WEBENCH.

#### 9.2.1.2.2 Custom Design With Excel Quickstart Tool

Select components based on the regulator specifications using the LM25148 *Quickstart Calculator* available for download from the LM25148 product folder.

#### 9.2.1.2.3 Buck Inductor

1. Use Equation 30 to calculate the required buck inductance based on a 30% inductor ripple current at nominal input voltages.

$$L_O = \frac{V_{OUT}}{\Delta I_{LO} \cdot F_{SW}} \cdot \left(1 - \frac{V_{OUT}}{V_{IN(nom)}}\right) = \frac{5\,V}{2.4\,A \cdot 2.1\,MHz} \cdot \left(1 - \frac{5\,V}{12\,V}\right) = 0.58\,\mu H \tag{30}$$

2. Select a standard inductor value of 0.56 µH or use a 0.68 µH to account for effective inductance derating with current of molded inductors. Use Equation 31 to calculate the peak inductor currents at maximum steady-state input voltage. Subharmonic oscillation occurs with a duty cycle greater than 50% for peak current-mode control. For design simplification, the LM25148 has an internal slope compensation ramp proportional to the switching frequency that is added to the current sense signal to damp any tendency toward subharmonic oscillation.

$$I_{LO(PK)} = I_{OUT} + \frac{\Delta I_{LO}}{2} = I_{OUT} + \frac{V_{OUT}}{2 \cdot L_O \cdot F_{SW}} \cdot \left(1 - \frac{V_{OUT}}{V_{IN(max)}}\right) = 8\,A + \frac{5\,V}{0.56\,\mu H \cdot 2.1\,MHz} \cdot \left(1 - \frac{5\,V}{18\,V}\right) = 9.53\,A \tag{31}$$

3. Based on Equation 8, use Equation 32 to cross-check the inductance to set a slope compensation close to the ideal one times the inductor current downslope.

$$L_{O(sc)} = \frac{V_{OUT} \cdot R_S}{24 \cdot F_{SW}} = \frac{5\,V \cdot 5\,m\Omega}{24 \cdot 2.1\,MHz} = 0.5\,\mu H \tag{32}$$

#### 9.2.1.2.4 Current-Sense Resistance

1. Calculate the current-sense resistance based on a maximum peak current capability of at least 25% higher than the peak inductor current at full load to provide sufficient margin during start-up and load-on transients. Calculate the current sense resistances using Equation 33.

$$R_S = \frac{V_{CS\text{-}TH}}{1.25 \cdot I_{LO(PK)}} = \frac{60\,mV}{1.25 \cdot 9.53\,A} = 5.04\,m\Omega \tag{33}$$


Copyright © 2021 Texas Instruments Incorporated

where

- $V_{CS-TH}$ is the 60-mV current limit threshold.

2. Select a standard resistance value of 5 mΩ for the shunt. An 0508 footprint component with wide aspect ratio termination design provides 1-W power rating, low parasitic series inductance, and compact PCB layout. Carefully adhere to the layout guidelines in Section 11.1 to make sure that noise and DC errors do not corrupt the differential current-sense voltages measured at the ISNS+ and VOUT pins.
3. Place the shunt resistor close to the inductor.
4. Use Kelvin-sense connections, and route the sense lines differentially from the shunt to the LM25148.
5. The CS-to-output propagation delay (related to the current limit comparator, internal logic, and power MOSFET gate drivers) causes the peak current to increase above the calculated current limit threshold. For a total propagation delay $t_{DELAY-ISNS+}$ of 40 ns, use Equation 34 to calculate the worst-case peak inductor current with the output shorted.

$$I_{LO-PK(SC)} = \frac{V_{CS-TH}}{R_S} + \frac{V_{IN(max)} \cdot t_{DELAY-ISNS+}}{L_O} = \frac{60\,mV}{5\,m\Omega} + \frac{18\,V \cdot 45\,ns}{0.56\,\mu H} = 13.5\,A \tag{34}$$

6. Based on this result, select an inductor with saturation current greater than 16 A across the full operating temperature range.

#### 9.2.1.2.5 Output Capacitors

1. Use Equation 35 to estimate the output capacitance required to manage the output voltage overshoot during a load-off transient (from full load to no load) assuming a load transient deviation specification of 1.5% (75 mV for a 5-V output).

$$C_{OUT} \geq \frac{L_O \cdot \Delta I_{OUT}{}^2}{\left(V_{OUT} + \Delta V_{OVERSHOOT}\right)^2 - V_{OUT}{}^2} = \frac{0.56\,\mu H \cdot \left(8\,A\right)^2}{\left(5\,V + 75\,mV\right)^2 - \left(5\,V\right)^2} = 47.4\,\mu F \tag{35}$$

2. Noting the voltage coefficient of ceramic capacitors where the effective capacitance decreases significantly with applied voltage, select four 47-µF, 10-V, X7R, 1210 ceramic output capacitors. Generally, when sufficient capacitance is used to satisfy the load-off transient response requirement, the voltage undershoot during a no-load to full-load transient is also satisfactory.
3. Use Equation 36 to estimate the peak-peak output voltage ripple at nominal input voltage.

$$\Delta V_{OUT} = \sqrt{\left(\frac{\Delta I_{LO}}{8 \cdot F_{SW} \cdot C_{OUT}}\right)^2 + \left(R_{ESR} \cdot \Delta I_{LO}\right)^2} = \sqrt{\left(\frac{2.54\,A}{8 \cdot 2.1\,MHz \cdot 44\,\mu F}\right)^2 + \left(1\,m\Omega \cdot 2.54\,A\right)^2} = 4.3\,mV \tag{36}$$

where

- $R_{ESR}$ is the effective equivalent series resistance (ESR) of the output capacitors.
- 44 µF is the total effective (derated) ceramic output capacitance at 5 V.

4. Use Equation 37 to calculate the output capacitor RMS ripple current using and verify that the ripple current is within the capacitor ripple current rating.

$$I_{CO(RMS)} = \frac{\Delta I_{LO}}{\sqrt{12}} = \frac{2.54\,A}{\sqrt{12}} = 0.73\,A \tag{37}$$

#### 9.2.1.2.6 Input Capacitors

A power supply input typically has a relatively high source impedance at the switching frequency. Good-quality input capacitors are necessary to limit the input ripple voltage. As mentioned earlier, dual-channel interleaved operation significantly reduces the input ripple amplitude. In general, the ripple current splits between the input capacitors based on the relative impedance of the capacitors at the switching frequency.

1. Select the input capacitors with sufficient voltage and RMS ripple current ratings.

Copyright © 2021 Texas Instruments Incorporated

2. Use Equation 38 to calculate the input capacitor RMS ripple current assuming a worst-case duty-cycle operating point of 50%.

$$I_{CIN(RMS)} = I_{OUT} \cdot \sqrt{D \cdot (1-D)} = 8A \cdot \sqrt{0.5 \cdot (1-0.5)} = 4\,A \tag{38}$$

3. Use Equation 39 to find the required input capacitance.

$$C_{IN} \geq \frac{D \cdot (1-D) \cdot I_{OUT}}{F_{SW} \cdot (\Delta V_{IN} - R_{ESR} \cdot I_{OUT})} = \frac{0.5 \cdot (1-0.5) \cdot 8\,A}{2.1MHz \cdot (120\,mV - 2m\Omega \cdot 8\,A)} = 9.2\ \mu F \tag{39}$$

where

- $\Delta V_{IN}$ is the input peak-to-peak ripple voltage specification.
- $R_{ESR}$ is the input capacitor ESR.

4. Recognizing the voltage coefficient of ceramic capacitors, select two 10-µF, 50-V, X7R, 1210 ceramic input capacitors. Place these capacitors adjacent to the power MOSFETs. See Section 11.1.1 for more details.
5. Use four 10-nF, 50-V, X7R, 0603 ceramic capacitors near the high-side MOSFET to supply the high di/dt current during MOSFET switching transitions. Such capacitors offer high self-resonant frequency (SRF) and low effective impedance above 100 MHz. The result is lower power loop parasitic inductance, thus minimizing switch-node voltage overshoot and ringing for lower conducted and radiated EMI signature. Refer to Section 11.1 for more details.

#### 9.2.1.2.7 Frequency Set Resistor

Calculate the RT resistance for a switching frequency of 2.1 MHz using Equation 40. Choose a standard E96 value of 9.53 kΩ.

$$R_T(k\Omega) = \frac{\frac{10^6}{F_{SW}(kHz)} - 53}{45} = \frac{\frac{10^6}{2100\,kHz} - 53}{45} = 9.4\,k\Omega \tag{40}$$

#### 9.2.1.2.8 Feedback Resistors

If an output voltage setpoint other than 3.3 V or 5 V is required (or to measure a bode plot when using either of the fixed output voltage options), determine the feedback resistances using Equation 41.

$$R_{FB1} = R_{FB2} \cdot \left( \frac{V_{OUT}}{V_{REF}} - 1 \right) = 15\,k\Omega \cdot \left( \frac{5\,V}{0.8\,V} - 1 \right) = 78.7\,k\Omega \tag{41}$$

#### 9.2.1.2.9 Compensation Components

Choose compensation components for a stable control loop using the procedure outlined as follows:

1. Based on a specified loop gain crossover frequency, $f_C$, of 60 kHz, use Equation 42 to calculate $R_{COMP}$, assuming an effective output capacitance of 100 µF. Choose a standard value for $R_{COMP}$ of 10 kΩ.

$$R_{COMP} = 2\pi \cdot f_C \cdot \frac{V_{OUT}}{V_{REF}} \cdot \frac{R_S \cdot G_{CS}}{g_m} \cdot C_{OUT} = 2\pi \cdot 60\,kHz \cdot \frac{5\,V}{0.8\,V} \cdot \frac{5m\Omega \cdot 10}{1200\,\mu S} \cdot 100\,\mu F = 9.82\,k\Omega \tag{42}$$

2. To provide adequate phase boost at crossover while also allowing a fast settling time during a load or line transient, select $C_{COMP}$ to place a zero at the higher of (1) one tenth of the crossover frequency, or (2) the load pole. Choose a standard value for $C_{COMP}$ of 2.7 nF.

$$C_{COMP} = \frac{10}{2\pi \cdot f_C \cdot R_{COMP}} = \frac{10}{2\pi \cdot 60\,kHz \cdot 10\,k\Omega} = 2.65\ nF \tag{43}$$


Copyright © 2021 Texas Instruments Incorporated

Such a low capacitance value also helps to avoid output voltage overshoot when recovering from dropout (when the input voltage is less than the output voltage setpoint and $V_{COMP}$ is railed high).

3. Calculate $C_{HF}$ to create a pole at the ESR zero and to attenuate high-frequency noise at COMP. $C_{BW}$ is the bandwidth-limiting capacitance of the error amplifier. $C_{HF}$ may not be significant enough to be necessary in some designs, like this one. $C_{HF}$ can be unpopulated, or used with a small 22 pF for more noise filtering.

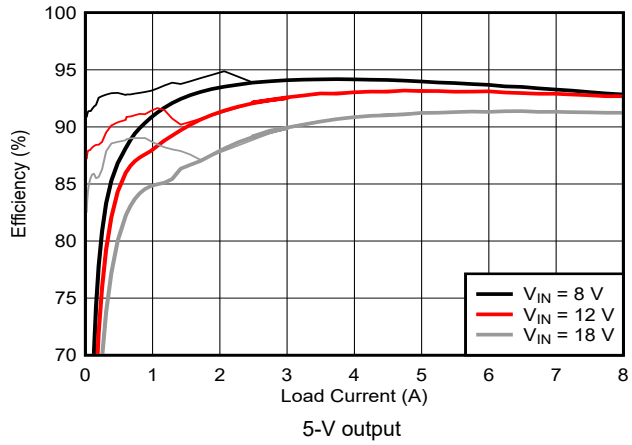
$$C_{HF} = \frac{1}{2\pi \cdot f_{ESR} \cdot R_{COMP}} - C_{BW} = \frac{1}{2\pi \cdot 500\,kHz \cdot 10\,k\Omega} - 31\,pF = 0.8\ pF \quad (44)$$

**Note**

Set a fast loop with high $R_{COMP}$ and low $C_{COMP}$ values to improve the response when recovering from operation in dropout.

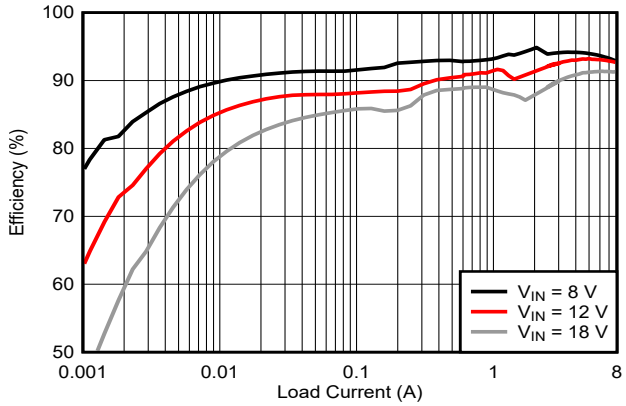
For technical solutions, industry trends, and insights for designing and managing power supplies, please refer to TI's technical articles.

### 9.2.1.3 Application Curves



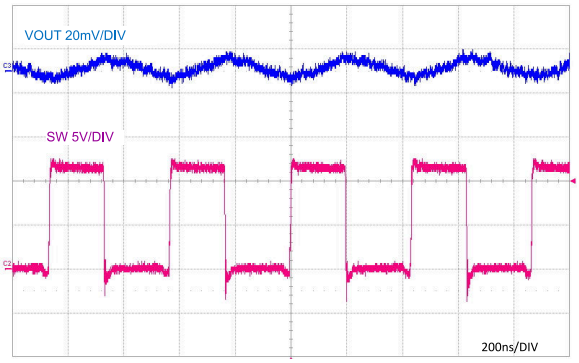

5-V output

**Figure 9-5. Efficiency vs $I_{OUT}$**



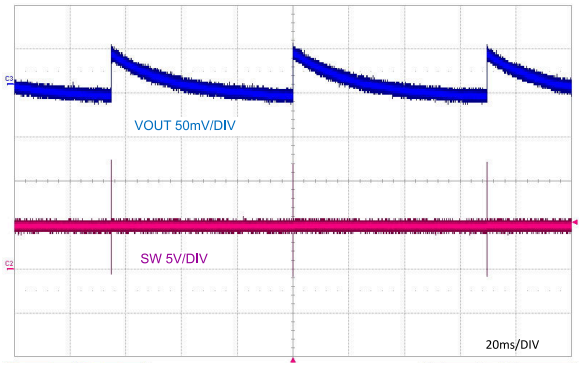

5-V output

**Figure 9-6. Efficiency vs $I_{OUT}$, Log Scale**



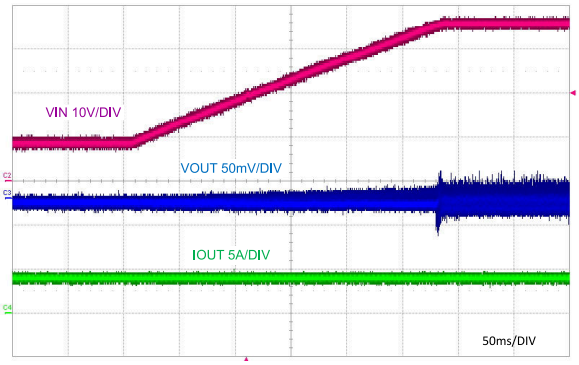

8-A resistive load

**Figure 9-7. Full Load Switching**



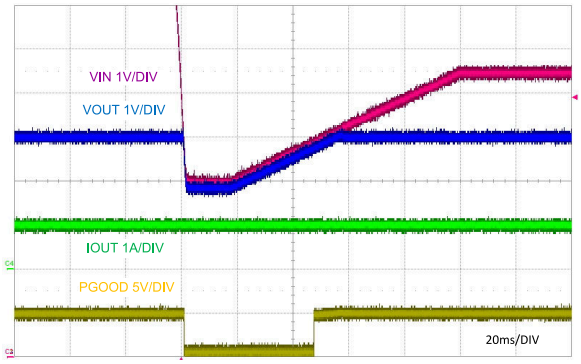

No load

**Figure 9-8. PFM Switching**




$V_{IN}$ ramps from 12 V to 36 V  5-A load

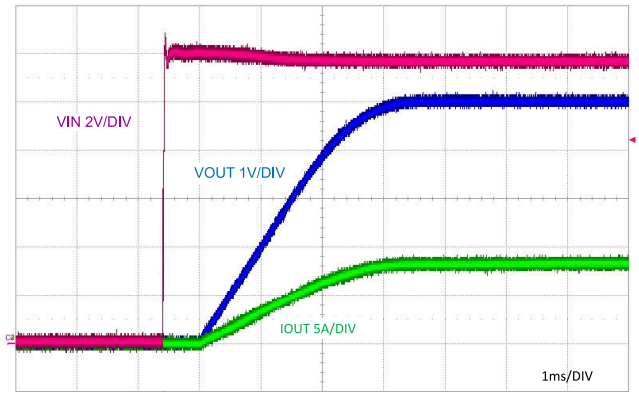
**Figure 9-9. Line Transient**




$V_{IN}$ falls to 3.8 V  5-A load

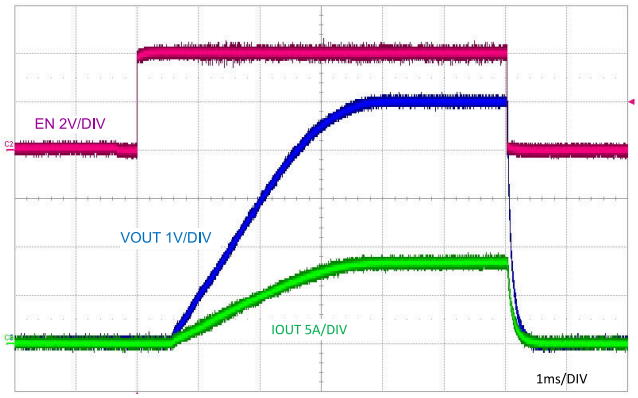
**Figure 9-10. Cold-Crank Response to $V_{IN}$ = 3.8 V**


Copyright © 2021 Texas Instruments Incorporated



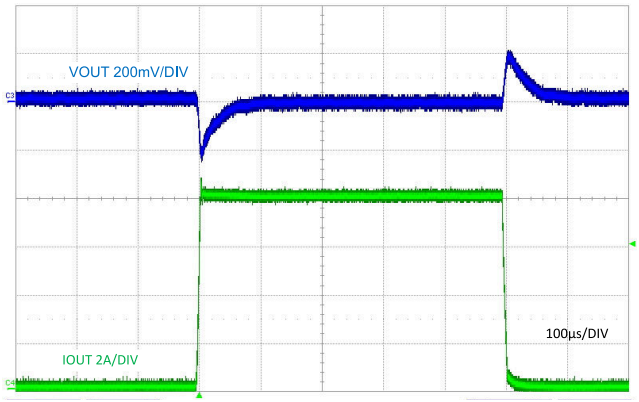

$V_{IN}$ step to 12 V 8-A resistive load

**Figure 9-11. Start-Up Characteristic**



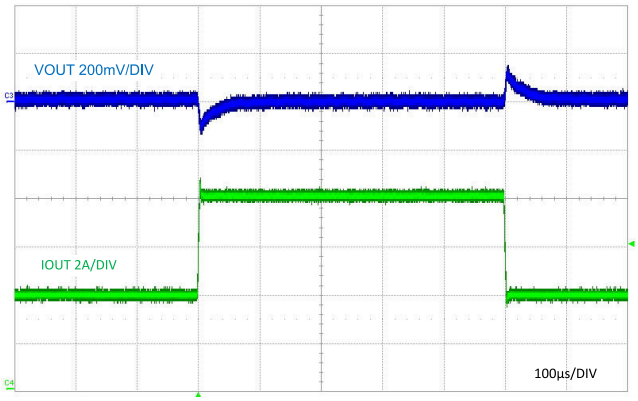

$V_{IN}$ = 12 V 8-A resistive load

**Figure 9-12. ENABLE ON and OFF Characteristic**



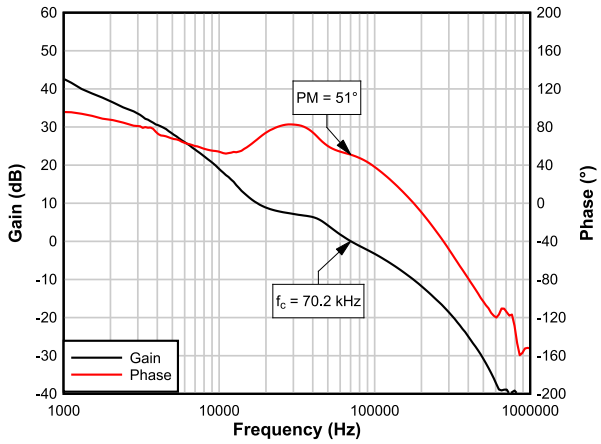

$V_{IN}$ = 12 V FPWM

**Figure 9-13. Load Transient, 0 A to 8 A**



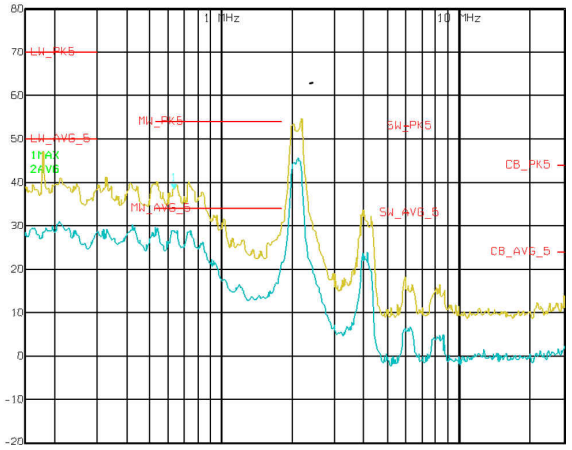

$V_{IN}$ = 12 V FPWM

**Figure 9-14. Load Transient, 4 A to 8 A**




$V_{IN}$ = 12 V 8-A resistive load

**Figure 9-15. Bode Plot, 5-V Output**




$V_{IN}$ = 13.8 V 150 kHz to 30 MHz 7-A resistive load

**Figure 9-16. CISPR 25 Class 5 Conducted EMI**

### 9.2.2 Design 2 – High Efficiency 440-kHz Synchronous Buck Regulator

Figure 9-17 shows the schematic diagram of a single-output synchronous buck regulator with an output voltage of 5 V and a rated load current of 10 A. In this example, the target half-load and full-load efficiencies are 97% and 95%, respectively, based on a nominal input voltage of 12 V that ranges from 5.5 V to 36 V. The switching frequency is set at 440 kHz by resistor $R_{RT}$. The 5-V output is connected to VCCX to reduce IC bias power dissipation and improve efficiency. An output voltage of 3.3 V is also feasible simply by connecting FB to VDDA (tie VCCX to GND in this case).

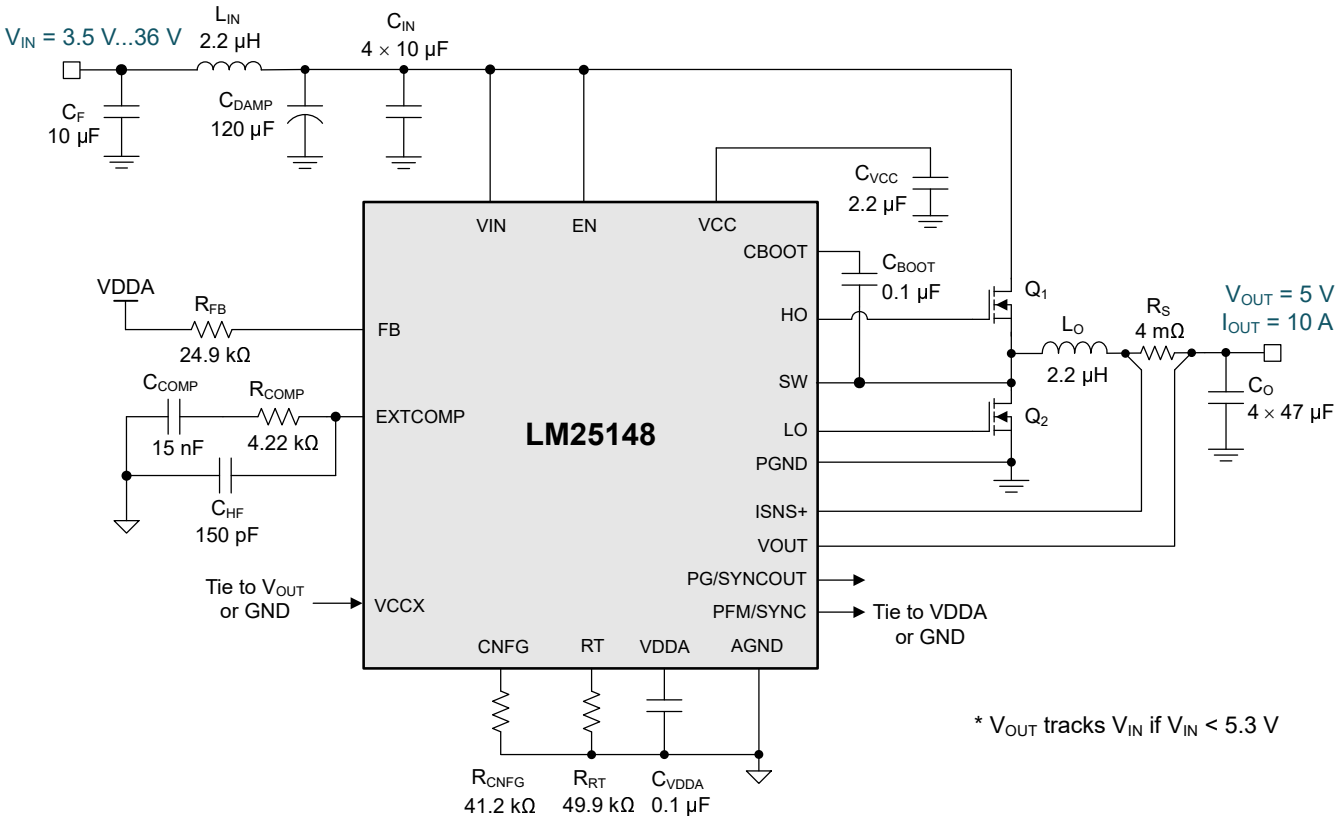



**Figure 9-17. Application Circuit 2 With LM25148 Buck Regulator at 440 kHz**


Copyright © 2021 Texas Instruments Incorporated

#### 9.2.2.1 Design Requirements

Table 9-4 shows the intended input, output, and performance parameters for this design example.

**Table 9-4. Design Parameters**

| DESIGN PARAMETER | VALUE |
|---|---|
| Input voltage range (steady-state) | 8 V to 36 V |
| Min transient input voltage | 5.5 V |
| Max transient input voltage | 40 V |
| Output voltage | 5 V |
| Output current | 10 A |
| Switching frequency | 440 kHz |
| Output voltage regulation | ±1% |
| Standby current, no-load | 12 µA |
| Shutdown current | 2.3 µA |
| Soft-start time | 3 ms |

The switching frequency is set at 440 kHz by resistor $R_{RT}$. The selected buck regulator powertrain components are cited in Table 9-5, and many of the components are available from multiple vendors. The MOSFETs in particular are chosen for both lowest conduction and switching power loss, as discussed in detail in Section 9.1.1.4.

**Table 9-5. List of Materials for Application Circuit 2**

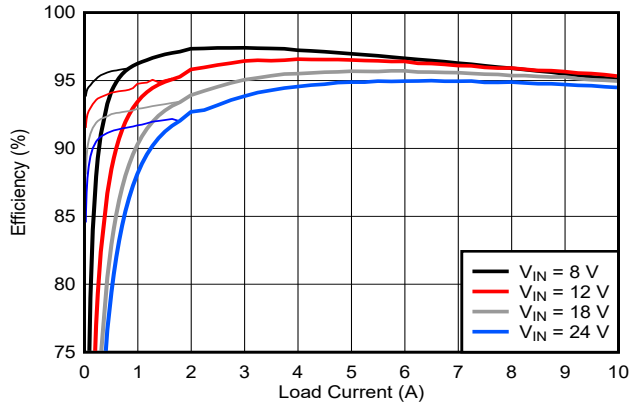
| REFERENCE DESIGNATOR | QTY | SPECIFICATION | MANUFACTURER | PART NUMBER |
|---|---|---|---|---|
| $C_{IN}$ | 4 | 10 µF, 50 V, X7R, 1210, ceramic | AVX | 12105C106K4Z2A |
| | | | TDK | C3225X7R1H106K250AC |
| | | | Murata | GRM32ER71H106KA12L |
| $C_O$ | 4 | 47 µF, 6.3 V, X7R, 1210, ceramic | Murata | GCM32ER70J476KE19L |
| | | | Taiyo Yuden | JMK325B7476KMHTR |
| | | 47 µF, 10 V, X7S, 1210, ceramic | TDK | CGA6P1X7S1A476M250AC |
| $L_O$ | 1 | 2.2 µH, 4.3 mΩ, 12.5 A, 6.7 × 6.5 × 6.1 mm | Coilcraft | XGL6060-222MEC |
| | | 2.2 µH, 6.5 mΩ, 10 A, 10 × 11 × 3.8 mm | Würth Electronik | 74437368022 |
| $Q_1$ | 1 | 40 V, 4.7 mΩ, 12 nC, SON 5 × 6 | Texas Instruments | CSD18503Q5A |
| $Q_2$ | 1 | 40 V, 2.7 mΩ, 35 nC, SON 5 × 6 | Texas Instruments | CSD18511Q5A |
| $R_S$ | 1 | Shunt, 4 mΩ, 0508, 1 W | Susumu | KRL2012E-M-R004-F-T5 |
| $U_1$ | 1 | LM25148 42-V synchronous buck controller | Texas Instruments | LM25148RGYR |

#### 9.2.2.2 Detailed Design Procedure

See Section 9.2.1.2.

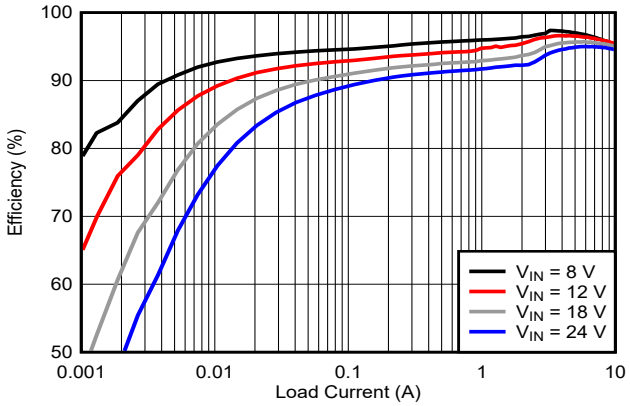
Copyright © 2021 Texas Instruments Incorporated

### 9.2.2.3 Application Curves



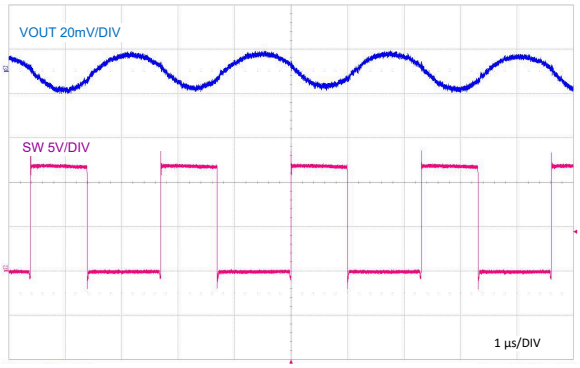

5-V output

**Figure 9-18. Efficiency vs $I_{OUT}$**



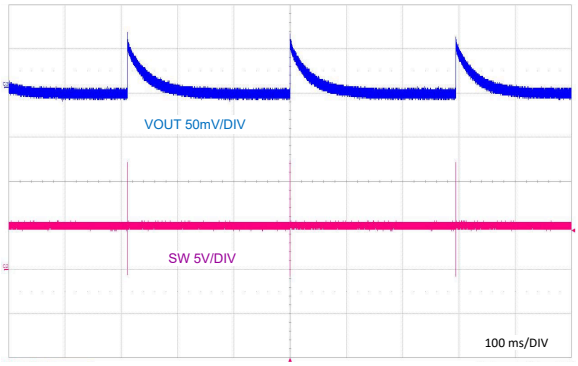

5-V output

**Figure 9-19. Efficiency vs $I_{OUT}$, Log Scale**



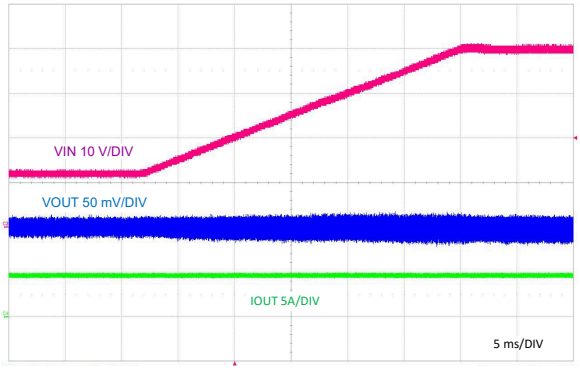

10-A resistive load

**Figure 9-20. Full Load Switching**



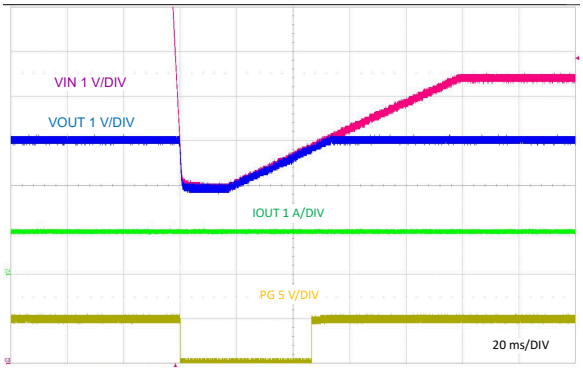

No load

**Figure 9-21. PFM Switching**




$V_{IN}$ ramps from 12 to 40 V  5-A load

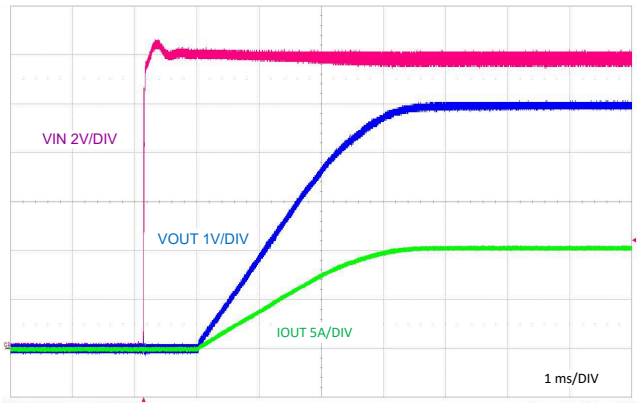
**Figure 9-22. Line Transient Response to $V_{IN}$ = 40 V**




$V_{IN}$ falls to 4 V  1-A load

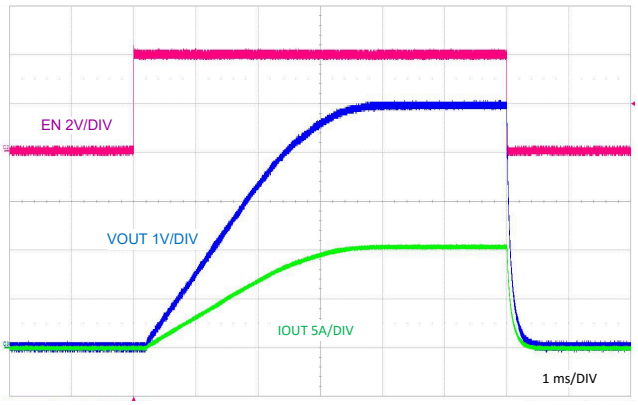
**Figure 9-23. Cold-Crank Response to $V_{IN}$ = 4 V**


Copyright © 2021 Texas Instruments Incorporated



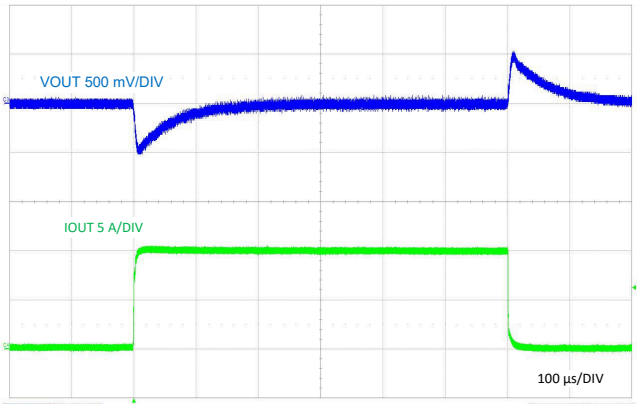

$V_{IN}$ step to 12 V 10-A resistive load

**Figure 9-24. Start-Up Characteristic**



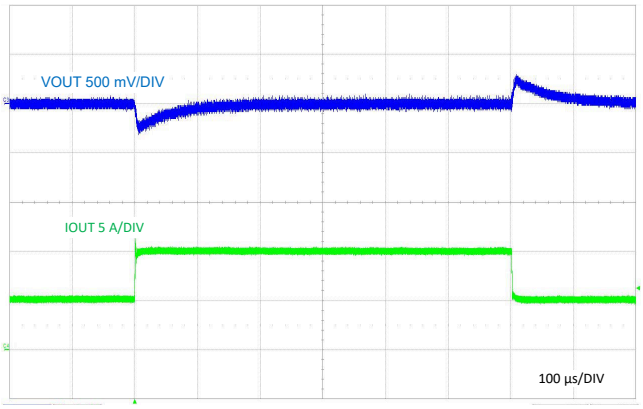

$V_{IN}$ = 12 V 10-A resistive load

**Figure 9-25. ENABLE ON and OFF Characteristic**




$V_{IN}$ = 12 V FPWM

**Figure 9-26. Load Transient, 0 A to 10 A**




$V_{IN}$ = 12 V FPWM

**Figure 9-27. Load Transient, 5 A to 10 A**

### 9.2.3 Design 3 – Dual-Phase 400-kHz 20-A Synchronous Buck Regulator

Figure 9-28 shows the schematic diagram of a dual-phase synchronous buck regulator with output voltage of 3.3 V and a rated load current of 20 A. In this example, the target half-load and full-load efficiencies are 95% and 92%, respectively, based on a nominal input voltage of 12 V that ranges from 4 V to 36 V. The switching frequency is set at 400 kHz by resistors $R_{RT1}$ and $R_{RT2}$.

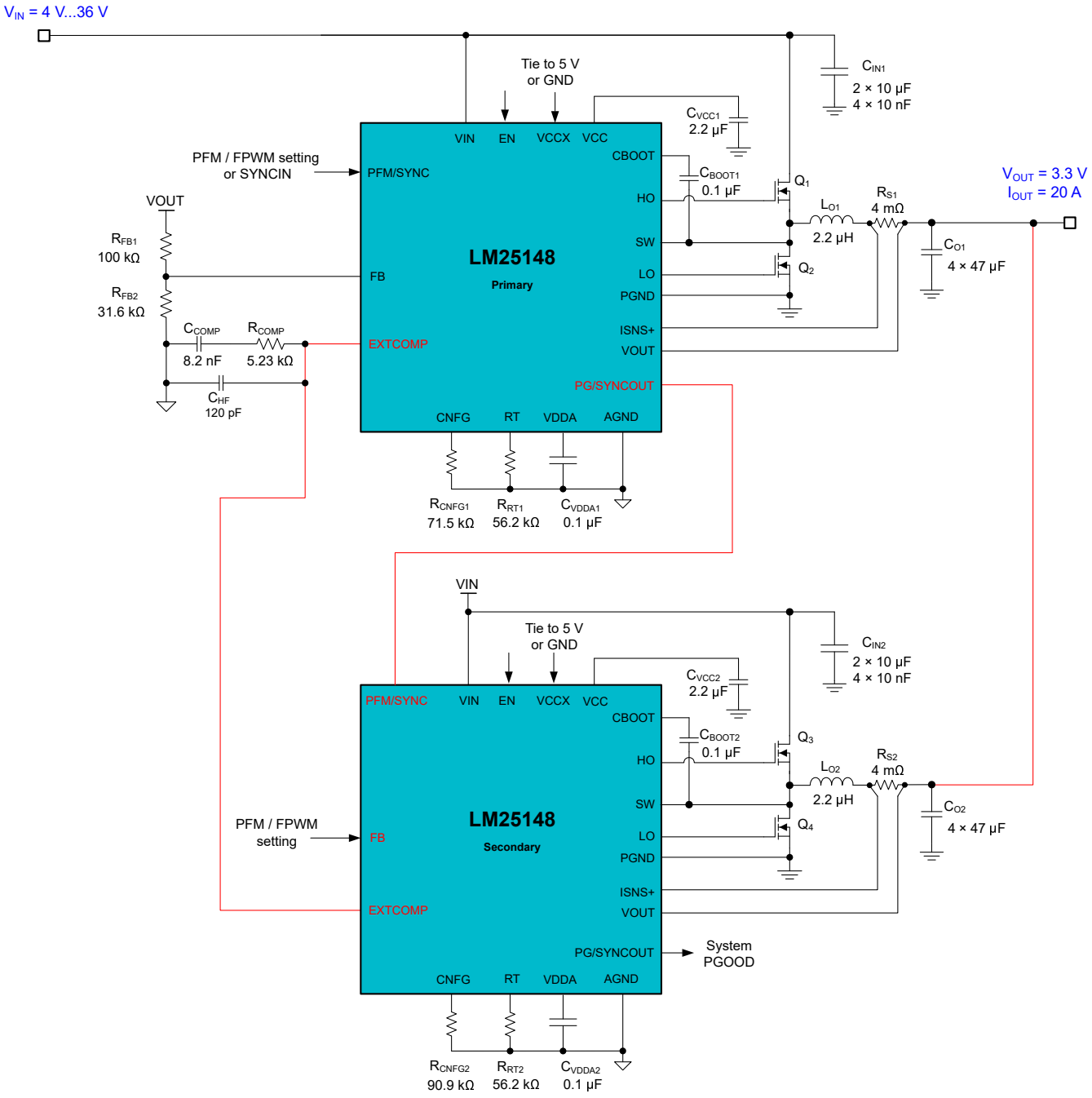



**Figure 9-28. Application Circuit 3 With Two LM25148 Buck Regulators at 400 kHz**


Copyright © 2021 Texas Instruments Incorporated

#### 9.2.3.1 Design Requirements

Table 9-6 shows the intended input, output, and performance parameters for this design example.

**Table 9-6. Design Parameters**

| DESIGN PARAMETER | VALUE |
|---|---|
| Input voltage range (steady-state) | 8 V to 36 V |
| Min transient input voltage | 4 V |
| Max transient input voltage | 40 V |
| Output voltage | 3.3 V |
| Output current | 20 A |
| Switching frequency | 400 kHz |
| Output voltage regulation | ±1% |
| Standby current, no-load | 44 µA |
| Shutdown current | 4.6 µA |
| Soft-start time | 3 ms |

The switching frequency is set at 400 kHz by resistors $R_{RT1}$ and $R_{RT2}$. The selected buck regulator powertrain components are cited in Table 9-7, and many of the components are available from multiple vendors. The MOSFETs in particular are chosen for both lowest conduction and switching power loss, as discussed in detail in Section 9.1.1.4.

**Table 9-7. List of Materials for Application Circuit 3**

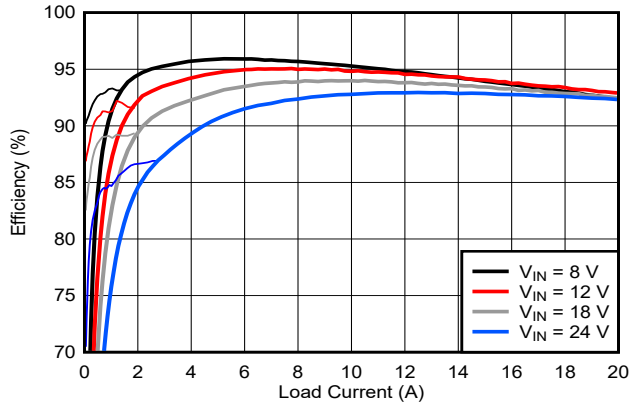
| REFERENCE DESIGNATOR | QTY | SPECIFICATION | MANUFACTURER | PART NUMBER |
|---|---|---|---|---|
| $C_{IN}$ | 4 | 10 µF, 50 V, X7R, 1210, ceramic | AVX | 12105C106K4Z2A |
| | | | TDK | C3225X7R1H106K250AC |
| | | | Murata | GRM32ER71H106KA12L |
| $C_O$ | 8 | 47 µF, 6.3 V, X7R, 1210, ceramic | Murata | GCM32ER70J476KE19L |
| | | 47 µF, 10 V, X7S, 1210, ceramic | TDK | CGA6P1X7S1A476M250AC |
| | 4 | 100 µF, 6.3 V, X7S, 1210, ceramic | Murata | GRT32EC70J107ME13 |
| $L_{O1}$, $L_{O2}$ | 2 | 2.2 µH, 4.5 mΩ, 32 A, 11.3 × 10 × 6 mm | Coilcraft | XKL1060-222MEC |
| | | 2.2 µH, 4.3 mΩ, 12.5 A, 6.7 × 6.5 × 6.1 mm | Coilcraft | XGL6060-222MEC |
| | | 2.2 µH, 6.5 mΩ, 10 A, 10 × 11 × 3.8 mm | Würth Electronik | 74437368022 |
| $Q_1$, $Q_3$ | 2 | 40 V, 4.7 mΩ, 12 nC, SON 5 × 6 | Texas Instruments | CSD18503Q5A |
| $Q_2$, $Q_4$ | 2 | 40 V, 2.7 mΩ, 35 nC, SON 5 × 6 | Texas Instruments | CSD18511Q5A |
| $R_{S1}$, $R_{S2}$ | 2 | Shunt, 4 mΩ, 0508, 1 W | Susumu | KRL2012E-M-R004-F-T5 |
| $U_1$, $U_2$ | 2 | LM25148 42-V synchronous buck controller | Texas Instruments | LM25148RGYR |

#### 9.2.3.2 Detailed Design Procedure

See Section 9.2.1.2.

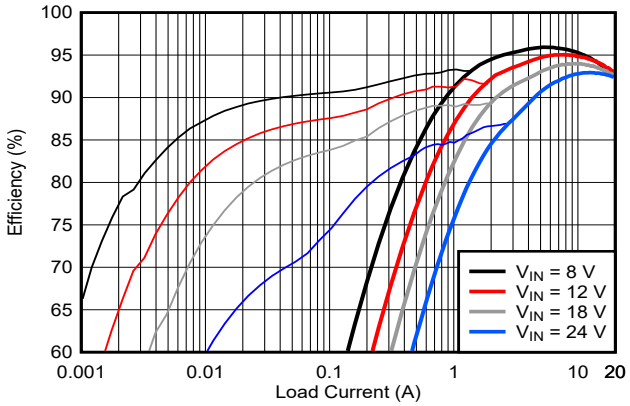
Copyright © 2021 Texas Instruments Incorporated

### 9.2.3.3 Application Curves



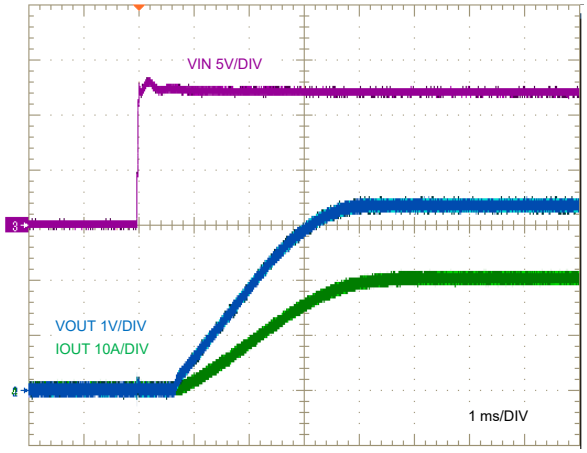

3.3-V output

**Figure 9-29. Efficiency vs $I_{OUT}$**



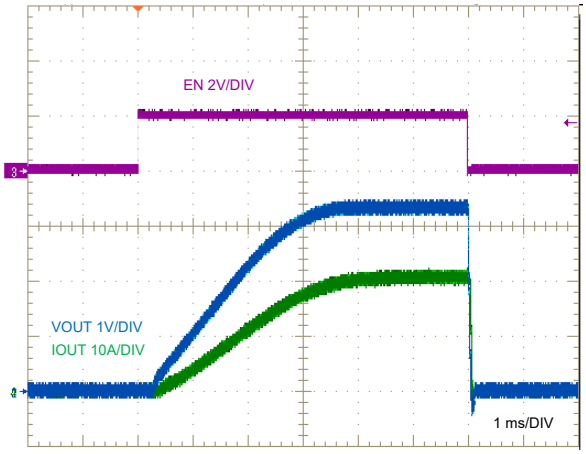

3.3-V output

**Figure 9-30. Efficiency vs $I_{OUT}$, Log Scale**



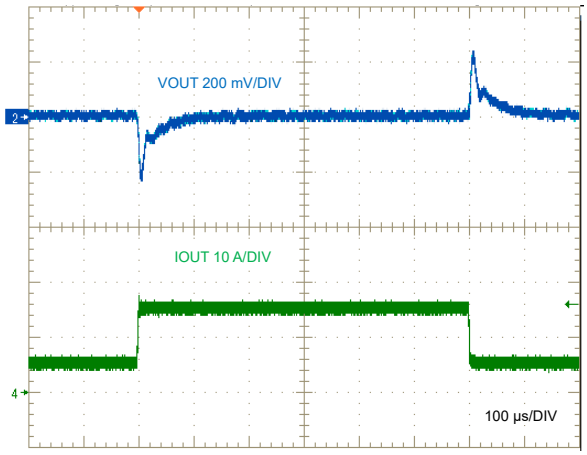

$V_{IN}$ step to 12 V 20-A load

**Figure 9-31. VIN Start-Up Characteristic**



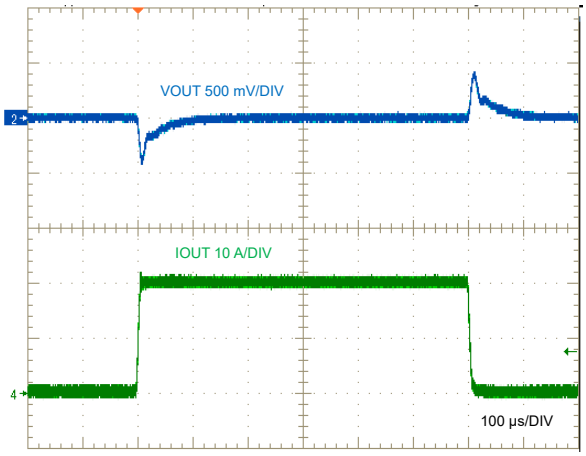

$V_{IN}$ = 12 V 20-A load

**Figure 9-32. ENABLE ON and OFF Characteristic**




$V_{IN}$ = 12 V FPWM

**Figure 9-33. Load Transient, 5 A to 15 A**




$V_{IN}$ = 12 V FPWM

**Figure 9-34. Load Transient, 0 A to 20 A**


Copyright © 2021 Texas Instruments Incorporated

## 10 Power Supply Recommendations

The LM25148 buck controller is designed to operate from a wide input voltage range of 3.5 V to 42 V. The characteristics of the input supply must be compatible with the *Absolute Maximum Ratings* and *Recommended Operating Conditions*. In addition, the input supply must be capable of delivering the required input current to the fully loaded regulator. Estimate the average input current with Equation 45.

$$I_{IN} = \frac{P_{OUT}}{V_{IN} \cdot \eta} \tag{45}$$

where

- η is the efficiency

If the regulator is connected to an input supply through long wires or PCB traces with a large impedance, take special care to achieve stable performance. The parasitic inductance and resistance of the input cables can have an adverse affect on converter operation. The parasitic inductance in combination with the low-ESR ceramic input capacitors form an underdamped resonant circuit. This circuit can cause overvoltage transients at VIN each time the input supply is cycled ON and OFF. The parasitic resistance causes the input voltage to dip during a load transient. The best way to solve such issues is to reduce the distance from the input supply to the regulator and use an aluminum or tantalum input capacitor in parallel with the ceramics. The moderate ESR of the electrolytic capacitors helps damp the input resonant circuit and reduce any voltage overshoots. A capacitance in the range of 10 µF to 47 µF is usually sufficient to provide parallel input damping and helps to hold the input voltage steady during large load transients.

An EMI input filter is often used in front of the regulator that, unless carefully designed, can lead to instability as well as some of the effects mentioned above. The *Simple Success with Conducted EMI for DC-DC Converters* application report provides helpful suggestions when designing an input filter for any switching regulator.

Copyright © 2021 Texas Instruments Incorporated

# 11 Layout

## 11.1 Layout Guidelines

Proper PCB design and layout is important in a high-current, fast-switching circuit (with high current and voltage slew rates) to achieve a robust and reliable design. As expected, certain issues must be considered before designing a PCB layout using the LM25148. The high-frequency power loop of a buck regulator power stage is denoted by loop 1 in the shaded area of Figure 11-1. The topological architecture of a buck regulator means that particularly high di/dt current flows in the components of loop 1, and it becomes mandatory to reduce the parasitic inductance of this loop by minimizing its effective loop area. Also important are the gate drive loops of the high-side and low-side MOSFETs, denoted by 2 and 3, respectively, in Figure 11-1.

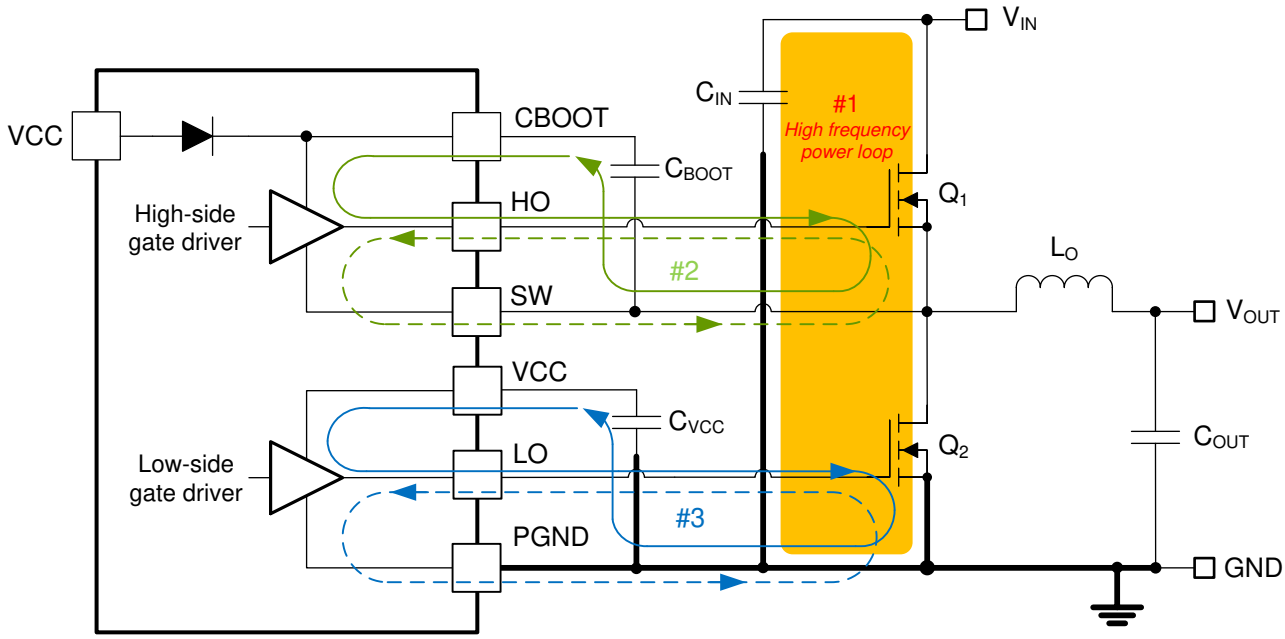



**Figure 11-1. DC/DC Regulator Ground System With Power Stage and Gate Drive Circuit Switching Loops**

### 11.1.1 Power Stage Layout

- Input capacitors, output capacitors, and MOSFETs are the constituent components of the power stage of a buck regulator and are typically placed on the top side of the PCB (solder side). The benefits of convective heat transfer are maximized because of leveraging any system-level airflow. In a two-sided PCB layout, small-signal components are typically placed on the bottom side (component side). Insert at least one inner plane, connected to ground, to shield and isolate the small-signal traces from noisy power traces and lines.
- The DC/DC regulator has several high-current loops. Minimize the area of these loops in order to suppress generated switching noise and optimize switching performance.
  - Loop 1: The most important loop area to minimize is the path from the input capacitor or capacitors through the high- and low-side MOSFETs, and back to the capacitor or capacitors through the ground connection. Connect the input capacitor or capacitors negative terminal close to the source of the low-side MOSFET (at ground). Similarly, connect the input capacitor or capacitors positive terminal close to the drain of the high-side MOSFET (at VIN). Refer to loop 1 of Figure 11-1.
  - Another loop, not as critical as loop 1, is the path from the low-side MOSFET through the inductor and output capacitor or capacitors, and back to source of the low-side MOSFET through ground. Connect the source of the low-side MOSFET and negative terminal of the output capacitor or capacitors at ground as close as possible.


Copyright © 2021 Texas Instruments Incorporated

- The PCB trace defined as SW node, which connects to the source of the high-side (control) MOSFET, the drain of the low-side (synchronous) MOSFET and the high-voltage side of the inductor, must be short and wide. However, the SW connection is a source of injected EMI and thus must not be too large.
- Follow any layout considerations of the MOSFETs as recommended by the MOSFET manufacturer, including pad geometry and solder paste stencil design.
- The SW pin connects to the switch node of the power conversion stage and acts as the return path for the high-side gate driver. The parasitic inductance inherent to loop 1 in Figure 11-1 and the output capacitance ($C_{OSS}$) of both power MOSFETs form a resonant circuit that induces high frequency (greater than 50 MHz) ringing at the SW node. The voltage peak of this ringing, if not controlled, can be significantly higher than the input voltage. Make sure that the peak ringing amplitude does not exceed the absolute maximum rating limit for the SW pin. In many cases, a series resistor and capacitor snubber network connected from the SW node to GND damps the ringing and decreases the peak amplitude. Provide provisions for snubber network components in the PCB layout. If testing reveals that the ringing amplitude at the SW pin is excessive, then include snubber components as needed.

### 11.1.2 Gate-Drive Layout

The LM25148 high-side and low-side gate drivers incorporate short propagation delays, adaptive dead-time control, and low-impedance output stages capable of delivering large peak currents with very fast rise and fall times to facilitate rapid turn-on and turn-off transitions of the power MOSFETs. Very high di/dt can cause unacceptable ringing if the trace lengths and impedances are not well controlled.

Minimization of stray or parasitic gate loop inductance is key to optimizing gate drive switching performance, whether it be series gate inductance that resonates with MOSFET gate capacitance or common source inductance (common to gate and power loops) that provides a negative feedback component opposing the gate drive command, thereby increasing MOSFET switching times. The following loops are important:

- Loop 2: high-side MOSFET, $Q_1$. During the high-side MOSFET turnon, high current flows from the bootstrap (boot) capacitor through the gate driver and high-side MOSFET, and back to the negative terminal of the boot capacitor through the SW connection. Conversely, to turn off the high-side MOSFET, high current flows from the gate of the high-side MOSFET through the gate driver and SW, and back to the source of the high-side MOSFET through the SW trace. Refer to loop 2 of Figure 11-1.
- Loop 3: low-side MOSFET, $Q_2$. During the low-side MOSFET turnon, high current flows from the VCC decoupling capacitor through the gate driver and low-side MOSFET, and back to the negative terminal of the capacitor through ground. Conversely, to turn off the low-side MOSFET, high current flows from the gate of the low-side MOSFET through the gate driver and GND, and back to the source of the low-side MOSFET through ground. Refer to loop 3 of Figure 11-1.

TI strongly recommends following circuit layout guidelines when designing with high-speed MOSFET gate drive circuits.

- Connections from gate driver outputs, HO and LO, to the respective gates of the high-side or low-side MOSFETs must be as short as possible to reduce series parasitic inductance. Be aware that peak gate drive currents can be as high as 3.3 A. Use 0.65 mm (25 mils) or wider traces. Use via or vias, if necessary, of at least 0.5 mm (20 mils) diameter along these traces. Route HO and SW gate traces as a differential pair from the LM25148 to the high-side MOSFET, taking advantage of flux cancellation.
- Minimize the current loop path from the VCC and HB pins through their respective capacitors as these provide the high instantaneous current, up to 3.3 A, to charge the MOSFET gate capacitances. Specifically, locate the bootstrap capacitor, $C_{BST}$, close to the CBOOT and SW pins of the LM25149 to minimize the area of loop 2 associated with the high-side driver. Similarly, locate the VCC capacitor, $C_{VCC}$, close to the VCC and PGND pins of the LM25148 to minimize the area of loop 3 associated with the low-side driver.

### 11.1.3 PWM Controller Layout

With the proviso to locate the controller as close as possible to the power MOSFETs to minimize gate driver trace runs, the components related to the analog and feedback signals as well as current sensing are considered in the following:

- Separate power and signal traces, and use a ground plane to provide noise shielding.
- Place all sensitive analog traces and components related to COMP, FB, ISNS+, and RT away from high-voltage switching nodes such as SW, HO, LO, or CBOOT to avoid mutual coupling. Use internal layer or

Copyright © 2021 Texas Instruments Incorporated

layers as ground plane or planes. Pay particular attention to shielding the feedback (FB) and current sense (ISNS+ and VOUT) traces from power traces and components.
- Locate the upper and lower feedback resistors (if required) close to the FB pin, keeping the FB trace as short as possible. Route the trace from the upper feedback resistor to the required output voltage sense point at the load.
- Route the ISNS+ and VOUT sense traces as differential pairs to minimize noise pickup and use Kelvin connections to the applicable shunt resistor (if shunt current sensing is used) or to the sense capacitor (if inductor DCR current sensing is used).
- Minimize the loop area from the VCC and VIN pins through their respective decoupling capacitors to the PGND pin. Locate these capacitors as close as possible to the LM25148.

### 11.1.4 Thermal Design and Layout

The useful operating temperature range of a PWM controller with integrated gate drivers and bias supply LDO regulator is greatly affected by the following:

- Average gate drive current requirements of the power MOSFETs
- Switching frequency
- Operating input voltage (affecting bias regulator LDO voltage drop and hence its power dissipation)
- Thermal characteristics of the package and operating environment

For a PWM controller to be useful over a particular temperature range, the package must allow for the efficient removal of the heat produced while keeping the junction temperature within rated limits. The LM25148 controller is available in a small 4-mm × 4-mm 24-pin VQFN PowerPAD package to cover a range of application requirements. Section 11.1.4 summarizes the thermal metrics of this package.

The 24-pin VQFN package offers a means of removing heat from the semiconductor die through the exposed thermal pad at the base of the package. While the exposed pad of the package is not directly connected to any leads of the package, it is thermally connected to the substrate of the LM25149 device (ground). This allows a significant improvement in heat sinking, and it becomes imperative that the PCB is designed with thermal lands, thermal vias, and a ground plane to complete the heat removal subsystem. The exposed pad of the LM25148 is soldered to the ground-connected copper land on the PCB directly underneath the device package, reducing the thermal resistance to a very low value.

Numerous vias with a 0.3-mm diameter connected from the thermal land to the internal and solder-side ground plane or planes are vital to help dissipation. In a multi-layer PCB design, a solid ground plane is typically placed on the PCB layer below the power components. Not only does this provide a plane for the power stage currents to flow but it also represents a thermally conductive path away from the heat generating devices.

The thermal characteristics of the MOSFETs also are significant. The drain pads of the high-side MOSFETs are normally connected to a VIN plane for heat sinking. The drain pads of the low-side MOSFETs are tied to the SW plane, but the SW plane area is purposely kept as small as possible to mitigate EMI concerns.

### 11.1.5 Ground Plane Design

As mentioned previously, TI recommends using one or more of the inner PCB layers as a solid ground plane. A ground plane offers shielding for sensitive circuits and traces and also provides a quiet reference potential for the control circuitry. In particular, a full ground plane on the layer directly underneath the power stage components is essential. Connect the source terminal of the low-side MOSFET and return terminals of the input and output capacitors to this ground plane. Connect the PGND and AGND pins of the controller at the DAP and then connect to the system ground plane using an array of vias under the DAP. The PGND nets contain noise at the switching frequency and can bounce because of load current variations. The power traces for PGND, VIN, and SW can be restricted to one side of the ground plane, for example on the top layer. The other side of the ground plane contains much less noise and is ideal for sensitive analog trace routes.


Copyright © 2021 Texas Instruments Incorporated

## 11.2 Layout Example

Figure 11-2 shows a single-sided layout of a synchronous buck regulator with discrete power MOSFETs, Q1 and Q2, in SON 5-mm × 6-mm case size. The power stage is surrounded by a GND pad geometry to connect an EMI shield if needed. The design uses layer 2 of the PCB as a power-loop return path directly underneath the top layer to create a low-area switching power loop of approximately 2 mm². This loop area, and hence parasitic inductance, must be as small as possible to minimize EMI as well as switch-node voltage overshoot and ringing.

The high-frequency power loop current flows through MOSFETs Q1 and Q2, through the power ground plane on layer 2, and back to VIN through the 0603 ceramic capacitors C15 through C18. The currents flowing in opposing directions in the vertical loop configuration provide field self-cancellation, reducing parasitic inductance. Figure 11-4 shows a side view to illustrate the concept of creating a low-profile, self-canceling loop in a multilayer PCB structure. The layer-2 GND plane layer, shown in Figure 11-3, provides a tightly-coupled current return path directly under the MOSFETs to the source terminals of Q2.

Four 10-nF input capacitors with small 0402 or 0603 case size are placed in parallel very close to the drain of Q1. The low equivalent series inductance (ESL) and high self-resonant frequency (SRF) of the small footprint capacitors yield excellent high-frequency performance. The negative terminals of these capacitors are connected to the layer-2 GND plane with multiple 12-mil (0.3-mm) diameter vias, further minimizing parasitic loop inductance.

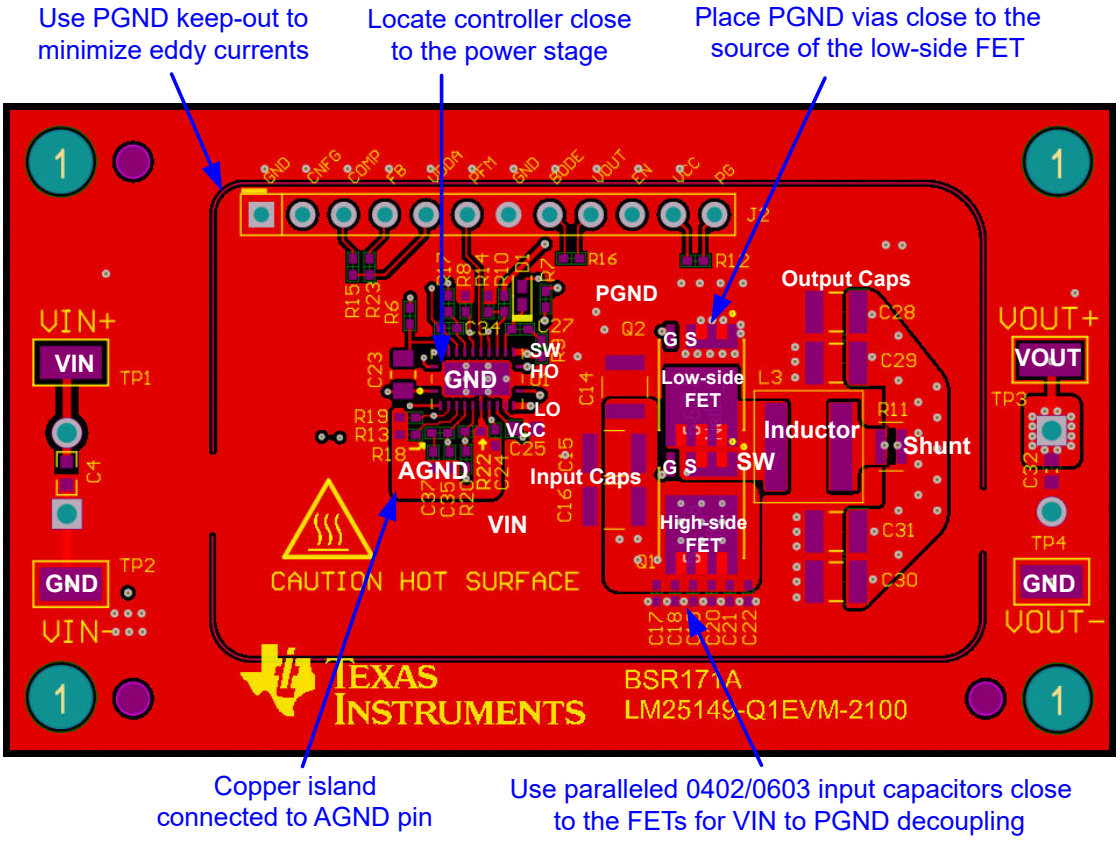



**Figure 11-2. PCB Top Layer – High Density, Single-sided Design**

Additional guidelines to improve noise immunity and reduce EMI are as follows:

- Make the ground connections to the LM25148-Q1 controller as shown in Figure 11-2. Create a power ground directly connected to all high-power components and an analog ground plane for sensitive analog components. The analog ground plane for AGND and power ground plane for PGND must be connected at a single point directly under the IC – at the die attach pad (DAP).
- Connect the MOSFETs (switch node) directly to the inductor terminal with short copper connections (without vias) as this net has high dv/dt and contributes to radiated EMI. The single-layer routing of the switch-node

Copyright © 2021 Texas Instruments Incorporated

connection means that switch-node vias with high dv/dt do not appear on the bottom side of the PCB. This avoids e-field coupling to the reference ground plane during the EMI test. VIN and PGND plane copper pours shield the polygon connecting the MOSFETs to the inductor terminal, further reducing the radiated EMI signature.

- Place the *EMI filter* components on the bottom side of the PCB so that they are shielded from the power stage components on the top side.

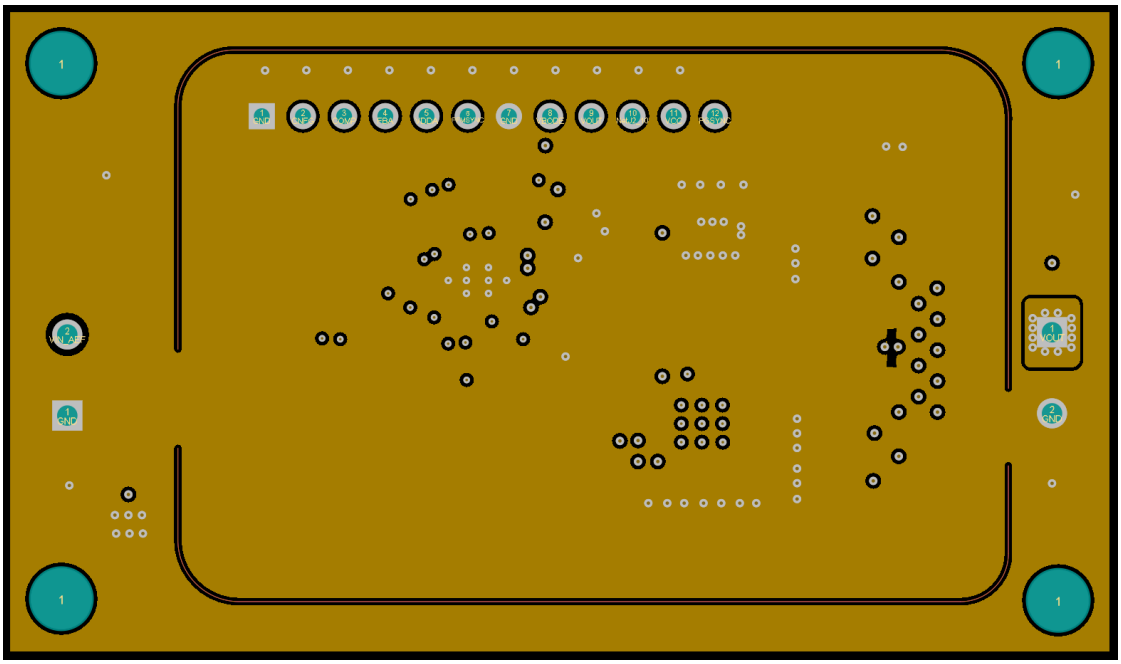


**Figure 11-3. Layer 2 Full Ground Plane Directly Under the Power Components**

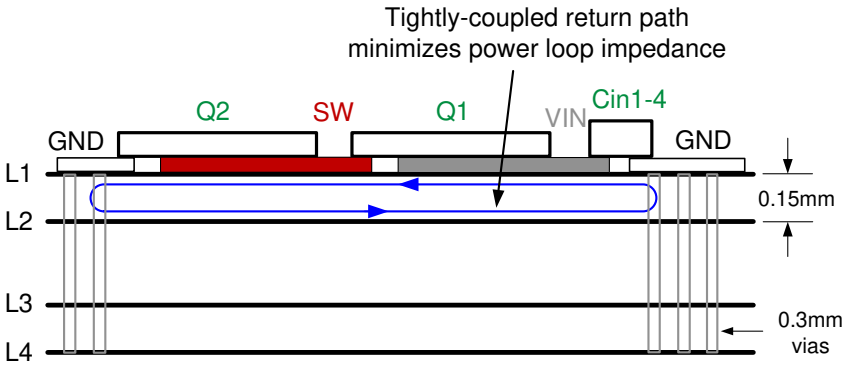



**Figure 11-4. PCB Stack-up Diagram With Low L1-L2 Intra-layer Spacing [1]**

[1] See *Improve High-current DC/DC Regulator Performance for Free with Optimized Power Stage Layout* for more detail.


Copyright © 2021 Texas Instruments Incorporated

# 12 Device and Documentation Support

## 12.1 Device Support

### 12.1.1 Development Support

With an input operating voltage as low as 3.5 V and up to 100 V as specified in Table 12-1, the LM(2)514x family of synchronous buck controllers from TI provides flexibility, scalability and optimized solution size for a range of applications. These controllers enable DC/DC solutions with high density, low EMI and increased flexibility. Available EMI mitigation features include dual-random spread spectrum (DRSS) or triangular spread spectrum (TRSS), split gate driver outputs for slew rate (SR) control, and integrated active EMI filtering (AEF).

**Table 12-1. Synchronous Buck DC/DC Controller Family**

| DC/DC CONTROLLER | SINGLE or DUAL | $V_{IN}$ RANGE | CONTROL METHOD | GATE DRIVE VOLTAGE | SYNC OUTPUT | EMI MITIGATION |
|---|---|---|---|---|---|---|
| LM25141 | Single | 3.8 V to 42 V | Peak current mode | 5 V | N/A | SR control, TRSS |
| LM25143 | Dual | 3.5 V to 42 V | Peak current mode | 5 V | 90° phase shift | SR control, TRSS |
| LM25145 | Single | 6 V to 42 V | Voltage mode | 7.5 V | 180° phase shift | N/A |
| LM25148 | Single | 3.5 V to 42 V | Peak current mode | 5 V | 180° phase shift | DRSS |
| LM25149 | Single | 3.5 V to 42 V | Peak current mode | 5 V | 180° phase shift | AEF, DRSS |
| LM5141 | Single | 3.8 V to 42 V | Peak current mode | 5 V | N/A | SR control, TRSS |
| LM5143 | Dual | 3.5 V to 65 V | Peak current mode | 5 V | 90° phase shift | SR control, TRSS |
| LM5145 | Single | 6 V to 75 V | Voltage mode | 7.5 V | 180° phase shift | N/A |
| LM5146 | Single | 5.5 V to 100 V | Voltage mode | 7.5 V | 180° phase shift | N/A |
| LM5148 | Single | 3.5 V to 80 V | Peak current mode | 5 V | 180° phase shift | DRSS |
| LM5149 | Single | 3.5 V to 80 V | Peak current mode | 5 V | 180° phase shift | AEF, DRSS |

For development support see the following:

- LM25148 Quickstart Calculator
- LM25148 Simulation Models
- For TI's reference design library, visit TI Designs
- For TI's WEBENCH Design Environment, visit the WEBENCH® Design Center
- TI Designs:
  - *ADAS 8-Channel Sensor Fusion Hub Reference Design with Two 4-Gbps Quad Deserializers*
  - *Automotive EMI and Thermally Optimized Synchronous Buck Converter Reference Design*
  - *Automotive High Current, Wide $V_{IN}$ Synchronous Buck Controller Reference Design Featuring LM5141-Q1*
  - *25W Automotive Start-Stop Reference Design Operating at 2.2 MHz*
  - *Synchronous Buck Converter for Automotive Cluster Reference Design*
  - *137W Holdup Converter for Storage Server Reference Design*
  - *Automotive Synchronous Buck With 3.3V @ 12.0A Reference Design*
  - *Automotive Synchronous Buck Reference Design*
  - *Wide Input Synchronous Buck Converter Reference Design With Frequency Spread Spectrum*
  - *Automotive Wide $V_{IN}$ Front-end Reference Design for Digital Cockpit Processing Units*
- Technical Articles:
  - *High-Density PCB Layout of DC/DC Converters*
  - *Synchronous Buck Controller Solutions Support Wide $V_{IN}$ Performance and Flexibility*
  - *How to Use Slew Rate for EMI Control*
- To view a related device of this product, see the LM25141

#### *12.1.1.1 Custom Design With WEBENCH® Tools*

Click here to create a custom design using the LM25148 device with the WEBENCH® Power Designer.

1. Start by entering the input voltage ($V_{IN}$), output voltage ($V_{OUT}$), and output current ($I_{OUT}$) requirements.
2. Optimize the design for key parameters such as efficiency, footprint, and cost using the optimizer dial.

Copyright © 2021 Texas Instruments Incorporated

3. Compare the generated design with other possible solutions from Texas Instruments.

The WEBENCH Power Designer gives a customized schematic along with a list of materials with real-time pricing and component availability.

In most cases, these actions are available:

- Run electrical simulations to see important waveforms and circuit performance
- Run thermal simulations to understand board thermal performance
- Export customized schematic and layout into popular CAD formats
- Print PDF reports for the design, and share the design with colleagues

Get more information about WEBENCH tools at www.ti.com/WEBENCH.

## 12.2 Documentation Support

### 12.2.1 Related Documentation

For related documentation see the following:

- User's Guides:
  - *LM25149-Q1 Synchronous Buck Controller High Density EVM*
  - *LM5141-Q1 Synchronous Buck Controller EVM*
  - *LM5143-Q1 Synchronous Buck Controller EVM*
  - *LM5146-Q1 EVM User's Guide*
  - *LM5145 EVM User's Guide*
- Application Reports:
  - *Improve High-current DC/DC Regulator Performance for Free with Optimized Power Stage Layout Application Report*
  - *AN-2162 Simple Success with Conducted EMI from DC-DC Converters*
  - *Maintaining Output Voltage Regulation During Automotive Cold-Crank with LM5140-Q1 Dual Synchronous Buck Controller*
- Technical Briefs:
  - *Reduce Buck Converter EMI and Voltage Stress by Minimizing Inductive Parasitics*
- White Papers:
  - *An Overview of Conducted EMI Specifications for Power Supplies*
  - *An Overview of Radiated EMI Specifications for Power Supplies*
  - *Valuing Wide $V_{IN}$, Low EMI Synchronous Buck Circuits for Cost-driven, Demanding Applications*

#### *12.2.1.1 PCB Layout Resources*

- Application Reports:
  - *Improve High-current DC/DC Regulator Performance for Free with Optimized Power Stage Layout*
  - *AN-1149 Layout Guidelines for Switching Power Supplies*
  - *AN-1229 Simple Switcher PCB Layout Guidelines*
  - *Low Radiated EMI Layout Made SIMPLE with LM4360x and LM4600x*
- Seminars:
  - *Constructing Your Power Supply – Layout Considerations*

#### *12.2.1.2 Thermal Design Resources*

- Application Reports:
  - *AN-2020 Thermal Design by Insight, Not Hindsight*
  - *AN-1520 A Guide to Board Layout for Best Thermal Resistance for Exposed Pad Packages*
  - *Semiconductor and IC Package Thermal Metrics*
  - *Thermal Design Made Simple with LM43603 and LM43602*
  - *PowerPAD™ Thermally Enhanced Package*
  - *PowerPAD Made Easy*
  - *Using New Thermal Metrics*


Copyright © 2021 Texas Instruments Incorporated

### 12.3 Receiving Notification of Documentation Updates

To receive notification of documentation updates, navigate to the device product folder on ti.com. Click on *Subscribe to updates* to register and receive a weekly digest of any product information that has changed. For change details, review the revision history included in any revised document.

### 12.4 Support Resources

TI E2E™ support forums are an engineer's go-to source for fast, verified answers and design help — straight from the experts. Search existing answers or ask your own question to get the quick design help you need.

Linked content is provided "AS IS" by the respective contributors. They do not constitute TI specifications and do not necessarily reflect TI's views; see TI's Terms of Use.

### 12.5 Trademarks

NexFET™ and TI E2E™ are trademarks of Texas Instruments.
PowerPAD™ is a trademark of Texas Instruments.
WEBENCH® is a registered trademark of Texas Instruments.
is a registered trademark of TI.
All trademarks are the property of their respective owners.

### 12.6 Electrostatic Discharge Caution



This integrated circuit can be damaged by ESD. Texas Instruments recommends that all integrated circuits be handled with appropriate precautions. Failure to observe proper handling and installation procedures can cause damage.

ESD damage can range from subtle performance degradation to complete device failure. Precision integrated circuits may be more susceptible to damage because very small parametric changes could cause the device not to meet its published specifications.

### 12.7 Glossary

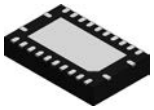
| | |
|---|---|
| TI Glossary | This glossary lists and explains terms, acronyms, and definitions. |

## 13 Mechanical, Packaging, and Orderable Information

The following pages show mechanical, packaging, and orderable information. This information is the most current data available for the designated devices. This data is subject to change without notice and revision of this document. For browser-based versions of this data sheet, refer to the left-hand navigation.

Copyright © 2021 Texas Instruments Incorporated

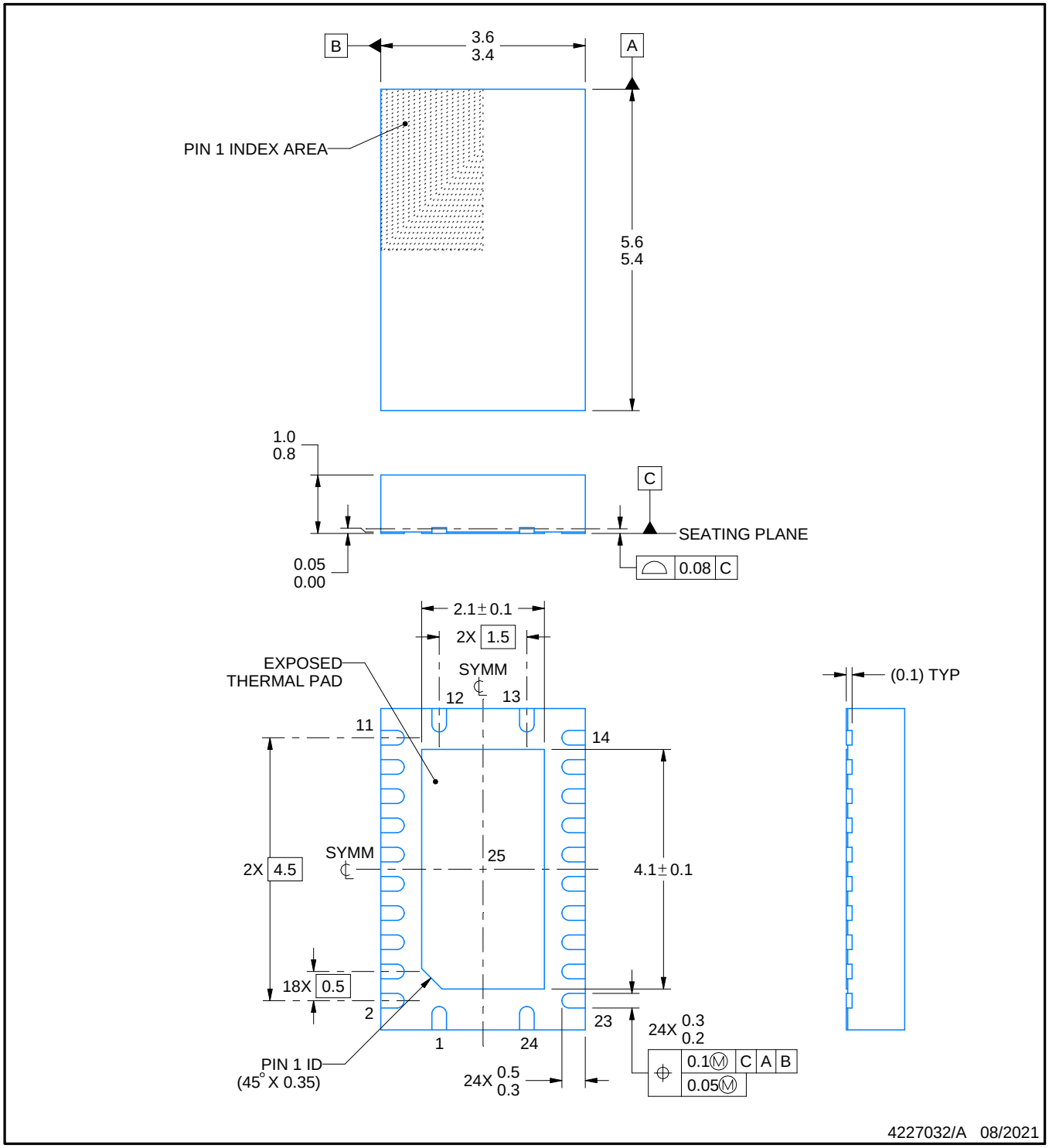
# RGY0024F



# PACKAGE OUTLINE

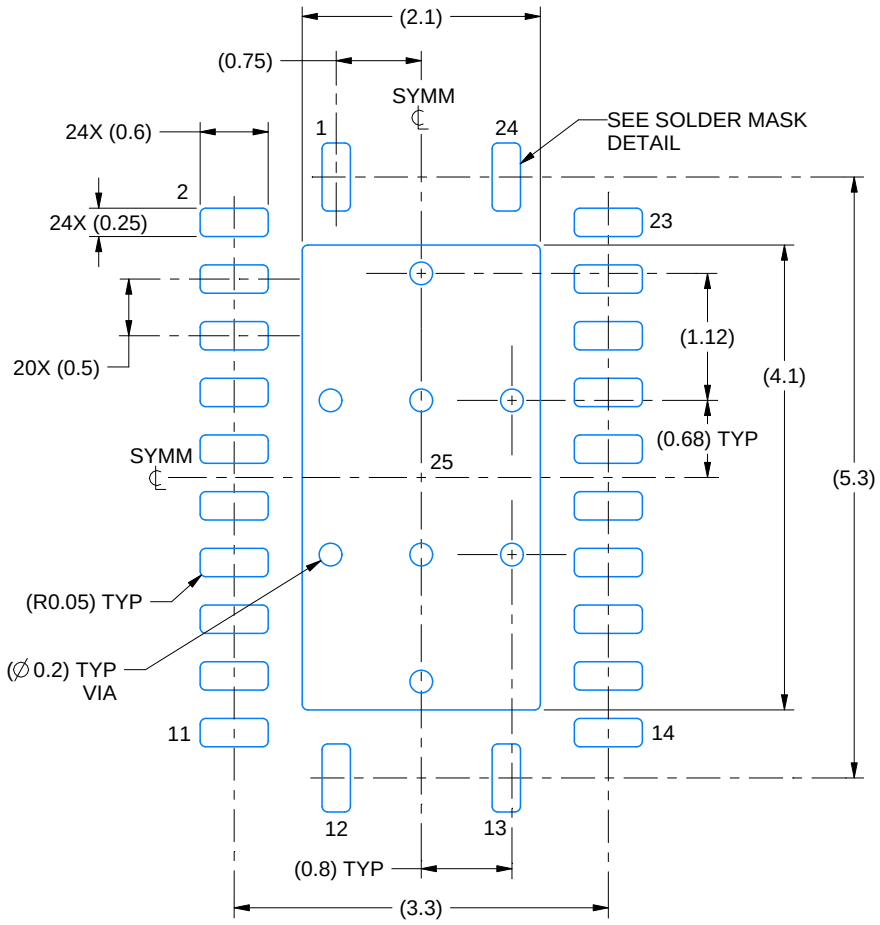
## VQFN - 1 mm max height

PLASTIC QUAD FLATPACK - NO LEAD

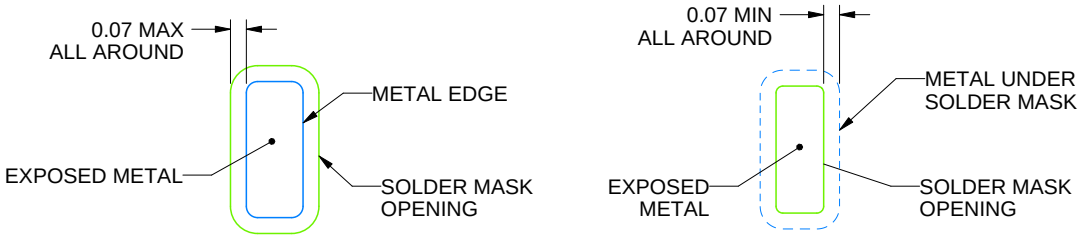



NOTES:

1. All linear dimensions are in millimeters. Any dimensions in parenthesis are for reference only. Dimensioning and tolerancing per ASME Y14.5M.
2. This drawing is subject to change without notice.
3. The package thermal pad must be soldered to the printed circuit board for thermal and mechanical performance.




LAND PATTERN EXAMPLE
EXPOSED METAL SHOWN
SCALE: 15X

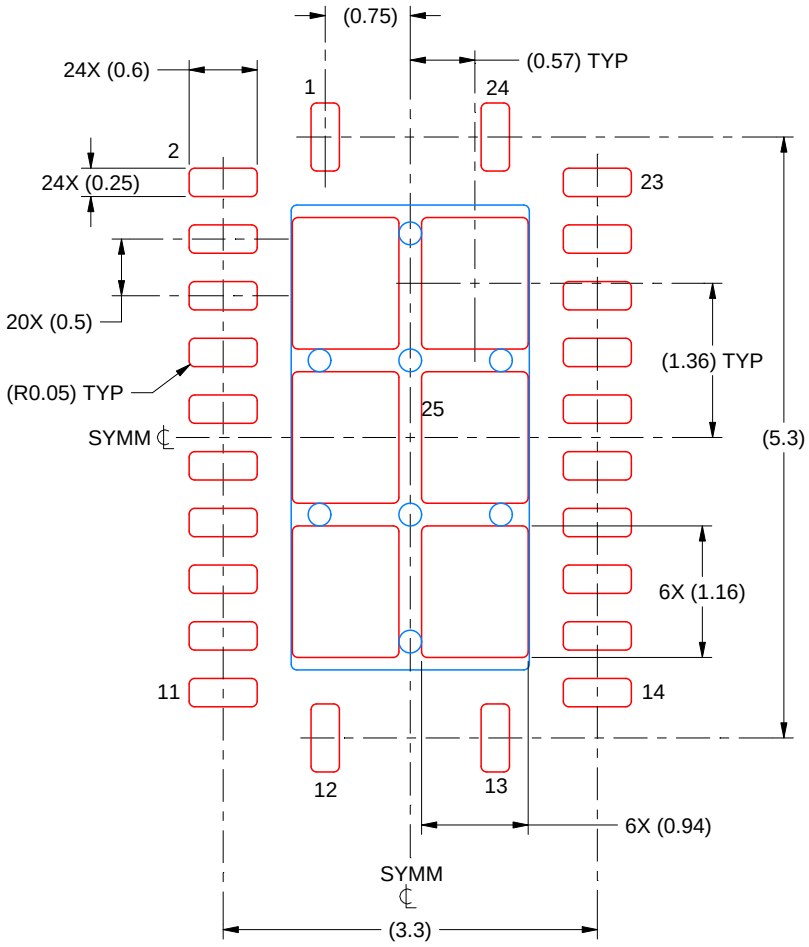



SOLDER MASK DETAILS

4227032/A 08/2021

NOTES: (continued)

4. This package is designed to be soldered to a thermal pad on the board. For more information, see Texas Instruments literature number SLUA271 (www.ti.com/lit/slua271).
5. Vias are optional depending on application, refer to device data sheet. If any vias are implemented, refer to their locations shown on this view. It is recommended that vias under paste be filled, plugged or tented.




SOLDER PASTE EXAMPLE
BASED ON 0.125 MM THICK STENCIL
SCALE: 15X

EXPOSED PAD 25
76% PRINTED SOLDER COVERAGE BY AREA UNDER PACKAGE

4227032/A 08/2021

NOTES: (continued)

6. Laser cutting apertures with trapezoidal walls and rounded corners may offer better paste release. IPC-7525 may have alternate design recommendations.

## PACKAGING INFORMATION

| Orderable part number | Status (1) | Material type (2) | Package \| Pins | Package qty \| Carrier | RoHS (3) | Lead finish/ Ball material (4) | MSL rating/ Peak reflow (5) | Op temp (°C) | Part marking (6) |
|---|---|---|---|---|---|---|---|---|---|
| LM25148RGYR | Active | Production | VQFN (RGY) \| 24 | 3000 \| LARGE T&R | Yes | SN | Level-1-260C-UNLIM | -40 to 150 | LM25148 |
| LM25148RGYR.A | Active | Production | VQFN (RGY) \| 24 | 3000 \| LARGE T&R | Yes | SN | Level-1-260C-UNLIM | -40 to 150 | LM25148 |

(1) **Status:** For more details on status, see our product life cycle.

(2) **Material type:** When designated, preproduction parts are prototypes/experimental devices, and are not yet approved or released for full production. Testing and final process, including without limitation quality assurance, reliability performance testing, and/or process qualification, may not yet be complete, and this item is subject to further changes or possible discontinuation. If available for ordering, purchases will be subject to an additional waiver at checkout, and are intended for early internal evaluation purposes only. These items are sold without warranties of any kind.

(3) **RoHS values:** Yes, No, RoHS Exempt. See the TI RoHS Statement for additional information and value definition.

(4) **Lead finish/Ball material:** Parts may have multiple material finish options. Finish options are separated by a vertical ruled line. Lead finish/Ball material values may wrap to two lines if the finish value exceeds the maximum column width.

(5) **MSL rating/Peak reflow:** The moisture sensitivity level ratings and peak solder (reflow) temperatures. In the event that a part has multiple moisture sensitivity ratings, only the lowest level per JEDEC standards is shown. Refer to the shipping label for the actual reflow temperature that will be used to mount the part to the printed circuit board.

(6) **Part marking:** There may be an additional marking, which relates to the logo, the lot trace code information, or the environmental category of the part.

Multiple part markings will be inside parentheses. Only one part marking contained in parentheses and separated by a "~" will appear on a part. If a line is indented then it is a continuation of the previous line and the two combined represent the entire part marking for that device.

**Important Information and Disclaimer:**The information provided on this page represents TI's knowledge and belief as of the date that it is provided. TI bases its knowledge and belief on information provided by third parties, and makes no representation or warranty as to the accuracy of such information. Efforts are underway to better integrate information from third parties. TI has taken and continues to take reasonable steps to provide representative and accurate information but may not have conducted destructive testing or chemical analysis on incoming materials and chemicals. TI and TI suppliers consider certain information to be proprietary, and thus CAS numbers and other limited information may not be available for release.

In no event shall TI's liability arising out of such information exceed the total purchase price of the TI part(s) at issue in this document sold by TI to Customer on an annual basis.

**OTHER QUALIFIED VERSIONS OF LM25148 :**

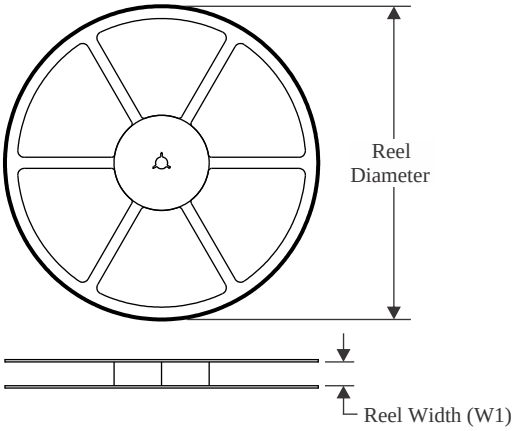
- Automotive : LM25148-Q1

NOTE: Qualified Version Definitions:

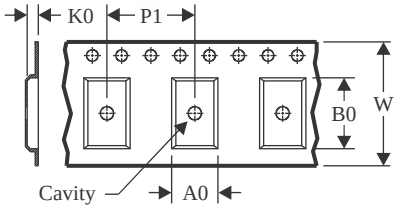
- Automotive - Q100 devices qualified for high-reliability automotive applications targeting zero defects

## TAPE AND REEL INFORMATION

**REEL DIMENSIONS**

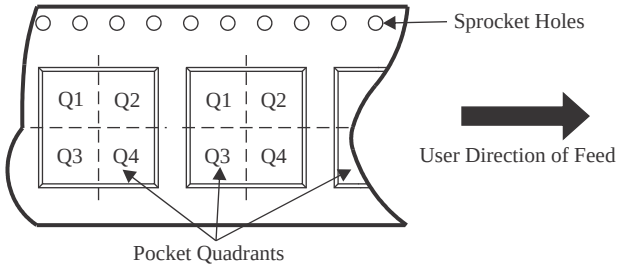



**TAPE DIMENSIONS**




| | |
|---|---|
| A0 | Dimension designed to accommodate the component width |
| B0 | Dimension designed to accommodate the component length |
| K0 | Dimension designed to accommodate the component thickness |
| W | Overall width of the carrier tape |
| P1 | Pitch between successive cavity centers |

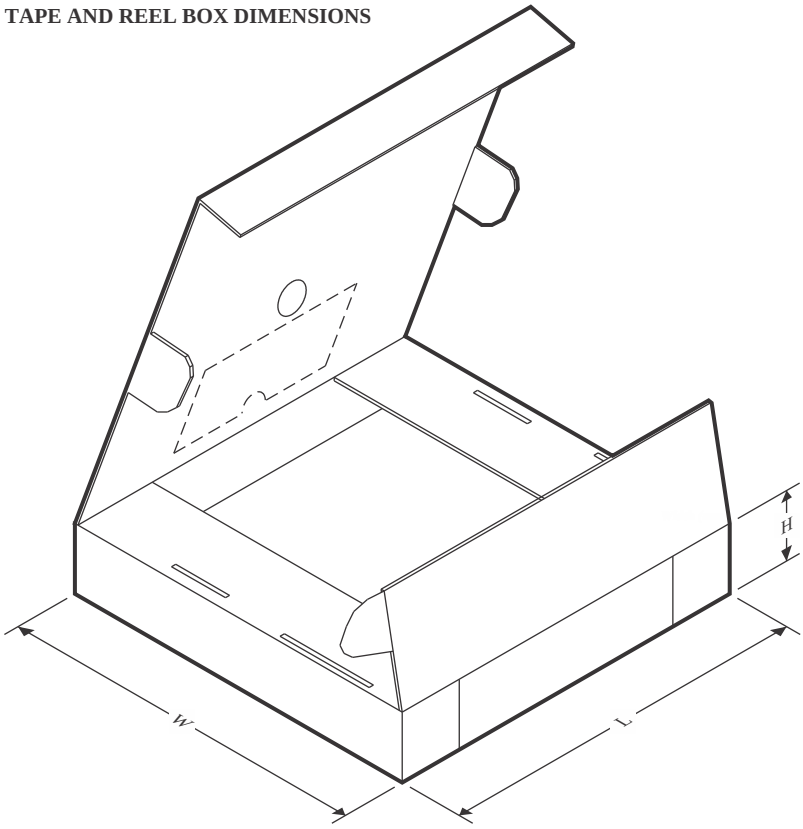
**QUADRANT ASSIGNMENTS FOR PIN 1 ORIENTATION IN TAPE**




*All dimensions are nominal

| Device | Package Type | Package Drawing | Pins | SPQ | Reel Diameter (mm) | Reel Width W1 (mm) | A0 (mm) | B0 (mm) | K0 (mm) | P1 (mm) | W (mm) | Pin1 Quadrant |
|---|---|---|---|---|---|---|---|---|---|---|---|---|
| LM25148RGYR | VQFN | RGY | 24 | 3000 | 330.0 | 12.4 | 3.8 | 5.8 | 1.2 | 8.0 | 12.0 | Q1 |

TAPE AND REEL BOX DIMENSIONS




*All dimensions are nominal

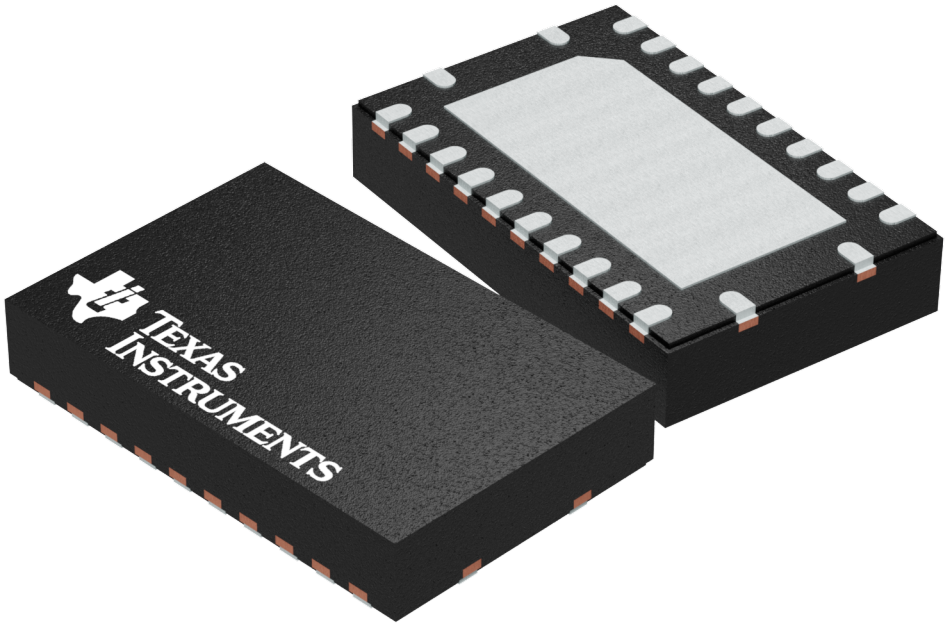
| Device | Package Type | Package Drawing | Pins | SPQ | Length (mm) | Width (mm) | Height (mm) |
|---|---|---|---|---|---|---|---|
| LM25148RGYR | VQFN | RGY | 24 | 3000 | 360.0 | 360.0 | 36.0 |

# RGY 24

# VQFN - 1 mm max height

**5.5 x 3.5 mm, 0.5 mm pitch**

PLASTIC QUAD FLATPACK - NO LEAD




Images above are just a representation of the package family, actual package may vary.
Refer to the product data sheet for package details.

# IMPORTANT NOTICE AND DISCLAIMER

TI PROVIDES TECHNICAL AND RELIABILITY DATA (INCLUDING DATASHEETS), DESIGN RESOURCES (INCLUDING REFERENCE DESIGNS), APPLICATION OR OTHER DESIGN ADVICE, WEB TOOLS, SAFETY INFORMATION, AND OTHER RESOURCES “AS IS” AND WITH ALL FAULTS, AND DISCLAIMS ALL WARRANTIES, EXPRESS AND IMPLIED, INCLUDING WITHOUT LIMITATION ANY IMPLIED WARRANTIES OF MERCHANTABILITY, FITNESS FOR A PARTICULAR PURPOSE OR NON-INFRINGEMENT OF THIRD PARTY INTELLECTUAL PROPERTY RIGHTS.

These resources are intended for skilled developers designing with TI products. You are solely responsible for (1) selecting the appropriate TI products for your application, (2) designing, validating and testing your application, and (3) ensuring your application meets applicable standards, and any other safety, security, regulatory or other requirements.

These resources are subject to change without notice. TI grants you permission to use these resources only for development of an application that uses the TI products described in the resource. Other reproduction and display of these resources is prohibited. No license is granted to any other TI intellectual property right or to any third party intellectual property right. TI disclaims responsibility for, and you fully indemnify TI and its representatives against any claims, damages, costs, losses, and liabilities arising out of your use of these resources.

TI’s products are provided subject to TI’s Terms of Sale, TI’s General Quality Guidelines, or other applicable terms available either on ti.com or provided in conjunction with such TI products. TI’s provision of these resources does not expand or otherwise alter TI’s applicable warranties or warranty disclaimers for TI products. Unless TI explicitly designates a product as custom or customer-specified, TI products are standard, catalog, general purpose devices.

TI objects to and rejects any additional or different terms you may propose.

Copyright © 2026, Texas Instruments Incorporated

Last updated 10/2025